OPTIMIZING THE PLANNING OF REMOTE CONSTRUCTION SITES TO MINIMIZE THE CONSEQUENCES OF EXPLOSIVE ATTACKS

BY

STEVEN JAMES SCHULDT

DISSERTATION

Submitted in partial fulfillment of the requirements
for the degree of Doctor of Philosophy in Civil Engineering
in the Graduate College of the
University of Illinois at Urbana-Champaign, 2017

Urbana, Illinois

Doctoral Committee:

Professor Khaled El-Rayes, Chair, Director of Research
Associate Professor Liang Liu
Associate Professor Mani Golparvar-Fard
Assistant Professor Nora El-Gohary
Dr. Ahmet Soylemezoglu, United States Army Corps of Engineers

ABSTRACT

Remote construction sites, such as oil production facilities and military forward operating bases, are often located in hostile areas that are vulnerable to the threat of explosive attacks. These attacks produce devastating and far-reaching consequences. From 2011-2015, explosive attacks targeting facilities and infrastructure resulted in more than 45,000 casualties and $73 billion in direct economic losses worldwide. Furthermore, the post-traumatic stress disorder rate among victims of explosive attacks is reported to be as high as 40%. To minimize the consequences of explosive attacks, site layout planners of remote construction sites utilize three primary protection measures that are designed to: (i) increase the standoff distances between site facilities and the potential location of an explosive device; (ii) construct perimeter walls to mitigate blast loads on facilities; and (iii) harden facilities to withstand blast loads. The integration of these protection measures increases construction costs and they can be challenging to implement when site space is limited. Accordingly, designers need to identify an optimum combination of these protection measures that minimizes the aforementioned explosive attack consequences while minimizing site construction costs.

The main goal of this research study is to develop novel models for optimizing the planning of remote construction sites that provide the capability of minimizing facility destruction levels and consequences resulting from explosive attacks. To accomplish this goal, the research objectives of this study are to: (1) develop an innovative blast effects assessment model capable of efficiently quantifying and visualizing blast effects on facilities behind blast walls; (2) develop an original multi-objective facility protection

model for optimizing the site layout and selection of perimeter blast walls and building materials in order to minimize facility destruction levels from explosive attacks while minimizing site construction costs; and (3) develop a novel multi-objective optimization model for the layout and security planning of remote construction sites that provides the capability of simultaneously minimizing the consequences of an explosive attack and the construction costs of remote sites.

The performance of the developed optimization models was analyzed using case studies of hypothetical remote construction sites. The results of analyzing these case studies illustrated the novel and distinctive capabilities of the developed models in enabling designers to search for and select optimum design configurations based on the mission of the remote construction site. These capabilities will result in the construction of cost-effective, secure sites that will reduce the risks to site personnel and facilities from the devastating effects of an explosive attack.

To My Loving Wife

“An excellent wife, who can find? She is far more precious than jewels.”

To Our Children

“I have no greater joy than to hear that my children are walking in the truth.”

ACKNOWLEDGEMENTS

While my name is listed on the cover of this dissertation, the real credit belongs to the many people who have graciously supported me throughout my studies. I am deeply humbled and honored by the guidance, support, and encouragement I have received over my last three years at the University of Illinois.

I first want to express my sincere appreciation and gratitude to my mentor and academic advisor, Professor Khaled El-Rayes. His advice, guidance, and unwavering support during my doctoral program was invaluable to my successful completion. His leadership will forever be cherished and I look forward to his continued support beyond my time at Illinois. I also want to extend my deepest appreciation to Professor Liang Liu, Professor Mani Golparvar-Fard, Professor Nora El-Gohary, and Dr. Ahmet Soylemezoglu for their dedicated service on my thesis supervisory committee and all their guidance and constructive feedback.

It is said that it takes an army, but in my case, it took the Army to facilitate many of the most critical aspects of my research. Thank you to the numerous employees at the United States Army Corps of Engineers, Engineer Research and Development Center, Construction Engineering Research Laboratory who provided technical assistance and invaluable operational feedback during my research. Specifically, I want to recognize the efforts of Dr. Soylemezoglu, Mr. Noah Garfinkle, and Mr. H. Garth Anderson. Additionally, I greatly acknowledge the financial support provided by the United States Air Force.

I would be remiss if I did not take the time to thank Ms. Deidre Bever, Ms. Joan Christian, Ms. Maxine Peyton, and the rest of the frontline staff of the Civil and Environmental Department. These individuals work tirelessly behind the scenes to help ensure the success of the department's graduate students and their dedication means the world to me.

I also want to sincerely thank my dear friends and colleagues Ernest-John Ignacio, Ayman Halabya, and Neetesh Sharma for their support during my doctoral study.

I owe my deepest gratitude to my lovely wife, Michelle Schuldt. She is my rock and I never could have finished this dissertation without her selfless love, patience, and understanding. I also want to thank my three wonderful children: Austin, Emmalyn, and Sophia. Their encouragement fills me with joy and motivates me to be better every day. Additionally, I want to thank my parents, Steve and Deborah Schuldt, and my in-laws, Wolfgang and Dorothea Kelly. So much of my strength can be directly attributed to the love and support of my entire family. Finally, I want to thank Pastor Paul Craig, Pastor Joel Hollins and the rest of my church family for the wisdom and counsel they have provided my family during this challenging venture.

The views expressed in this paper are those of the author and do not reflect the official policy or position of the United States Air Force, Department of Defense, or the United States government.

TABLE OF CONTENTS

CHAPTER 1

INTRODUCTION

1.1 Problem Statement

Remote construction sites are encountered in many projects such as oil exploration and production operations and the construction of remote military bases. With proven oil reserves in 101 countries (CIA 2015), oil exploration and production operations have increased 20% worldwide since 2000 (USEIA 2015) to accommodate the increasing demand for energy for the growing global population and the increased industrialization of developing countries. Similarly, the construction of remote military bases has increased in recent years to address heightened national security threats and confront conflicts worldwide. These construction projects are located in remote and often hostile areas. Project managers and planners of this type of construction are often confronted with a number of unique and critical challenges, including how to: (1) analyze and select blast walls and building materials to protect site facilities; (2) minimize the destruction of site facilities in the event of an explosive attack; and (3) mitigate the consequences of an explosive attack on site personnel, facilities, and operations. The following sections highlight the significance of these three pressing challenges confronting remote construction sites and the research needs to address them, as shown in Figure 1.1.

1.1.1 Blast Effect Assessment Challenges

Explosive attacks on constructed facilities are a significant threat worldwide, producing devastating consequences including loss of life, property damages, and economic losses (Wu and Hao 2007; Dillon et al. 2009). In 2014 alone, explosive

attacks targeting facilities and infrastructure resulted in 8,024 casualties and $13.1 billion in direct economic losses (Hunter and Perkins 2015; Institute for Economics and Peace 2015). In an effort to mitigate blast effects on facilities, it is necessary for designers to harden facilities and/or construct blast walls (Ward 2004; Remennikov and Rose 2007). Therefore, designers must carefully analyze and select the most effective combination of utilizing blast walls and hardening facilities to reduce the security risks to site personnel and facilities from the threat of an explosive attack (Carper 2011).

A number of research studies were conducted to: (1) predict the impact of blast on facilities; and (2) analyze and quantify the effectiveness of blast walls in protecting facilities from an explosion. First, several models were developed to predict the impact of blast on facilities, employing empirical and numerical methods. Empirical methods are presented in several technical reports and design manuals (DoD 2002, 2008a; ASCE 2011) and integrated into the software system, ConWep (Kingery and Bulmash 1984). Numerical methods include both (a) blast models that predict blast loads on facilities (McGlaun et al. 1990; Crepeau 1998; Britt et al. 1999; Nichols and Doyle 2014); and (b) coupled analysis models (Hibbitt, Karlsson & Sorensen, Inc. 2004; Ansys 2013; LSTC 2016) that are capable of accounting for structural motion as the blast calculation proceeds by combining both blast load and structural response calculations (Ngo et al. 2007).

Second, a number of studies conducted live tests and used numerical methods to quantify the effectiveness of blast walls. Live tests were conducted on rigid steel walls (Beyer 1986; Jones et al. 1987; Chapman et al. 1995a; Rose et al. 1995, 1997), as well as non-rigid or frangible materials, including sand-filled containers, wood and ice walls

(Rose et al. 1998), concrete masonry units (CMUs) and thin precast concrete panels (Bogosian and Piepenburg 2002), full-size, soil-filled HESCO Bastion concertainers (Scherbatiuk and Rattanawangcharoen 2008), and water walls (Chen et al. 2015). Numerical method studies utilized computational fluid dynamics software packages to test and examine blast wall effectiveness (Chapman et al. 1995b; Ngo et al. 2004; Rickman et al. 2006). Numerical simulation data was also used to train artificial neural networks (Remennikov and Rose 2007; Bewick et al. 2011) and develop "pseudo-analytical" formulae (Zhou and Hao 2008) that can be used with existing design manuals.

Despite the significant contributions of the aforementioned research studies and blast models, they are incapable of: (1) efficiently predicting the performance of all feasible blast wall and building material design alternatives (Bogosian et al. 2002; Sorensen and McGill 2012); (2) quantifying the effectiveness of feasible blast wall types in reducing blast loads on facilities; and (3) visualizing the anticipated facility damage areas based upon blast charge weight, blast wall type, and building material combinations. Accordingly, there is an urgent need for a novel model that is capable of efficiently quantifying and visualizing blast effects on facilities behind blast walls of various materials in order to support designers in their critical task of identifying the most effective design for blast walls and facility hardening.

1.1.2 Facility Protection Challenges

Remote construction sites such as oil production facilities and military forward operating bases are often located in remote and hostile areas that are vulnerable to the threat of explosive attacks that seek to destroy facilities and infrastructure (DoD 2008a,

2012; Johnson and Gilbert 2013). To minimize the destructive effects of these explosive attacks, planners of these remote construction sites need to incorporate a number of security measures including: (i) increasing the standoff distances between site facilities and the potential location of an explosive device; (ii) constructing perimeter walls to mitigate blast loads on facilities; and (iii) hardening facilities to withstand blast loads (Longinow and Mniszewski 1996; Remennikov and Rose 2007; DoD 2012). The integration of these site layout security measures increases construction costs; therefore, construction planners need to identify an optimum combination of these security measures that minimizes facility destruction while minimizing site construction costs (Stewart 2008).

To address the aforementioned challenging site layout planning task, a number of research studies were conducted to assess and maximize the security of facilities and construction sites. These related research studies can be grouped in two categories that focused on: (1) improving the selection of security measures; and (2) optimizing site layout planning to improve the security of construction sites. The first category of related research studies focused on improving the selection of security measures. Grassie et al. (1990) proposed a six-step security measure selection process to assist designers in implementing a cost-effective approach to site security. Longinow and Mniszewski (1996) analyzed the interaction between air blasts and facilities in an effort to identify potential design changes and security guidelines that can minimize the damages and casualties caused by vehicle bombs. In another study, Little et al. (2002) proposed a decision framework for security and natural hazard risk mitigation that identifies the maximum level of damage to be tolerated for a facility based on its risk groups and

design event magnitudes. Dillon et al. (2009) developed an anti-terrorism risk-based decision aid to prioritize upgrade measures of existing facilities.

The second group of related research studies focused on optimizing site layout planning to improve the security of construction sites. Khalafallah and El-Rayes (2008) utilized genetic algorithm to develop a multi-objective optimization model capable of simultaneously minimizing construction-related security breaches and minimizing site layout costs for airport expansion projects. Said and El-Rayes (2010) developed an automated multi-objective framework that minimizes site security risks from the threat of theft or destruction of classified materials while minimizing overall site costs. In two separate studies, Li et al. (2015a; b) utilized multi-objective, bi-level optimization algorithms to address the dynamic construction site layout and security planning problem.

Despite the significant contributions of the aforementioned research studies, there is no reported research that focused on: (1) quantifying and minimizing the impact of potential explosive attacks on facilities; (2) optimizing the selection of blast walls and building materials to minimize blast damage levels on facilities; (3) generating optimal tradeoffs between the two critical site layout planning objectives of minimizing facility destruction levels from explosive attacks and minimizing site construction costs. Accordingly, there is a pressing need for a novel model that addresses these three key research areas and enables the optimization of the site layout of remote construction sites and their selection of perimeter blast walls and building materials to minimize both destruction levels and construction costs.

1.1.3 Blast Consequence Mitigation Challenges

The consequences of explosive attacks targeting remote construction sites can be grouped into four main categories: personnel loss, psychological impact, economic loss, and operational impact (FEMA 2011). The magnitude of these consequences has significantly increased in recent years. During a five-year period from 2011-2015, explosive attacks targeting facilities and infrastructure resulted in more than 45,000 casualties and $73 billion in direct economic losses worldwide (Hunter and Perkins 2015; Institute for Economics and Peace 2015; Perkins 2015). Furthermore, the post-traumatic stress disorder (PTSD) rate among victims of explosive attacks is reported to be as high as 40% (Neria et al. 2008).

Designers and site layout planners of remote construction sites are confronted with two critical and challenging tasks in their efforts to construct resilient sites. First, they must be able to accurately and efficiently predict the potential consequences of explosive attacks. Second, they need to identify optimal combinations of site layouts and protection strategies that are capable of minimizing the consequences of an explosive attack while minimizing the construction costs of remote sites that have limited available site layout space. Research studies investigating these challenging tasks focused on three main areas: (1) evaluating the consequences of disasters and explosive attacks; (2) quantifying and aggregating explosive attack consequences; and (3) optimizing construction site layouts in order to maximize site security. These three research areas are briefly discussed below.

The first area of research studies focused on evaluating the four main consequences of disasters and explosive attacks: personnel loss, psychological impact,

economic loss, and operational impact. Personnel loss studies examined the most frequent injury types suffered in explosive attacks, including severe head trauma, (Mellor 1992; Mallonee et al. 1996; Wightman and Gladish 2001), damage to the ears (Garth 1995; Cave et al. 2007), eyes (Abbotts et al. 2007; Morley et al. 2010), and lungs (Avidan et al. 2005; Sasser et al. 2006; Stuhmiller et al. 1996), as well as injuries from flying glass debris (Norville et al. 1999; Thompson et al. 2004; Ataei and Anderson 2012). Psychological impact studies consist of applied epidemiological investigations on victims of a number of historical terrorist attacks, including the Oklahoma City bombing (North et al. 1999, 2002), September 11, 2001 attacks on New York City (Schuster et al. 2001; Galea et al. 2002; Schlenger et al. 2002), 2004 Madrid train bombing (Gabriel et al. 2007; Vázquez et al. 2008), and French bombings of 1982-1987 (Abenhaim et al. 1992) and 1995-1996 (Verger et al. 2004). Economic loss studies analyzed and differentiated between the macroeconomic (Blomberg et al. 2004; Enders and Olson 2012) and microeconomic costs (Enders 2007), and between the direct (Dillon et al. 2009) and indirect costs (Kazimi and Mackenzie 2016) of attacks. Operational impact studies investigated facility downtime caused by disasters (Comerio 2000; Pachakis and Kiremidjian 2004; Comerio 2006; Bailey and Levitan 2008; Porter and Ramer 2012) and methods of determining facility importance to a site mission (Karydas and Gifun 2006; Antelman et al. 2008; Grussing et al. 2010).

The second group of research studies developed frameworks to quantify and aggregate the consequences of disasters and explosive attacks. For example, Ayyub et al. (2007) and McGill et al. (2007) created quantitative methods for performing critical asset risk analysis based upon five consequence types: casualty, economic, mission

disruption, environmental damage, and recuperation time. These studies provided a methodology to aggregate the five consequences into a single measure of monetary loss. Dillon et al. (2009) utilized multi-attribute utility theory to integrate owner value preferences between the mission, personnel, and economic consequences of terrorist attacks. The third area of research studies consists of the aforementioned site layout optimizing models designed to maximize construction site security.

Despite the significant contributions of the aforementioned research studies, existing risk analysis and layout-based security optimization models are incapable of: (1) efficiently quantifying the consequences of explosive attacks because they rely on the use of time-consuming external blast analysis software packages; (2) evaluating the impact of serious and minor injuries on total personnel losses; (3) quantifying the extent of psychological impacts on survivors of explosive attacks; (4) measuring the impact of explosive attacks on the operational capacity of the site in terms of the total number of days the site is unable to perform its primary mission; and (5) generating a set of optimal combinations of site layout solutions and protection strategies that provide optimal tradeoffs between minimizing the consequences of explosive attacks and minimizing site construction costs. Accordingly, there is an urgent need for the development of a novel optimization model that is designed to overcome the above five limitations of existing models.

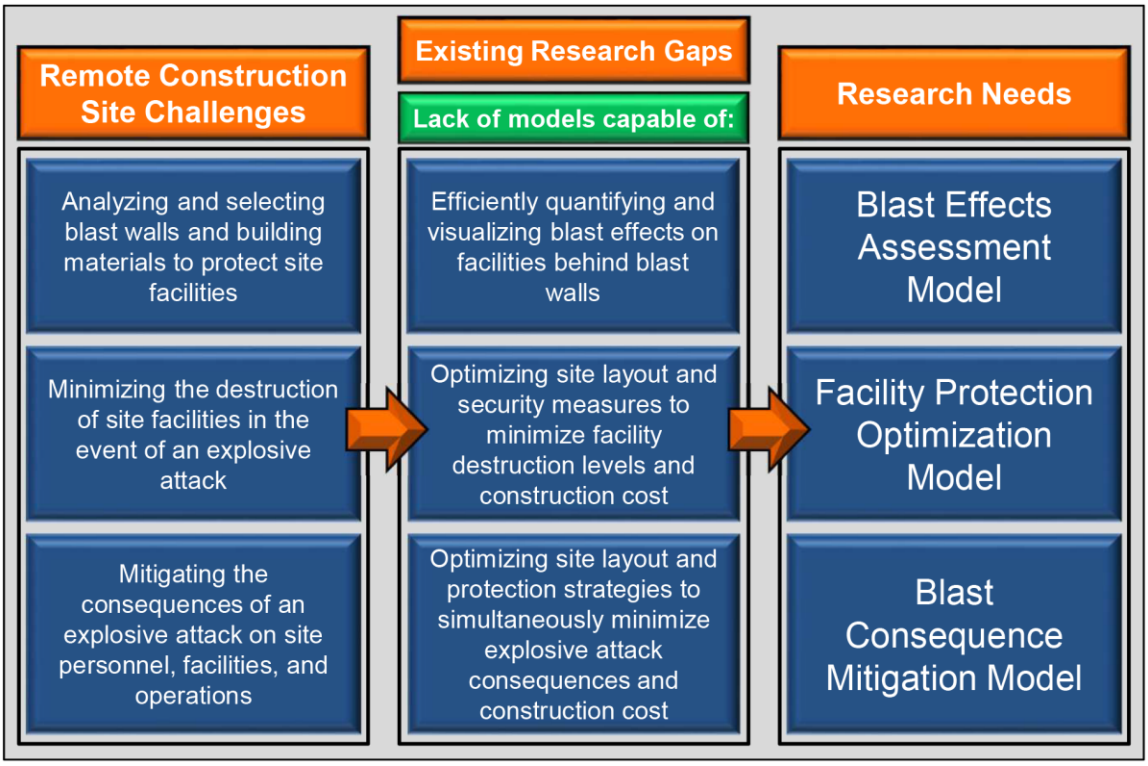

Figure 1.1 Challenges and Research Needs in Remote Construction Sites

1.2 Research Objectives

The primary goal of this research study is to develop novel models for optimizing the planning of remote construction sites that provide the capability of minimizing facility destruction levels and consequences resulting from explosive attacks. To accomplish this goal, the objectives of this research study along with its research questions and hypotheses are summarized below:

Objective 1:

Conduct a comprehensive literature review on the latest research in: (1) quantifying blast effects on facilities behind blast walls; (2) quantifying the consequences that explosive attacks and disasters inflict on site personnel and facilities; (3) analyzing models and best practices developed for remote construction site security planning; (4) modeling and optimizing the layout of construction sites; and (5)

investigating multi-objective optimization techniques that are capable of addressing the unique challenges of remote construction sites.

Research Questions:

(a) What methods are available to predict blast impacts on facilities? (b) What impact do feasible rigid and frangible blast walls have in reducing blast loads on remote facilities? (c) What are the primary consequences inflicted on site personnel and facilities in the event of an explosive attack? (d) What methods are available to quantify the various consequences of explosive attacks? (e) What design decisions and security measures can be selected to reduce the consequences of these threats? (f) What methods exist to optimize the selection of numerous facility locations on a remote construction site? and (g) What decision-making and optimization techniques are available to model the unique challenges presented in this research?

Objective 2:

Develop an innovative blast effects assessment model that is capable of efficiently quantifying and visualizing blast effects on facilities behind blast walls of various materials in order to support designers in their critical task of identifying the most effective design for blast walls and facility hardening.

Research Questions:

(a) What are the feasible blast wall types that can be constructed to reduce blast loading on facilities? (b) How do blast wall type, building material, and facility location affect the expected damages to a facility in the event of an explosive attack? and (c) How can visualizations of the anticipated facility damage

areas based upon blast charge weight, blast wall type, and building material be generated to enable the performance of visual risk management assessments of the design scenario?

Hypothesis:

A blast effects assessment model for remote construction sites can provide the capability of quantifying and visualizing blast effects on facilities behind blast walls of various materials.

Objective 3:

Develop an original multi-objective facility protection model for optimizing the site layout and selection of perimeter blast walls and building materials in order to minimize facility destruction levels from explosive attacks while minimizing site construction costs.

Research Questions:

(a) What metrics can be utilized to quantify the destruction of site facilities? (b) What modeling techniques are available to represent the site area and location of multiple site facilities? and (c) Which optimization techniques can be utilized to generate optimal tradeoffs between minimizing facility destruction levels from explosive attacks and minimizing site construction costs?

Hypothesis:

A multi-objective facility protection optimization model for remote construction sites can be used to analyze and optimize tradeoffs between minimizing site facility destruction levels and minimizing total site construction cost.

Objective 4:

Develop a novel multi-objective optimization model for the layout and security planning of remote construction sites that provides the capability of minimizing the consequences of an explosive attack and minimizing the construction costs of remote sites.

Research Questions:

(a) What metrics can be used to quantify the consequences of explosive attacks inflicted on site personnel, facility assets, and the site's ability to conduct operations? (b) How can the extent of serious injuries and minor injuries be computed? (c) How can the psychological impacts experienced by explosive attack survivors be defined and quantified? and (d) How can the various consequence metrics that have inherently different units of measure be aggregated to model the overall explosive attack consequences on remote construction sites?

Hypothesis:

A blast consequence mitigation model can be used to generate and analyze optimal tradeoffs between minimizing the consequences of an explosive attack and minimizing the construction costs of remote construction sites.

1.3 Research Methodology

This section outlines the proposed methodology for achieving the objectives of this research study. As shown in Figure 1.2, the proposed methodology can be divided into four major tasks: (1) conduct a comprehensive literature review; (2) develop a blast effects assessment model for remote construction site facilities; (3) create a facility

protection optimization model for remote construction sites; and (4) develop a blast consequence mitigation model for remote construction sites.

1.3.1 Task 1: Conduct a Comprehensive Literature Review

This task will focus on conducting a comprehensive literature review to identify and investigate the latest research focusing on remote construction site challenges. The work in this research task can be subdivided into the following subtasks:

Task 1.1: Evaluate methods for quantifying blast effects on remote facilities behind blast walls

The objective of this task is to investigate available blast assessment methods for quantifying blast effects on remote facilities. Furthermore, this task examines feasible blast walls that can be constructed to reduce blast loading on facilities in hostile and remote locations. Blast walls may be rigid, such as steel or reinforced concrete, or frangible, such as sand-filled, water-filled, and wood walls.

Task 1.2: Analyze the consequences of explosive attacks on remote construction sites

The purpose of this task is to analyze the consequences of explosive attacks on remote construction sites. These consequences include fatalities, serious injuries, and minor injuries suffered by site personnel, psychological impacts inflicted on survivors of an explosive attack, direct and indirect economic losses, and degradation of operational or mission capability. Additionally, this task investigates methods to aggregate consequences that have inherently different units of measure into a single consequence score.

Task 1.3: Examine construction site security planning models and best practices

This research task analyzes available security planning models and best practices for the design and construction of remote sites. The areas investigated include criteria for selecting security countermeasures, blast mitigation techniques, and methods to prioritize anti-terrorism upgrade decisions.

Task 1.4: Study the latest research on construction site layout models

The purpose of this task is to review available methodologies for modeling construction site layout planning including heuristics and genetic algorithms. Furthermore, this task will review how each of these methodologies handles the required constraints of construction site layouts including boundary, overlap, and zone conditions.

Task 1.5: Analyze available multi-objective optimization techniques

This task focuses on analyzing available multi-objective optimization techniques that can be used in addressing the unique challenges of remote construction sites. The reviewed multi-objective optimization techniques in this task can be grouped in three main categories: (1) weighted linear and integer programming; (2) genetic algorithms; (3) and nature-inspired metaheuristic algorithms.

1.3.2 Task 2: Develop a Blast Effects Assessment Model

The purpose of this task is to develop a blast effects assessment model capable of efficiently quantifying and visualizing blast effects on constructed facilities behind blast walls. The model is intended to support designers in their critical task of analyzing and comparing all feasible design alternatives in order to select the most effective combination of blast wall type and building material to reduce the security risks to site

personnel and facilities from the threat of an explosive attack. The work in this research task can be subdivided into the following tasks:

Task 2.1: Develop a frangible wall effectiveness metric

In this task, a new metric will be developed to quantify the performance of feasible frangible wall types including sand-filled, water-filled, and wood walls in reducing peak reflected pressure and impulse loading on facilities. Development of this metric includes novel analytical formulae and a set of frangible blast wall effectiveness factors for pressure and impulse.

Task 2.2: Formulate a blast effects assessment model

Formulate a blast effects assessment model to compute an overall facility damage level for constructed facilities behind blast walls. This model will consider design combinations of blast wall type, building material, and facility location for a specified blast charge weight. The model will also generate visualizations that display anticipated facility damage areas based upon blast charge weight, blast wall type, and building material combinations.

Task 2.3: Implement the blast effects assessment model

Implement the developed blast effects assessment model utilizing the Python programming language (Rossum 1995) and the 2-D plotting library matplotlib (Hunter 2007).

Task 2.4: Confirm model performance and evaluate model performance using a case study

First, the accuracy and efficiency of the blast effects assessment model will be confirmed by comparing it to an existing blast damage assessment tool. Next, the model performance will be evaluated, refined, and improved using a case study of a remote construction site.

1.3.3 Task 3: Develop a Facility Protection Optimization Model

This task will focus on developing a multi-objective facility protection optimization model capable of quantifying and minimizing facility destruction levels from explosive attacks while minimizing site construction costs. The model is intended to equip planners of remote construction sites with the capability to efficiently analyze and compare all feasible design alternatives in order to construct remote sites that minimize the destruction levels of site facilities from the threat of explosive attacks in the most cost-effective manner. The work in this research task can be subdivided into the following subtasks:

Task 3.1: Formulate a facility protection optimization model

The purpose of this task is to formulate a multi-objective facility protection optimization model for remote construction sites that is capable of generating optimal tradeoffs between minimizing site facility destruction levels from an explosive attack and minimizing the total site construction cost.

Task 3.2: Identify site layout geometric constraints

The objective of this task is to identify all practical geometric constraints that can be encountered in the planning of remote construction sites, including: (1) site boundary; (2) facility overlap; (3) minimum distance; and (4) maximum distance.

Task 3.3: Implement the facility protection optimization model

This task focuses on implementing the developed facility protection optimization model using multi-objective genetic algorithms.

Task 3.4: Evaluate model performance using a case study

This task evaluates, refines, and improves the performance of the developed facility protection optimization model by analyzing a case study of a hypothetical remote construction site.

1.3.4 Task 4: Develop a Blast Consequence Mitigation Model

The objective of this task is to develop a multi-objective blast consequence mitigation model capable of quantifying and minimizing the consequences of an explosive attack and minimizing the construction costs of remote sites. The model is intended to support designers in their critical task of searching for and identifying optimal remote construction site layouts in order to construct remote sites that minimize the personnel loss, psychological impact, economic loss, and operational impact in the event of an explosive attack while minimizing site construction costs. The work in this research task is organized in the following subtasks:

Task 4.1: Identify explosive attack consequence metrics

In this task, new metrics will be developed to quantify the consequences of explosive attacks on remote construction sites. These metrics include personnel loss, psychological impact, economic loss, and operational impact.

Task 4.2: Formulate a blast consequence mitigation model

Formulate a multi-objective blast consequence mitigation model that is capable of generating optimal tradeoffs between minimizing the consequences of an explosive attack and minimizing the construction costs of remote sites.

Task 4.3: Implement the blast consequence mitigation model

Implement the developed blast consequence mitigation model using the NSGA-2 genetic algorithm (Deb et al. 2002).

Task 4.4: Evaluate model performance using a case study

Evaluate and refine the performance of the developed blast consequence mitigation model using a case study of a hypothetical remote construction site.

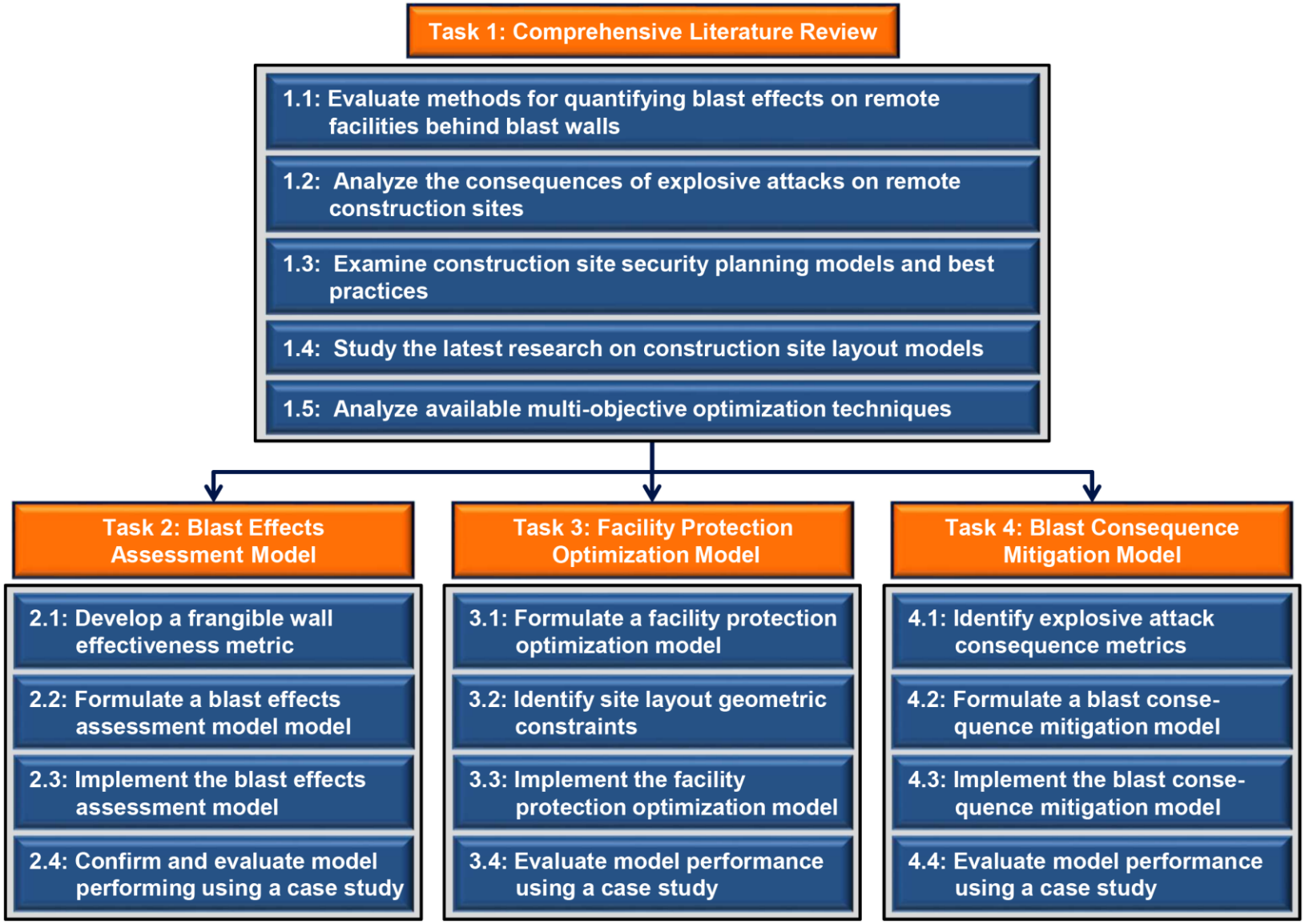

Figure 1.2: Research Methodology

1.4 Research Significance

The developments of this research study are expected to have significant and broad impacts on: (1) quantifying and visualizing blast effects on facilities behind frangible blast walls; (2) minimizing facility destruction levels; and (3) mitigating the consequences of explosive attacks on remote construction sites.

1. Quantifying and visualizing blast effects on facilities behind frangible blast walls

This research study holds a strong potential to improve blast wall and facility design at remote construction sites by developing a model that allows designers to efficiently and accurately analyze and compare the performance of all feasible frangible blast wall types in reducing blast loading on facilities. Furthermore, the model generates visualizations of the anticipated facility damage levels based upon the selected design. These generated visualizations will enable designers to rapidly perform visual risk management assessments of their design scenarios and determine if any design changes are needed to provide the required level of protection for constructed facilities.

2. Minimizing facility destruction levels

The present study is expected to support site layout planners of multi-facility remote construction sites in minimizing facility destruction levels from explosive attacks. The proposed multi-objective optimization model is designed to generate a broad spectrum of Pareto-optimal solutions that represent unique and optimal tradeoffs between the two optimization objectives of minimizing site facility destruction levels and minimizing site construction costs. Accordingly, site layout planners can select the design from the spectrum of Pareto-optimal solutions that best fit the maximum acceptable level of destruction based on the mission of the remote construction site or

complies with the maximum available budget. This capability will result in the construction of cost-effective, high-performance sites that will lower the risks to facilities from the devastating effects of an explosive attack.

3. Mitigating explosive attack consequences

The developed blast consequence mitigation model provides site layout planners with the capability of minimizing explosive attack consequences in remote construction sites while keeping site construction costs to a minimum. The model provides much-needed support for designers and enables them to identify an optimal and cost-effective site layout that minimizes security risks in remote construction sites. This can lead to numerous and significant improvements in the performance of this type of project, including minimized risks of personnel fatalities and injuries, fewer diagnoses of post-traumatic stress disorder among explosive attack survivors, reduced economic losses from damage to facilities, and fewer disruptions to the overall mission of the site.

1.5 Report Organization

The organization of this report and its relation with research objectives, tasks and deliverables is described as follows:

Chapter 2 presents a comprehensive literature review that establishes baseline knowledge of the latest research in: (1) quantifying blast effects on facilities behind blast walls; (2) evaluating and aggregating the consequences of explosive attacks on remote construction sites; (3) analyzing existing models and best practices for improving construction site security; (4) modeling and optimizing construction site layouts; and (5) investigating available decision-making and multi-objective optimization techniques that are capable of addressing the unique challenges of remote construction sites.

Chapter 3 discusses the development of a novel blast effects assessment model capable of efficiently quantifying and visualizing blast effects on constructed facilities behind blast walls. This chapter presents the model in five main stages: (1) blast wall analysis stage that develops a novel analytical formula and a set of effectiveness factors to quantify the performance of feasible frangible blast wall types including sand-filled, water-filled, and wood walls in reducing peak reflected pressure loading on facilities; (2) facility damage assessment stage that computes the percent area of each facility within five specified damage levels in order to calculate an overall facility damage level; (3) blast damage visualization stage that displays anticipated facility damage areas based upon blast charge weight, blast wall type, and building material combinations; (4) model validation stage that confirms the accuracy and efficiency of the developed model; and (5) performance evaluation stage that analyzes the performance of the developed model using a case study.

Chapter 4 displays the development of a multi-objective model for optimizing the site layout and selection of perimeter blast walls and building materials in order to minimize facility destruction levels from explosive attacks while minimizing site construction costs. This chapter presents the model in three main stages: (1) formulation stage that defines the relevant decision variables, formulates the objective functions, and identifies practical model constraints; (2) implementation stage that performs the optimization computations using multi-objective genetic algorithm; and (3) performance evaluation stage that analyzes an application example to evaluate and improve model performance.

Chapter 5 presents the development of a novel multi-objective optimization model for the layout and security planning of remote construction sites that provides the capability of minimizing the consequences of an explosive attack and minimizing the construction costs of remote sites. This chapter presents the developed model in three main stages: (1) consequence identification stage that quantifies the consequences of explosive attacks targeting facilities; (2) formulation stage that identifies the relevant decision variables, formulates the objective functions, and defines all practical constraints; and (3) implementation stage that performs the optimization computations using genetic algorithm and specifies the model input and output data. The performance of the developed model is then analyzed using a case study that is designed to illustrate the use of the model and demonstrate its unique capabilities.

Chapter 6 presents the conclusions, research contributions, and recommended future research of the present study.

CHAPTER 2

LITERATURE REVIEW

2.1 Introduction

A comprehensive literature review has been conducted to establish a firm foundation for the proposed study. The literature review focused on investigating and analyzing the current practices as well as relevant research studies in the security planning of remote construction sites. This chapter summarizes and organizes the reviewed literature in five main sections: (1) quantifying blast effects on facilities behind blast walls; (2) quantifying the consequences of explosive attacks and disasters on facilities; (3) security planning for remote construction sites; (4) construction site layout modeling; and (5) decision-making and optimization techniques.

2.2 Quantifying Blast Effects on Facilities behind Blast Walls

Explosive attacks on constructed facilities are a significant threat worldwide, producing devastating consequences including loss of life, property damages, and economic losses (Wu and Hao 2007; Dillon et al. 2009). In 2014 alone, explosive attacks targeting facilities and infrastructure resulted in 8,024 casualties and $13.1 billion in direct economic losses (Hunter and Perkins 2015; Institute for Economics and Peace 2015). Designers attempt to minimize blast effects on facilities by maximizing the standoff distance between the facility and the likely location of an explosive device, hardening facilities, and/or constructing blast walls to mitigate potential blast effects (Longinow and Mniszewski 1996; Ward 2004; Remennikov and Rose 2007; DoD 2012). In order to analyze and select the most effective design combination of utilizing blast walls and hardening facilities to reduce security risks to site personnel from the threat of

an explosive attack, designers must have accurate methods to quantify blast impacts on facilities behind blast walls. This section discusses a number of studies that were conducted to: (1) predict the impact of blast on facilities; and (2) analyze and quantify the effectiveness of blast walls in protecting facilities from an explosion.

2.2.1 Blast Assessment Methods

Several models were developed to predict the impact of blast on facilities, employing empirical and numerical methods. Empirical methods provide best-fit design curves of experimental data (Goel and Matsagar 2014). These methods consolidated and incorporated extensive experimental blast data into several technical reports and design manuals, including American Society of Civil Engineers Structural Engineering Institute (ASCE/SEI) 59-11 (ASCE 2011), Unified Facilities Criteria (UFC) 3-340-01 (DoD 2002), which superseded Technical Manual (TM) 5-855-1 (USACE 1984), and UFC 3-340-02 (DoD 2008a), which superseded TM 5-1300 (U.S. Dept. of the Army 1990). The equations and design curves presented by Kingery and Bulmash (1984) form the basis of the UFCs above and have also been incorporated into a software system named ConWep (Hyde 1988), which is capable of modeling and calculating blast loads on constructed facilities (Stewart and Netherton 2015). Numerical methods typically utilize computational fluid dynamics to solve mathematical equations of the laws of physics governing the problem such as the conservation of mass, momentum, and energy (Remennikov 2003). Numerical methods can be subdivided into: (a) blast models that predict blast loads on facilities; and (b) coupled analysis models, which are capable of accounting for structural motion as the blast calculation proceeds by combining both blast load and structural response calculations (Ngo et al. 2007).

Examples of blast models are BlastX (Britt et al. 1999), CTH (McGlaun et al. 1990), ProSAIR (ProSAir 2009), SHAMRC (Crepeau 1998) and VAPO (Nichols and Doyle 2014). Coupled analysis models include ABAQUS (Hibbitt, Karlsson & Sorensen, Inc. 2004), AUTODYN (Ansys 2013) and LS-DYNA (LSTC 2016).

2.2.2 Blast Walls

A blast wall is a physical barrier that separates valuable facilities from explosive threats (Smith 2010), as shown in Figure 2.1. Blast walls function by reflecting a portion of the explosive blast energy, thereby reducing peak reflected pressure loading on the facility (Remennikov and Rose 2007). A number of studies conducted live tests and used numerical methods to quantify the effectiveness of blast walls. This section will discuss these experimental methods for both rigid and frangible blast walls.

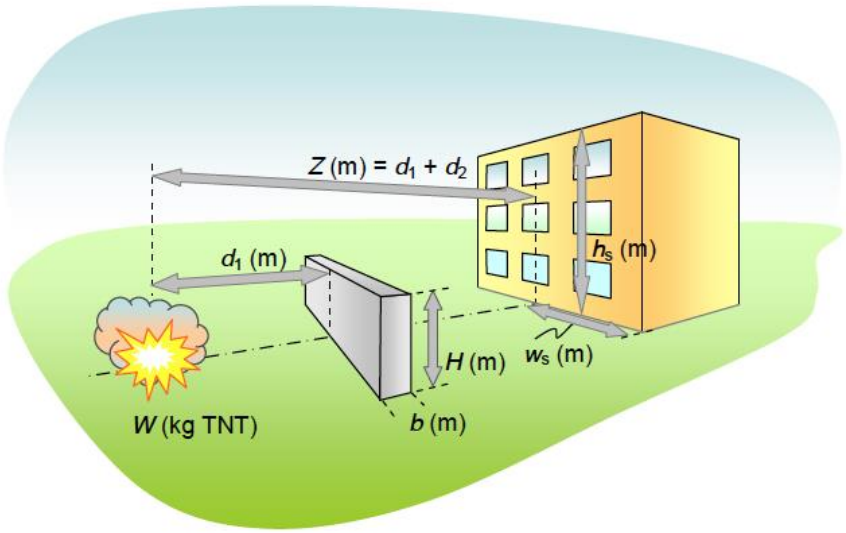

Figure 2.1 Blast Wall Configuration (Bewick et al. 2011)

2.2.2.1 Live Tests

Beyer et al. (1986) and Jones et al. (1987) conducted two of the earliest studies on rigid blast walls. Both studies recorded reflected pressure-time history

measurements behind rigid steel walls to quantify the blast parameters behind a vertical wall and the subsequent reduction in blast loads on a facility. Beyer et al. (Beyer 1986) performed tests on a 1/6th scale, vertical cantilever wall constructed of steel armor plate. The authors tested combinations of three blast charge weights (1, 8, and 15 pounds of spherical C4) and three blast wall designs. Jones et al. (1987) simulated vehicle-borne improvised explosive device (VBIED) attacks on a facility by conducting live tests on 1/10th scale models of a rigid steel wall. Appropriately scaled charges, representing the most probable security threats faced by designers, were detonated at various standoff distances from the model facility.

In response to frequent VBIED attacks on facilities in Northern Ireland, researchers from Cranfield University at the Defence Academy of the United Kingdom conducted a series of live test experiments on rigid steel walls. Rose et al. (1995) performed 1/10th scale tests on a plane, non-deforming steel wall. Pressure-time histories were measured in a grid of locations behind the wall and results were presented as contour plots of peak pressure and scaled impulse at increments of “wall heights” from the wall. This study demonstrated that a plane, non-deforming steel wall significantly reduces the pressure and impulse behind a wall out to approximately six wall heights.

Seeking to expand the work conducted by Rose et al. (1995), Chapman et al. (1995a) performed experiments on steel walls to quantify the impact that considering additional design parameters, namely the distance from the blast to the blast wall, would have on altering blast loads on facilities behind blast walls. The authors were able to

develop a “protection factor” based upon the resulting pressure-time history contour plots as functions of the geometric parameters shown in Figure 2.2.

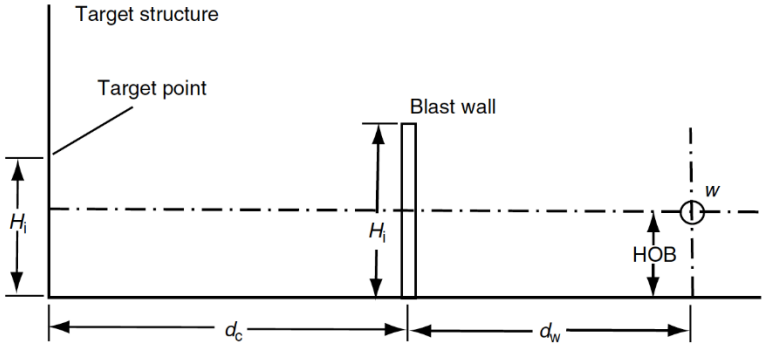

Figure 2.2 Geometrical Parameters Included in a “Protection Factor” (Chapman et al. 1995a)

Several design charts from the work of Chapman et al. (1995a) were published in Rose et al. (1997). The design charts plotted peak overpressure (kPa) and peak scaled impulse (kPa ms/kg$^{1/3}$) versus scaled distance (standoff distance/blast charge weight$^{1/3}$) at various heights on the protected facility for selected ratios of distance from the blast to the wall and distance from the wall to the protected facility. It is worth noting that the results of these scale model experiments correlated well with the full-scale experiments conducted by Hulton et al. (1995), thereby validating the scale model approach to blast wall experiments.

Live tests were also conducted on blast walls constructed of non-rigid or frangible materials. Rose et al. (1998) concluded the Cranfield University blast wall research stream by performing a series of 1/10th scale tests on seven different materials (sand-filled containers, balsa wood, polystyrene, polythene, revetting fabric, water-filled and ice walls) in 23 experimental configurations. The different configurations served to compare variations in wall geometry, height, thickness, and stabilization method. The tests were conducted by detonating a 57g spherical charge of Demex explosive

(equivalent to 75g TNT) at a distance of 138mm from the wall and a height of 109mm above the ground. Peak pressure and peak scaled impulse measurements were recorded at four distances between 1.35 and 1.8m behind the wall. The results of the study showed that frangible materials provide comparable and often greater reductions in blast loading than rigid walls.

Bogosian and Piepenburg (2002) performed a series of 35 live tests, analyzing the effectiveness of rigid concrete walls as well as four frangible wall types: concrete masonry units (CMUs), thin precast concrete panels, thin water, and thick water. The authors developed a frangible wall effectiveness factor (EF), which is defined as the ratio of the pressure or impulse behind a frangible blast wall divided by the same metric behind a rigid blast wall, as shown in Eqs (2.1)-(2.2). Each test series measured EF_p values at several scaled heights on the building. In order to create a more useable metric, a single EF_p value was calculated for each frangible wall type by consolidating and averaging the effectiveness factors over all building elevations. Experimental results showed that all four frangible wall types performed better than the rigid concrete wall with regard to mitigation of pressure. For mitigation of impulse, the CMU, thin precast concrete panels, and thick water walls performed better than the rigid concrete wall, while the thin water wall performed worse than the rigid concrete wall.

$$EF_P = \frac{P_{frangible}}{P_{rigid}} \tag{2.1}$$

$$EF_I = \frac{I_{frangible}}{I_{rigid}} \tag{2.2}$$

where,

EF_P = frangible wall effectiveness factor for pressure;

$P_{frangible}$ = blast pressure behind a frangible wall (kPa);

P_{rigid} = blast pressure behind a rigid wall (kPa);

EF_I = frangible wall effectiveness factor for impulse;

$I_{frangible}$ = blast impulse behind a frangible wall (kPa-ms); and

I_{rigid} = blast impulse behind a rigid wall (kPa-ms).

Two recent research efforts have performed live tests with numerical simulations. The purpose of the live tests was to calibrate the developed numerical models, which could then be used to run additional simulations without the inherent expense or safety concerns associated with live tests. Scherbatiuk and Rattanawangcharoen (2008) executed three full-size tests on soil-filled HESCO Bastion concertainers, a prefabricated unit, made of galvanized welded steel mesh lined with non-woven polypropylene geotextile. Chen et al. (2015) performed nine in-situ experiments on scale-size water walls in an explosion chamber. Both research studies utilized LS-DYNA (LSTC 2016) to develop their numerical simulations. Scherbatiuk and Rattanawangcharoen (2008) developed a finite element model capable of predicting displacement-time histories of soil-filled concertainers subjected to blast loading. Chen et al. (2015) utilized their numerical simulation to derive empirical formulae capable of predicting the blast environment behind water walls.

2.2.2.2 Numerical Methods

Numerical methods were also used to quantify the effectiveness of blast walls. For example, Chapman et al. (1995b) utilized AUTODYN2D (Ansys 2013) to analyze the simulation of blast waves over protective barriers. The authors recorded high correlation between the simulation data and the experimental results from Rose et al.

(1995). This work demonstrated that numerical simulation methods can accurately simulate blast wave and blast wall interactions in both simple and complex geometries in two dimensions.

Ngo et al. (2004) used LS-DYNA (LSTC 2016) and Air3D (2001) to produce three-dimensional visualizations of the complex flow of a blast wave propagating over a wall. Their study aimed to visualize the effectiveness of blast walls for a range of standoff distances, wall heights, and geometries.

Rickman et al. (2006) conducted a series of small-scale experiments and employed SHAMRC simulations (Crepeau 1998) to examine the effect of wall height, charge-to-wall distances, and charge-to-facility standoff distances on the shielding capability of blast walls. Their analysis yielded four main conclusions. First, all barriers, even relatively short ones, can significantly reduce the peak reflected pressures on facilities behind the wall. Second, blast walls may provide significant protection for facilities that are taller than the walls themselves. Third, blast walls can still provide significant protection for facilities at relatively large wall-to-facility distances. Fourth, the primary source of protection provided by blast walls is likely from the slowing of the air shock wave as it diffracts over the blast wall toward a facility.

As the quality of numerical simulations matured and the capability of blast walls to significantly reduce blast loads on facilities was confirmed, the emphasis of research studies shifted to quantifying blast wall effectiveness based upon individual design scenarios. The focus was on developing adjustment factors capable of quantifying the reduction in peak reflected pressure and peak impulse on facilities behind blast walls. The earliest paper to introduce this concept was Rose et al. (1995), with the

development of pressure and improvement benefit factors. The remaining papers in this section used various methods to quantify blast wall adjustment factors based upon a number of input factors.

Remennikov and Rose (2007) and Bewick et al. (2011) utilized both test data from live scaled experiments and numerical simulation data to train artificial neural networks (ANNs) to predict the area of effectiveness behind a blast wall and subsequent blast loads on structures. The purpose of the research was to develop stand-alone, fast-running tools capable of quantifying pressure and impulse adjustment factors based upon blast charge weight, blast wall height, wall-to-facility distance, charge-to-facility distance, and height on the building. The pressure and impulse adjustment factors are defined as the ratio of reflected pressure or impulse behind a blast wall to the original pressure or impulse when no wall is present, as shown in Eqs. (2.3)-(2.4). For example, a pressure adjustment factor of 0.4 represents a 60% reduction in pressure behind a wall compared to a no-wall configuration. The advantage of using ANNs to predict blast wall adjustment factors is the ability to obtain accurate results in significantly less time than methods requiring complex numerical computational fluid dynamics (CFD) simulations. The disadvantages of using ANNs to predict blast wall adjustment factors is acquiring the amount of validated test data that is needed to train the ANN. Further, while extremely capable, these ANNs still do not realize the level of flexibility that exists with numerical CFD simulations.

$$AF_P = \frac{P_{wall}}{P_{no\ wall}} \tag{2.3}$$

$$AF_I = \frac{I_{wall}}{I_{no\ wall}} \tag{2.4}$$

where,

AF_P = pressure adjustment factor for a blast wall;

P_{wall} = blast pressure behind a wall (kPa);

$P_{no\ wall}$ = blast pressure with no wall (kPa);

AF_I = impulse adjustment factor for a blast wall;

I_{wall} = blast impulse behind a wall (kPa-ms); and

$I_{no\ wall}$ = blast impulse behind a rigid barrier (kPa-ms).

Zhou and Hao (2008) developed “pseudo-analytical” formulae to estimate the reflected pressure-time histories on a facility behind a blast wall. These formulae were developed as best-fit curves of AUTODYN3D numerical simulations (Ansys 2013). They are expressed in terms of the following parameters: blast charge weight (W), distance from the explosion to the facility (D), facility height (H_B), the height of the gauge point on the facility (H_e), blast wall height (H_1), and the ratio of the distance between the blast wall and the explosion to that between the facility and the explosion (L_1/D), as shown in Figure 2.3. The formulae can be combined with existing design manuals, such as UFC 3-340-02 (DoD 2008a), to predict blast loading on facilities behind a rigid wall.

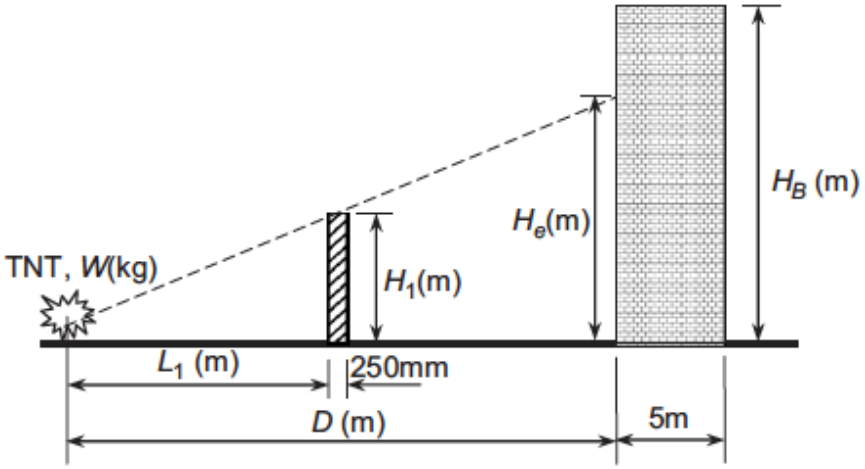

Figure 2.3 Problem Configuration (Zhou and Hao 2008)

2.2.3 Limitations of Available Blast Models and Blast Wall Research Studies

Despite the significant contributions of the aforementioned research studies and blast models, they are incapable of: (1) efficiently predicting the performance of all feasible blast wall and building material design alternatives due to the significant computational time and effort required by numerical blast assessment models to analyze each possible combination of blast wall type, building material, and facility location (Bogosian et al. 2002; Sorensen and McGill 2012); (2) quantifying the effectiveness of feasible frangible blast wall types including sand-filled, water-filled, and wood walls in reducing peak reflected pressure loading on facilities; and (3) visualizing the anticipated facility damage areas based upon blast charge weight, blast wall type, and building material combinations. Accordingly, there is an urgent need for a novel model that is capable of efficiently quantifying and visualizing blast effects on facilities behind blast walls of various materials in order to support designers in their critical task of identifying the most effective design for blast walls and facility hardening.

2.3 Quantifying Consequences of Explosive Attacks and Disasters

Explosive attacks targeting remote construction sites, such as oil production facilities and military forward operating bases, cause devastating consequences. The magnitude of these consequences has significantly increased in recent years. During a five-year period from 2011-2015, explosive attacks targeting facilities and infrastructure resulted in more than 45,000 casualties and $73 billion in direct economic losses worldwide (Hunter and Perkins 2015; Institute for Economics and Peace 2015; Perkins 2015). Furthermore, the post-traumatic stress disorder (PTSD) rate among victims of explosive attacks is reported to be as high as 40% (Neria et al. 2008). The Federal Emergency Management Agency (FEMA) groups explosive attack consequences into four primary categories: personnel loss, psychological impact, economic loss, and operational impact (FEMA 2011). The following sections present the most relevant and recent research on these consequences as well as methodologies to aggregate various consequence types into a single combined consequence value.

2.3.1 Personnel Loss

Personnel loss measures the extent of fatalities, serious injuries, and minor injuries suffered by victims of explosive attacks. Trauma from explosives is traditionally divided into three groups: primary, secondary, and tertiary injuries.

Primary blast injuries occur when the force of the blast overpressure or shock wave causes direct tissue damage (Wolf et al. 2009). Explosive tests indicate that human blast tolerance varies by both the magnitude of the shock wave and the shock duration, i.e. the pressure tolerance for short-duration blast loads is significantly higher than that for long-duration blast loads. For example, for a short-duration blast of 3-5 ms,

50 percent of personnel are expected to suffer eardrum rupture, lung damage, and lethality at 15 psi, 80 psi, and 130-180 psi, respectively (DoD 2008a).

Secondary blast injuries occur when a person is struck by debris that is displaced by the blast overpressure or winds, such as glass, ball bearings, nails and rocks. This flying debris causes a combination of penetrating and blunt trauma. Because debris fragments can travel much greater distances than the blast shock wave, secondary injuries are more frequent than primary injuries and can occur in individuals hundreds to thousands of meters from the explosion's epicenter (Wolf et al. 2009).

Tertiary blast injuries are caused when a person is physically displaced by the force of the blast shock wave and strikes an object. Examples of tertiary injuries include blunt head trauma, blunt abdominal trauma, tissue contusions, and fractures. Furthermore, the risk of tertiary injuries is exacerbated by the collapse of buildings or surrounding structures. Consequently, tertiary injuries result in the highest level of mortality among blast victims (Wolf et al. 2009).

Researchers have performed epidemiological studies to examine the causes and extent of the most prevalent injury types, including severe head trauma, (Mellor 1992; Mallonee et al. 1996; Wightman and Gladish 2001), damage to the ears (Garth 1995; Cave et al. 2007), eyes (Abbotts et al. 2007; Morley et al. 2010), and lungs (Stuhmiller et al. 1996; Avidan et al. 2005; Sasser et al. 2006), as well as injuries from flying glass debris (Norville et al. 1999; Thompson et al. 2004; Ataei and Anderson 2012).

2.3.2 Psychological Impact

Psychological impact measures the frequency and severity of emotional and psychological disorders among survivors of explosive attacks. The psychological

impacts of explosive attacks encompass a range of emotional, behavioral, and cognitive reactions including: (1) distress responses, such as insomnia and increased feelings of anxiety or anger; (2) behavioral changes, like avoiding air travel or increasing alcohol consumption; and (3) psychiatric illnesses, such as post-traumatic stress disorder (PTSD) or clinical depression (Butler et al. 2003). The majority of psychological impact studies focused on analyzing the causes, frequency, and severity of PTSD because it is the best-defined and one of the most frequent and debilitating psychological disorders experienced in the aftermath of explosive attacks (Gabriel et al. 2007; Neria et al. 2008).

Researchers have conducted applied epidemiological studies on victims of a number of historical terrorist attacks, including the Oklahoma City bombing (North et al. 1999, 2002), September 11, 2001 attacks on New York City (Schuster et al. 2001; Galea et al. 2002; Schlenger et al. 2002), 2004 Madrid train bombing (Gabriel et al. 2007; Vázquez et al. 2008), and French bombings of 1982-1987 (Abenhaim et al. 1992) and 1995-1996 (Verger et al. 2004). These studies show that injured survivors, uninjured survivors, first responders, and residents of the local area around an attack frequently experience symptoms of PTSD. Furthermore, injured survivors of explosive attacks experience the highest reported rates of PTSD, normally ranging from 30-40%, while 10-20% of first responders suffer PTSD, and 5-10% of uninjured survivors and local residents are inflicted with PTSD.

2.3.3 Economic Loss

Economic loss measures the total financial cost inflicted on a site by an attack and is the sum of direct losses and indirect losses. Direct losses include all damage to fixed assets, capital, inventories, raw materials, and spare parts. Indirect losses

represent the flow of goods that will not be produced and services that will not be provided by the damaged facility (Pelling et al. 2002). Indirect losses can far exceed the direct losses of an explosive attack (Kazimi and Mackenzie 2016). Examples of indirect loss include increased unemployment, decreased property values, reduction in travel and tourism, and reduction in foreign direct investment and trade (Enders and Olson 2012; Rose 2009).

Studies have analyzed and differentiated between the macroeconomic (Blomberg et al. 2004; Enders and Olson 2012) and microeconomic costs (Enders 2007), and between the direct (Dillon et al. 2009) and indirect costs (Kazimi and Mackenzie 2016) of attacks. Furthermore, researchers have developed frameworks that integrate a site's economic resilience and behavioral linkages in estimating total losses from an attack (Rose 2009; Rose and Blomberg 2010).

2.3.4 Operational Impact

Operational impact measures the level of mission degradation on a site resulting from the downtime of critical facilities damaged by a disaster or explosive attack. Mission degradation is a function of the downtime of a damaged facility and the importance of a facility to the overall site mission.

Several studies have investigated the downtime of damaged facilities following disasters, such as earthquakes (Comerio 2000; Pachakis and Kiremidjian 2004; Porter and Ramer 2012), damaging snow loads (Strobel and Liel 2013), and hurricanes (Bailey and Levitan 2008). Two of the most significant studies regarding facility downtime are Comerio (2006) and Comerio and Belcher (2010). Comerio 2006 estimates facility downtime following a disaster by considering both rational and irrational components.

Rational components include the construction cost to repair the damaged facility and the time needed for construction. Irrational components are situationally specific and include the time needed to secure financing and mobilize for repairs, and the availability of qualified workers to perform the repairs. The author then presented a simplified method for estimating facility downtime based upon total facility area and facility damage level. Building on this study, Comerio and Belcher (2010) analyzed the impact of several other factors on facility downtime, including facility area, number of units, and facility height. The authors found no statistical significance that any of these factors had a significant impact on facility downtime. The authors concluded that modeling facility downtime requires the incorporation of three critical elements: (1) an estimate of construction repair time for the damaged facility; (2) an estimate of project mobilization time; and (3) a representation of the economic conditions within the region at the time of the event.

Two primary methods have been developed to calculate the importance of individual facilities to the overall site mission. The first method was developed to prioritize infrastructure projects at the Massachusetts Institute of Technology (Karydas and Gifun 2006). The model utilizes multi-attribute utility theory and the analytical hierarchy process to prioritize facilities based on 16 criteria, including minimization of risk, optimization of economic impact, and coordination with applicable policies, programs, and operations. The second method was developed to determine infrastructure criticality for the United States Navy (Antelman et al. 2008). This method has since been adopted and tailored to meet the specific programming needs of the other branches of the United States Department of Defense, including the United States

Army (Grussing et al. 2010). Antelman et al. (2008) developed the scoring methodology for a facility's mission dependency index (MDI), which represents the percentage that the overall site operations will be degraded if the facility is unable to perform its primary function. MDI is calculated by assigning scores from a scoring matrix based upon designers' answers to questions designed to assess the: (a) length of time a facility can be inoperable before having an adverse impact on the site mission; (b) ability of another facility to perform the mission of the damaged facility; and (c) difficulty to replace the services provided by the damaged facility. MDI is measured on a normalized scale of 0% to 100%, with 100% representing facilities the highest risk to the site mission.

2.3.5 Consequence Aggregation Models

Several research studies have developed frameworks to quantify and aggregate the consequences of disasters and explosive attacks. For example, Ayyub et al. (2007) and McGill et al. (2007) created quantitative methods for performing critical asset risk analysis based upon five consequence types: casualty, economic, mission disruption, environmental damage, and recuperation time. To calculate these five consequence types, McGill et al. (2007) recommended using system modeling techniques and subject matter experts to estimate consequences, while Ayyub et al. (2007) assumes the severity of consequences follows a normal distribution within three pre-defined damage levels. Both studies utilized conversion factors to aggregate the five consequences into a single measure of monetary loss; however, their methodology to calculate these consequences for a specific threat was reported to be limited by Dillon et al. (2009) due to its inability to consider the risk tolerance levels of owners and designers. To address this reported limitation, Dillon et al. (Dillon et al. 2009) utilized multi-attribute utility

theory to calculate a single consequence score as the weighted sum of mission, personnel, and economic impacts, where weights represent the importance of each consequence type to site owners and the shape of utility curves reflects owner risk tolerance.

2.3.6 Limitations of Available Disaster Consequence Quantification Models

Despite the significant contributions of the aforementioned consequence quantification models, they are incapable of: (1) efficiently quantifying the consequences of explosive attacks because they rely on the use of time-consuming external blast analysis software packages; (2) evaluating the impact of serious and minor injuries on total personnel losses; (3) quantifying the extent of psychological impacts on survivors of explosive attacks; and (4) measuring the impact of explosive attacks on the operational capacity of the site in terms of the total number of days the site is unable to perform its primary mission. Accordingly, there is an urgent need for the development of a novel model that is designed to overcome these four limitations of existing models.

2.4 Security Planning for Remote Construction Sites

A number of security planning models have been developed to assist designers in selecting security measures and procedures to minimize the risks from threats faced on remote construction sites. This section highlights the most relevant and recently developed heuristics and optimization-based security models.

2.4.1 Heuristics Security Models

Grassie et al. (1990) proposed a six-step structured countermeasures selection process to assist design engineers in implementing a cost-effective approach to site security. The six steps are: (1) identify all assets to be protected; (2) determine asset

criticality; (3) identify potential threats; (4) ascertain likely modes of attack; (5) determine asset vulnerability based upon attack severity; and (6) select protection required when considering financial and operational constraints. The design team then concentrates on developing asset, facility and site-specific countermeasures that are physical, electronic, operational, or procedural in nature. Countermeasures are then selected based upon their cost effectiveness, which considers the operational impact, vulnerability reduction, and the cost of operation including installation, lifecycle operations and maintenance, and savings in security manpower over the life of the system.

Longinow and Mniszewski (1996) analyzed the interaction between air blasts and building structures in an effort to identify potential design changes and security guidelines that could be followed to minimize the damages and casualties caused by vehicle bombs. Using the bombings of the World Trade Center (1992) and the Alfred P. Murrah Federal Building (1995) as case studies, the authors investigated vehicle bomb damage and casualty mechanisms, building structural systems that are capable of resisting progressive collapse, and nonstructural building components and building systems that are able to reduce secondary damages such as those caused by flying debris. They concluded that it is impractical to either design conventional buildings to withstand the effects of a close-in blast or to retrofit existing buildings against blast. Rather, the authors stated that a strong perimeter fence at a sufficient distance from the building provides the greatest defense. Six design guidelines were provided to establish the recommended perimeter including providing the maximum possible standoff distance, creating redundancy in protection measures, and constructing a robust, well-lit fence, capable of completely denying or sufficiently delaying unauthorized site access.

Hicks et al. (1999) utilized Cost and Performance Analysis (CPA), which is the integration of Activity Based Cost (ABC) estimating and performance-based analysis, to evaluate physical protection systems effectiveness. Cost estimation was performed with Cost Analysis Tool for Security Systems (CATSS), a tool that is built around Automated Cost Estimating Integrated Tools (ACEIT), an existing Department of Defense tool that supports a full lifecycle cost analysis, from procurement to decommissioning. Performance analysis was completed via PERFORM, which is the integration of two existing tools, Analytic System and Software for Evaluating Safeguards and Security (ASSESS), a Department of Energy software designed to assess the performance of physical protection systems of nuclear assets, and Joint Tactical Simulation (JTS). System effectiveness is defined as the probability of interruption, P(I), multiplied by the probability of neutralization, P(N) for each attacker and response combination. P(I) is a function of detection probabilities and delay times of the attackers and the response time of security personnel. The overall model objective is to compare the costs of physical protection system components with probabilistic methods of performance in order to facilitate operational and strategic management decisions.

Little et al. (2002) proposed a simplistic decision framework for security and natural hazard risk mitigation. The decision framework identifies the maximum level of damage to be tolerated for a facility based on its risk groups and design event magnitudes. The maximum level of damage to be tolerated can be mild, moderate, high or severe, as shown in Table 2.1. Based upon the identified tolerable level of damage, decision makers recommend the required upgrade measures for the facility. For example, a small, unoccupied storage facility that is not critical to a site's operations

may be assigned into risk group I, which represents buildings that require lower levels of protection. If the threat assessment and risk analysis identifies a high probability of a very large event, such as a 5,000-pound vehicle bomb, the chart shows that a severe amount of damage could be tolerated on the storage facility. Conversely, a critical facility assigned to risk group IV would only be able to tolerate moderate levels of damage in a very large event. Depending on the risk group and anticipated design event magnitude in this example, upgrade measures would need to be identified and constructed in order for the risk group IV category building to only experience moderate levels of expected damage.

Table 2.1 Maximum Level of Damage to be Tolerated Based on Risk Groups and Design Event Magnitudes (adapted from Little et al. 2002)

		RISK GROUPS INCREASING LEVEL OF RISK →			
		Risk Group I (Prot. Level Low)	**Risk Group II** (Prot. Level Medium/Low)	**Risk Group III** (Prot. Level Medium)	**Risk Group IV** (Prot. Level Higher)
MAGNITUE OF DESIGN EVENT (TACTIC) INCREASING MAGNITUDE OF EVENT	**VERY LARGE** (Very Rare) (Higher Risk)	**SEVERE**	**SEVERE**	**HIGH**	**MODERATE**
	LARGE (Rare) (Medium Risk)	**SEVERE**	**HIGH**	**MODERATE**	**MILD**
	MEDIUM (Less Frequent) (Med/Low Risk)	**HIGH**	**MODERATE**	**MILD**	**MILD**
	SMALL (Frequent) (Low Risk)	**MODERATE**	**MILD**	**MILD**	**MILD**

Dillon et al. (2009) developed an anti-terrorism risk-based decision aid (ARDA) to prioritize anti-terrorism upgrade measures of existing facilities. The framework considered 15 potential attack modes, from hostage situations to chemical warfare agent attacks, and 160 existing facility types. Total potential consequences of an attack were calculated as the weighted sum of mission impact, personnel loss, and economic

loss. Weights are defined through project managers' utilization of the multi-attribute utility theory. Upgrade decisions are then made based upon a reduction in risk versus cost ratio. While this model does provide a standardized and organized method by which to prioritize upgrade measures of existing facilities, it does not consider the cost investment for mitigation alternatives. Additionally, this model cannot be directly applied to new construction.

2.4.2 Security Optimization Models

Khalafallah and El-Rayes (2008) investigated the security risks associated with the planning of airport expansion projects. The authors developed a multi-objective optimization model capable of simultaneously minimizing construction-related security breaches and minimizing site layout costs, while complying with all Federal Aviation Administration (FAA) guidelines. Security decision variables included security response distances and physical security measures. The physical security measures include both FAA-required items such as physical barriers (e.g. fences) and access control systems (e.g. keypad entry and fingerprint scan) and three FAA-recommended items: (1) anti-intrusion systems such as CCTV and motion detectors; (2) detection technologies such as x-ray scanning and explosives detection; and (3) security lighting systems. Using a weighted-average approach, the authors combined two criterions, Security Response Distance Criterion (SRDC) and Security Systems Criterion (SSC) into a combined Construction-Related Security Level (CRSL). Costs are a product of the security systems and the travel costs of resources, which are based on the following three factors: (1) planned travel frequency of crews; (2) crew hourly cost rate; and (3) average speed of travel (El-Rayes and Khalafallah 2005). The model only considers security

breaches from an aggressor reaching a targeted facility. It does not consider explosive threats at the site perimeter.

Said and El-Rayes (2010) developed an automated multi-objective optimization framework that provides the capability to: (1) minimize site security risks; and (2) minimize overall site costs. The security threat analyzed in this model was the threat of theft or destruction of classified materials in the targeted facility, a Sensitive Compartmented Information Facility (SCIF). The model utilized the Crime Prevention through Environmental Design (CPTED) theory (Crowe 2000), relying on a combination of natural surveillance, target hardening and lighting to deter criminal acts. The considered countermeasures consisted of security lighting, fencing, intrusion detection systems, security guard response forces, and natural surveillance. The site consisted of three layers: (1) site fence; (2) site grounds; and (3) target fence, and the model considered both security and layout decision variables over multiple phases of construction. Facilities were characterized as fixed, moveable or stationary, which for practical purposes, are considered fixed due to the excessive cost of relocation (e.g. cranes). Costs included security system costs and layout costs (resource travel costs and facility relocation costs over the phases of construction). The probability and consequence of a potential attack was a product of the attacker intrusion speed and response time of security personnel. Attacker intrusion speed considered delays from all site security countermeasures including the delay inflicted by the site fence, site grounds, target fence, and target buffer (distance between target fence and targeted facility). The security system effectiveness was calculated based on the probability of interruption, a deterrence index, and the probability of detaining the attacker. Site

security risks were limited to an individual reaching one targeted facility. There was no consideration of the risk of explosive. As a result, the choice of building materials or facility hardening was not considered.

Li et al. (2015a) utilized a multi-objective, bi-level Particle Swarm Optimization Algorithm (MOBLPSO), to address security planning in a dynamic construction site layout scenario. The proposed scenario is bi-level as the project manager and attacker are involved in a Stackelberg game (Simaan and Cruz Jr 1973). The upper-level programming is based on the decisions of the project manager in seeking two objectives: (1) minimize the efficiency consequence of a facility system, measured by the reduction in operational efficiency of a facility following an attack; and (2) minimize the site layout cost, security system cost, and economic consequences of a potential attack. To quantify economic and efficiency consequences, the model employed twofold random uncertainty, that is, the use of random variables with random parameters. The lower-level programming denotes the decision of the attacker, who will attempt to destroy a subset of facilities that will result in the greatest economic consequences. As a result, the model can consider potential attackers' strategies.

2.4.3 Limitations of Available Security Models

Despite the significant contributions of the aforementioned security models, there is no reported research that focused on: (1) minimizing the consequences of explosive terrorist attacks on remote construction sites; and (2) generating a set of optimal combinations of site layout solutions and protection strategies that provide optimal tradeoffs between minimizing the consequences of explosive attacks and minimizing site construction costs. Accordingly, there is a pressing need for a novel multi-objective

blast consequence mitigation model for remote construction sites that is capable of overcoming these limitations of existing models.

2.5 Construction Site Layout Planning Models

The primary purpose of site layout planning is to allocate site space to resources so that they can be accessible and functional during construction (Zouein and Tommelein 1999). Optimizing site layouts can assist in achieving multiple objectives such as minimizing resource transportation and facility relocation costs (Zouein and Tommelein 1999; Mawdesley et al. 2002; Tam et al. 2002), improving site safety (Elbeltagi et al. 2004; El-Rayes and Khalafallah 2005), and minimizing site security risks (Khalafallah and El-Rayes 2008; Said and El-Rayes 2010; Li et al. 2015a). Site layout models can also be static (one phase) or dynamic (multiple phases of construction). The following sections discuss several methodologies used in the literature to accomplish site layout planning tasks.

2.5.1 Heuristics

Zouein and Tommelein (1999) approached the problem of dynamic site layout planning with a combination of constraint satisfaction, heuristics, and linear programming. The model objective is to minimize total cost, which is the sum of transportation and relocation costs. Resources are represented as rectangles in a two-dimensional space. The facility centroid, its dimensions, and its orientation identify the location of each facility. A series of hard constraints determine which positions are acceptable and soft constraints gauge the quality of the layout. Resources are analyzed one at a time and a position is selected for each resource based upon two heuristics: (1) resources with the largest relocation weights; and (2) resources with the greatest

interaction with other positioned resources. Tiebreaker heuristics are also identified, if required. A linear program is then used to minimize overall costs. The main limitation of the system is that layouts are selected chronologically, meaning earlier optimized layouts cannot be reanalyzed. As a result, the system cannot achieve global optimality.

Tam et al. (2002) analyzed a site layout-planning problem using nonstructural fuzzy decision support system (NSFDSS). NSDFSS consists of three steps: (1) decomposition, which is breaking the problem down in a hierarchal fashion; (2) conducting pairwise comparisons on a three-point scale (better, the same, or worse); and (3) synthesis of priorities that combines decision criteria with weighting factors. The authors claim that their method offers three advantages over the traditional analytical hierarchy process (AHP): (1) a simplified comparative rating scale (1, 0.5, and 0) in evaluating the relative importance of decision criteria; (2) built-in consistency checking by placing a greater level of reliability on higher rows and automatically resetting the values of lower rows if inconsistencies are found; and (3) elimination of consistency deviation by providing absolute consistency during evaluation. The data is then arranged in matrix form to display comparison and score assignment. Project managers can then use the priorities identified by the NSFDSS to aid in decision making. The authors reported two main limitations in this model: (1) decisions and comparisons are still not automated although the process is less labor intensive than AHP; and (2) quality of results is highly dependent on the knowledge and expertise of the project management team.

2.5.2 Genetic Algorithms

Mawdesley et al. (2002) utilized an augmented genetic algorithm to model the cost to move and position temporary facilities on a construction site over time. A user-defined grid system was established to create potential locations within site boundaries. Facilities are assumed to be rectangular and are represented by coordinates of two opposite corners. The model allows for user-defined minimum and maximum interfacility distances. There are three sources of costs considered in this model: (1) the cost to setup a facility; (2) the cost to remove a facility; and (3) the cost of transporting materials between locations. Minimum travel distances can be calculated using either Manhattan (follows only axis-aligned directions) or Euclidean (straight line between two points) geometry. Additionally, the model allows for varying site conditions and can account for unequal transportation costs in north-south, south-north, east-west, and west-east directions. The authors identify two primary limitations of their model: (1) its sensitivity to the relative costs assigned to facility setup and material transport; and (2) modeling the dynamic nature of a project by considering the site layout to be correlated with the work phases.

Elbeltagi et al. (2004) developed a GA that was able to consider the effects of safety in dynamic layout planning. The model aimed to minimize distances between facilities for the purpose reducing resource travel costs, but only to the extent that it did not move facilities into unsafe zones around high-risk buildings. The authors adapted existing closeness relationships from Malakooti (1987) and introduced large negative values when safety concerns arose between two facilities. The model was built into Excel using macros, which allowed for linking to widely used scheduling software.

Furthermore, model results can be exported to Geographical Information System (GIS) to automate site mapping.

While many other studies have investigated the optimization of construction site layout planning, considering security of critical infrastructure projects as an objective has been limited to only a few studies, namely Khalafallah and El-Rayes (2008) and Said and El-Rayes (2010). The main limitation of these studies is that they only consider the security risk of human breaches, not the risk of explosive attacks. As both of these papers were discussed in section 2.4.2 above, the discussion of these papers in this section will focus on their facility layout component.

Khalafallah and El-Rayes (2008) developed a multi-objective genetic algorithm capable of minimizing construction-related security breaches while keeping the site layout costs of airport expansion projects to a minimum. The location of temporary facilities such as security fences, site offices and hazardous material storage facilities affect numerous aspects of this model including: (1) the response distances required by security personnel; (2) the buffer zone sizes between secure areas and temporary facilities; and (3) the travel costs of resources. The travel costs of resources are estimated based on the planned travel frequency of crews, the crew hourly cost rate, and the average speed of travel (El-Rayes and Khalafallah 2005). In order to perform the optimization, project planners must provide the dimensions of each temporary facility, the available options for temporary fence placement, the location and dimension of each secure facility on the construction site and the recommended security response distances between secure areas. The output of the model includes identifying the

optimal location of temporary facilities and the security fence and the optimal utilization of security control systems in order to achieve the aforementioned objectives.

Said and El-Rayes (2010) developed an automated multi-objective optimization framework, using genetic algorithm, to simultaneously minimize the site security risks and minimize the overall site costs associated with the construction of critical infrastructure projects. The main security threat in this model was the theft or destruction of classified materials located in a Sensitive Compartmented Facility (SCIF). The construction site was separated into three layers: (1) site fence; (2) site grounds; and (3) target fence. Additionally, multiple phases of construction were considered, potentially requiring the relocation of temporary facilities and construction materials. The model is designed to dynamically position all temporary facilities and relocate moveable facilities in each stage of the project. Facility location impacts the length of an attacker's intrusion path (which impacts the likelihood of a successful attack), the degree or amount of natural surveillance, and site layout costs, which are the sum of resource travel costs and facilities relocation costs. Analogous to Zouein and Tommelein (1999), the facilities are represented by their centroid, dimensions and orientation. Four types of geometric constraints must be satisfied in order to successfully place a facility within the site boundary: 1) boundary; 2) overlap; 3) distance; and 4) zone constraints (El-Rayes and Said 2009). The model generates an optimal combination of security measures and facility positions over multiple phases of construction to minimize site security risks and to minimize overall site costs.

2.6 Multi-objective Optimization Techniques for Remote Construction Sites

This section presents a number of available multi-objective optimization techniques for addressing the unique challenges of remote construction sites, including: (1) weighted linear and integer programming; (2) nature-inspired metaheuristic algorithms; and (3) genetic algorithms.

2.6.1 Weighted Linear and Integer Programming

A multi-objective optimization problem can be transformed into a scalar problem by using the weighted-sum method in the form, minimize:

$$\sum_{i=1}^{k} w_i f_i(\bar{x}) \tag{2.5}$$

where,

k = number of objective functions;

$f_i(\bar{x})$ = scalar objective functions; and

w_i = weighting coefficients representing the relative importance of the objectives.

In this method, it is generally assumed that all weighting coefficients are positive and the sum of the coefficients equal one (Coello 1999). The two main advantages of this method over other optimization techniques are: (1) the ability to achieve a global optimum solution, as opposed to the sub-optimal solutions reached when using metaheuristic optimization methods, and (2) faster computational efficiency. The main disadvantage is the difficulty in determining the appropriate weighting coefficients when little is known about the problem or how the relative weights will affect the solution

(Coello 1999). To overcome this shortcoming, it is necessary to solve the same problem for many different values of w_i in order to generate the Pareto front (Caramia and Dell'Olmo 2008). This approach is simple and effective when solving problems with a convex Pareto front (Figure 2.4); however, if the problem is non-convex, there is a set of points that cannot be achieved for any combination of the weighting coefficients (Figure 2.5).

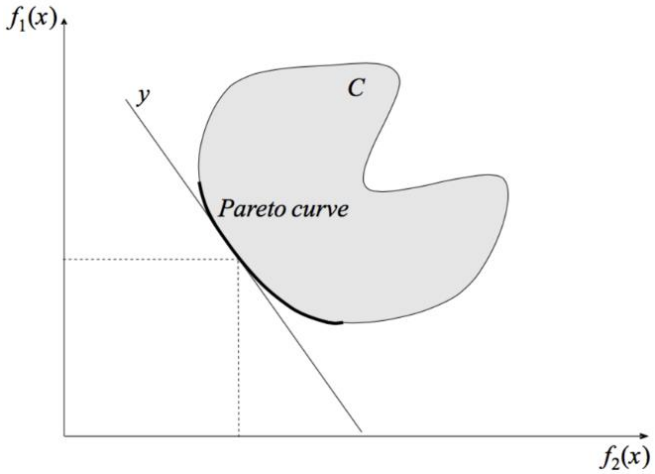

Figure 2.4 Weighted-sum Approach with Convex Pareto Curve (Caramia and Dell'Olmo 2008)

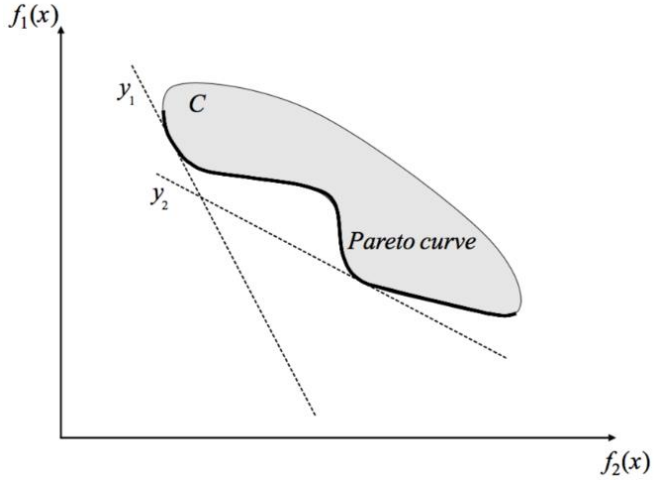

Figure 2.5 Weighted-sum Approach with Non-convex Pareto Curve (Caramia and Dell'Olmo 2008)

The weighted-sum method can be employed in linear, integer or mixed-integer programming problems. A main limitation to linear programming is the requirement for all objective functions and constraints to be linear. Integer programming refers to decision variables that are non-continuous and non-fractions such as the number of personnel required to complete a task. Mixed-integer programming is when some decision variables require integers and others are continuous (Abdallah 2014). These techniques have been used to solve many complex optimization problems in construction, including facility layout modeling (Foulds et al. 1998; Kim and Kim 2000).

2.6.2 Nature-inspired Metaheuristic Algorithms

Hard optimization problems can be defined as problems that cannot be solved by any deterministic method within a reasonable amount of time (Boussaïd et al. 2013). Metaheuristics can be used to solve these hard optimization problems. Metaheuristics are “higher-level” heuristics, meaning that they are designed to approximately solve a wide range of optimization problems without having to deeply adapt to each specific scenario (Boussaïd et al. 2013). Most metaheuristic algorithms are nature-inspired, seeking optimality by mimicking some physical, biological or ethological process. In a recent survey, Fister Jr. et al. (2013), identified more than 40 nature-inspired metaheuristic algorithms based upon such natural processes as migratory bird patterns (Eberhart and Kennedy 1995), ant colony behaviors (Dorigo et al. 1996), bacterial foraging (Chu et al. 2008), firefly bioluminescence (Yang 2009), slime mold life cycle (Monismith and Mayfield 2008), cockroach infestation (Havens et al. 2008), mosquito host-seeking (Feng et al. 2009), and bat echolocation (Yang 2010). This section will

analyze the two most prevalent nature-inspired metaheuristic algorithms: particle swarm optimization and ant colony optimization.

2.6.2.1 Particle Swarm Optimization

Particle swarm optimization (PSO) is a population-based, stochastic optimization technique, inspired by the migratory patterns of birds attempting to reach an unknown destination (Zhou et al. 2011). PSO was originally developed by Eberhart and Kennedy (1995) and was later expanded to include multi-objective optimization by Moore and Chapman (1999). In PSO, each solution is a “bird” in the migrating flock. As the flock flies, the birds communicate with one another, identifying the bird in the best location. The rest of the flock then flies toward this bird and investigates their surrounding environment. This social behavior is repeated until the birds reach their destination. PSO successfully incorporates both intelligence and social interaction, combining local search, where the birds learn from their own experience, and global search, where the birds learn from the experience of others around them (Elbeltagi et al. 2005). PSO has been widely used in multi-objective optimization problems in construction, including modeling construction site layout (Zhang and Wang 2008; Rezazadeh et al. 2009; Ohmori et al. 2010).

2.6.2.2 Ant Colony Optimization

Dorigo et al. (1996) developed ant colony optimization (ACO), a naturally inspired optimization technique that mimics the process of ants determining the shortest route between their nest and a food source (Elbeltagi et al. 2005). As ants travel, they deposit pheromone trails on the ground that are detected by other ants (Zhou et al. 2011). As the search for food begins, ants will randomly travel around all sides of an encountered

obstacle, initially depositing equal concentrations of pheromones from the left and right direction. Ants with the shortest path to food will return to their nest following their original path, thus depositing more pheromones. Future ants will detect this greater concentration of pheromones and follow the established path from their nest to the food source (Elbeltagi et al. 2005). Over time, favored paths that are shorter and more efficient will emerge because of this positive feedback mechanism (Yang 2014). ACO has been effectively utilized to address many multi-objective optimization problems in construction, including construction site layout (Baykasoglu et al. 2006; Pour and Nosraty 2006; Komarudin and Wong 2010), sustainability and building energy performance (Marzouk et al. 2012; Yuan et al. 2012). One limitation of ACO is that it can only be used in discrete problems (Elbeltagi et al. 2005).

2.6.3 Genetic Algorithms

Genetic algorithms, developed by John Holland in 1975 (Holland 1975), are search algorithms that mimic genetic operations based up Darwin's theory of natural selection (Goldberg 1989). Genetic algorithms apply survival of the fittest to obtain near-optimum solutions by following a six-step process: (1) create a population of individual solutions (chromosomes); (2) calculate the value of the objective function(s) for each individual within the population; (3) assign a fitness value to each individual based upon the objective function(s); (4) perform reproduction with higher-fitness individuals having a higher probability of survival than individuals with lower fitness values; (5) create offspring by combining or varying the genotypes in the parent solutions through the processes of crossover and mutation; (6) repeat steps 2-5 until termination conditions are satisfied (Weise 2008). The structured randomness of genetic algorithms coupled

with the inclusion of mutation to avoid local minima give genetic algorithms the ability to deal with complex problems and parallelism. Genetic algorithms have been successfully employed in various types of optimization, where the objective function is static or dynamic, linear or nonlinear, continuous or discontinuous, or contains random noise (Yang 2014). Genetic algorithm is the most reported optimization tool used to solve multi-objective problems in construction engineering and management, including construction site layout planning (Elbeltagi et al. 2004; Khalafallah and El-Rayes 2008; Said and El-Rayes 2010); and renewable-energy system optimization (Bernal-Agustín et al. 2006; Koutroulis et al. 2006; Yang et al. 2008; Piacenza et al. 2012).

CHAPTER 3

ASSESSMENT OF BLAST EFFECTS

3.1 Introduction

This chapter presents the development of a novel blast effects assessment model (BEAM) capable of efficiently quantifying and visualizing blast effects on constructed facilities behind blast walls. The model is intended to support designers in their critical task of analyzing and comparing all feasible design alternatives in order to select the most effective combination of blast wall type and building material to reduce the security risks to site personnel and facilities from the threat of an explosive attack. The model is developed in five main stages: (1) blast wall analysis stage that develops novel analytical formulas and a set of effectiveness factors to quantify the performance of feasible frangible blast wall types including sand-filled, water-filled, and wood walls in reducing reflected pressure and impulse loading on facilities; (2) facility damage assessment stage that computes the percent area of each facility within five specified damage levels in order to calculate an overall facility damage level; (3) blast damage visualization stage that displays anticipated facility damage areas based upon blast charge weight, blast wall type, and building material combinations; (4) performance analysis stage that evaluates the accuracy and efficiency of the developed model; and (5) case study stage that analyzes the performance of the developed model using an application example. The following sections provide a concise description of these five model development stages.

3.2 Blast Wall Analysis

A blast wall is a physical barrier that separates valuable facilities from explosive threats (Smith 2010). Blast walls function by reflecting a portion of the explosive blast energy, thereby reducing reflected pressure and impulse loading on the facility (Remennikov and Rose 2007). This reduction in blast environment for rigid walls can be quantified using Eqs. (3.1) and (3.2) for reflected pressure and impulse, respectively (Zhou and Hao 2008). These equations, however, are limited to rigid walls and need to be expanded to consider feasible frangible wall types such as sand-filled, water-filled and wood walls that were reported to provide greater reduction in blast loading on facilities (Rose et al. 1997; Bogosian and Piepenburg 2002).

$$AF_{P_{max,rigid}} = -0.1359 + \left(0.3272 + 0.1995\, log\left(\frac{H}{S}\right)\right) log\left(\frac{S}{W^{1/3}}\right) - 0.5626\, log\left(\frac{H}{S}\right) + 0.4666\left(\frac{L}{S}\right) \quad (3.1)$$

$$AF_{I_{max,rigid}} = 0.0274 + \left(0.4146 + 0.2393\, log\left(\frac{H}{S}\right)\right) log\left(\frac{S}{W^{1/3}}\right) - 0.5044\, log\left(\frac{H}{S}\right) + 0.2538\left(\frac{L}{S}\right) \quad (3.2)$$

where,

$AF_{P_{max,rigid}}$ = maximum reflected pressure adjustment factor for rigid walls;

H = blast wall height (m);

S = standoff distance from explosive to facility (m);

W = blast charge weight (kg TNT equivalent);

L = distance from explosive to blast wall (m); and

$AF_{I_{max,rigid}}$ = maximum reflected impulse adjustment factor for rigid walls.

To address the aforementioned limitation of Eqs. (3.1)-(3.2), this stage develops analytical formulas to quantify the performance of feasible frangible blast wall types in reducing reflected pressure and impulse loading on facilities, as shown in Eqs. (3.3)-(3.4). These equations utilize a newly developed set of effectiveness factors that consider a wide range of frangible blast wall types including various thicknesses of balsa wood, ice walls, polystyrene, polythene sheets, revetting material, various thicknesses of sand-filled containers, water bag walls, and water-filled containers, as shown in Table 3.2.

$$AF_{P_{max,frangible}} = AF_{P_{max,rigid}} \times EF_P \tag{3.3}$$

$$AF_{I_{max,frangible}} = AF_{I_{max,rigid}} \times EF_I \tag{3.4}$$

where,

$\mathrm{AF}_{\mathrm{P}_{\mathrm{max,frangible}}}$ = maximum reflected pressure adjustment factor for frangible walls;

EF_P = frangible wall pressure effectiveness factor;

$AF_{I_{max,frangible}}$ = maximum reflected pressure adjustment factor for frangible walls; and

EF_P = frangible wall impulse effectiveness factor.

The frangible wall pressure and impulse effectiveness factors measure the performance of frangible blast walls compared to a standard, rigid blast wall (Bogosian and Piepenburg 2002). A set of frangible wall effectiveness factors is calculated in this stage for 12 feasible frangible wall types by analyzing experimental data from previous blast wall research studies (Rose et al. 1997, 1998). Previous studies record pressure and impulse measurements at incremental distances or heights behind a blast wall. The frangible wall effectiveness factors [Eq. (3.5)-(3.6)] are computed in three steps that are

designed to: (1) utilize existing experimental data of recorded blast measurements at various locations (k) behind the blast wall; (2) calculate the ratio between the frangible wall pressure or impulse and rigid wall pressure or impulse for each location; and (3) compute the effectiveness factor by averaging all the ratios calculated in the previous step. For example, the pressure effectiveness factor for a thick sand wall is calculated using Eq. (3.5), as shown in Table 3.1.

$$EF_P = \frac{\sum_{k=1}^{K}\left(\frac{P_{frangible_k}}{P_{rigid_k}}\right)}{K} \tag{3.5}$$

$$EF_I = \frac{\sum_{k=1}^{K}\left(\frac{I_{frangible_k}}{I_{rigid_k}}\right)}{K} \tag{3.6}$$

where,

k = pressure/impulse measurement location behind the blast wall at varying distances and/or heights (m);

K = total number of pressure/impulse measurement locations behind blast wall;

$P_{frangible}$ = blast pressure behind a frangible barrier at location k (kPa);

P_{rigid} = blast pressure behind a rigid barrier at location k (kPa)

$I_{frangible}$ = blast impulse behind a frangible barrier at location k (kPa-ms/kg$^{1/3}$); and

I_{rigid} = blast impulse behind a rigid barrier at location k (kPa-ms/kg$^{1/3}$).

Table 3.1 Example Calculation for Effectiveness Factor of a Thick Sand Wall

Pressure measurement location, k	Distance from blast wall, S (m)	Measured pressure, $P_{frangible_k}$ (kPa) (Rose et al. 1998)	Measured pressure, P_{rigid_k} (kPa) (Rose et al. 1997)	Calculated ratio, $\left(\frac{P_{frangible_k}}{P_{rigid_k}}\right)$	Pressure Effectiveness factor, EF_P
1	1.35	41	56	0.72	0.74
2	1.50	38	49	0.78	
3	1.65	35	46	0.76	
4	1.80	28	39	0.71	

In this stage, Eqs. (3.5)-(3.6) were used to calculate a set of newly developed pressure and impulse effectiveness factors for 12 feasible frangible blast wall types, where a value greater than one means the material will perform worse than a standard steel wall while a value less than one signifies that a wall will perform better than a standard steel wall, as shown in Table 3.2. The significance of these calculated effectiveness factors can be illustrated using a simplified example, as shown in Figure 3.1 and Table 3.3. In this example, it is assumed that a 250 kg TNT explosive is detonated at a distance of 40 meters from a facility. The example shows the impact of utilizing three blast design alternatives: no wall, standard steel wall, and thick sand wall. The lack of a blast wall exposes the facility to a reflected pressure load of 65 kPa. The use of a rigid steel wall at a distance of four meters from the explosion reduces this peak reflected pressure by 31%, resulting in a reflected pressure load of 45 kPa, while a thick sand wall reduces the pressure load by 51%, resulting in a pressure load of 33 kPa. This example shows that the use of frangible blast walls can substantially reduce peak reflected pressure loading on a facility. This reduction in pressure load decreases damages to the facility resulting in reduced loss of life, property damages and economic losses.

Table 3.2 Blast Wall Effectiveness Factors

Wall Material	Material Thickness (m)	Pressure Effectiveness Factor (EF_P)	Impulse Effectiveness Factor (EF_I)
Balsa wood, thick	.08	0.70	1.06
Balsa wood, thin	.02	1.33	1.33
Ice wall, thick	0.6	0.80	0.86
Ice wall, thin	0.3	0.97	0.93
Polystyrene	.05	0.78	1.01
Polythene sheet	<.01	1.26	1.29
Revetting material	.02	0.79	1.15
Sand wall, thick	1.5	0.74	0.64
Sand wall, medium	1.0	0.82	0.71
Sand wall, thin	0.5	0.86	0.78
Steel, standard	0.2	1.00	1.00
Water, bag wall	0.1	0.71	0.91
Water, filled wall	0.6	0.81	0.84

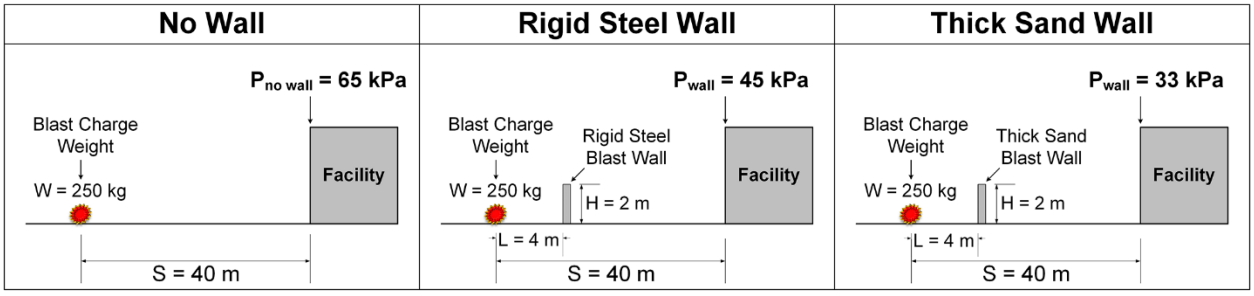

Figure 3.1 Impact of Blast Walls on Reflected Pressure at a Constructed Facility: (a) No Blast Wall; (b) Rigid Steel Blast Wall; (c) Thick Sand Blast Wall

Table 3.3 Blast Wall Effectiveness Factor Example Calculations

Wall Type	Pressure Effectiveness Factor (EF_P)	Pressure Adjustment Factor (AF_{Pmax})	Pressure (kPa) [Eqs. (3.9)-(3.10), (3.12)]
No wall	N/A	N/A	65
Rigid Steel	1.0	0.70	45
Thick Sand	0.74	0.52	33

Equipped with the capability of quantifying the pressure-mitigating effects of all feasible blast wall types, the next section will focus on the development of a blast effects assessment model, which is designed to calculate the percent area of each

facility within specified damage levels in order to determine an overall facility damage level from an explosive attack.

3.3 Facility Blast Damage Assessment

This stage presents the development of a blast effects assessment model (BEAM) that is capable of efficiently quantifying and visualizing blast effects on constructed facilities behind blast walls. This stage is accomplished in four steps: (1) identifying model input parameters; (2) calculating standoff distances between the explosive location and facilities; (3) quantifying the percent facility area within specified damage levels; and (4) computing total facility damages.

3.3.1 Input Parameters

The input parameters of the developed model are selected to represent all feasible design alternatives in order to determine the most effective combination of blast wall type and building material to reduce the security risks to site personnel and facilities from the threat of an explosive attack. The model requires three main types of input parameters: (1) facility parameters: building material, facility location and orientation, and facility geometry; (2) blast wall parameters: wall material type, wall height and location; and (3) explosive parameters: blast charge weight and the location of the explosive. Locations within the model are identified using a grid system that allows decision makers to specify the grid interval. Facility locations are defined by the placement of their centroids on the grid system, as shown in Figure 3.2.

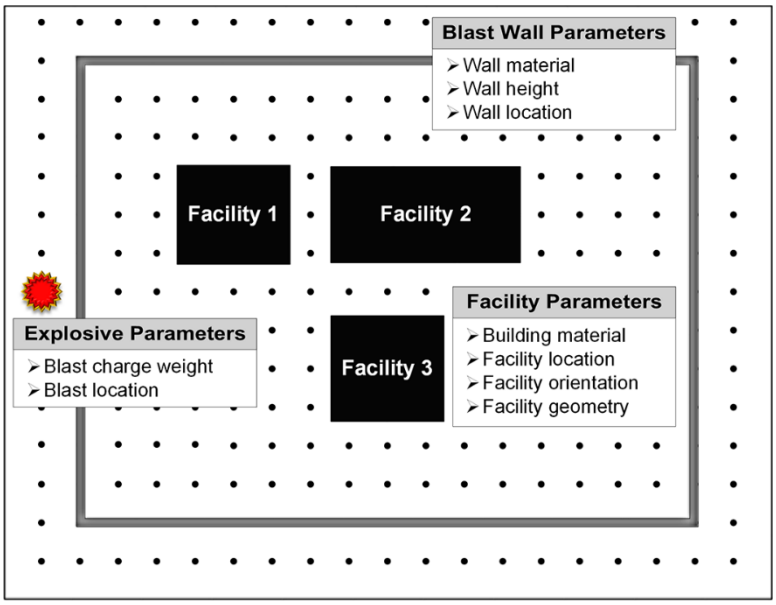

Figure 3.2 Model Input Parameters

3.3.2 Calculate Standoff Distances Between Explosive and Facility

Based on the aforementioned input parameters, the model is designed to perform blast effect assessments by computing the percent area of each facility that is exposed to five specified damage levels: minimal, minor, moderate, heavy and severe, as shown in Figure 3.3. These five damage levels (DL_j) are identified in the present model to ensure consistency with the levels of protection and damage utilized in UFC 4-020-01 (DoD 2008b). In order to compute these percent facility areas (PFA_j), standoff distances (S_j) must be calculated for each combination of damage level (j), blast charge weight (W), blast wall type and building material. These standoff distances represent the minimum allowable separation distance between a facility and an explosive threat that will provide the desired level of protection (U.S. Dept. of the Air Force 1997). For example, if a reinforced concrete facility is located at a standoff distance (S_2) of 55 meters or more from a 250 kg TNT explosive, then this facility will be outside the range of minor damage. Existing design manuals are incapable of identifying these standoff

distances for facilities located behind blast walls. To address this limitation, a novel methodology is used to calculate blast wall-adjusted standoff distances (AS_j) that provide an equivalent level of protection for facilities behind blast walls compared to existing standoff distances for facilities with no blast wall, as shown in Figure 3.4.

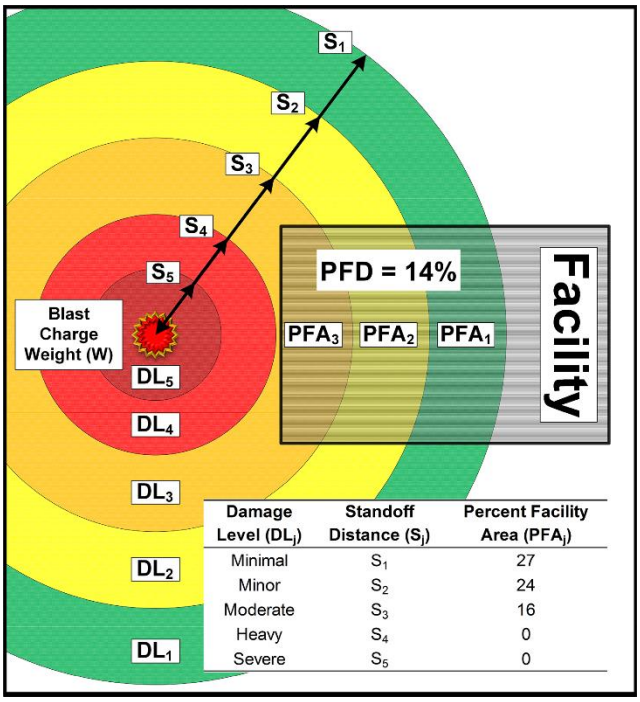

Figure 3.3 Percent Facility Areas Subjected to Varying Damage Levels

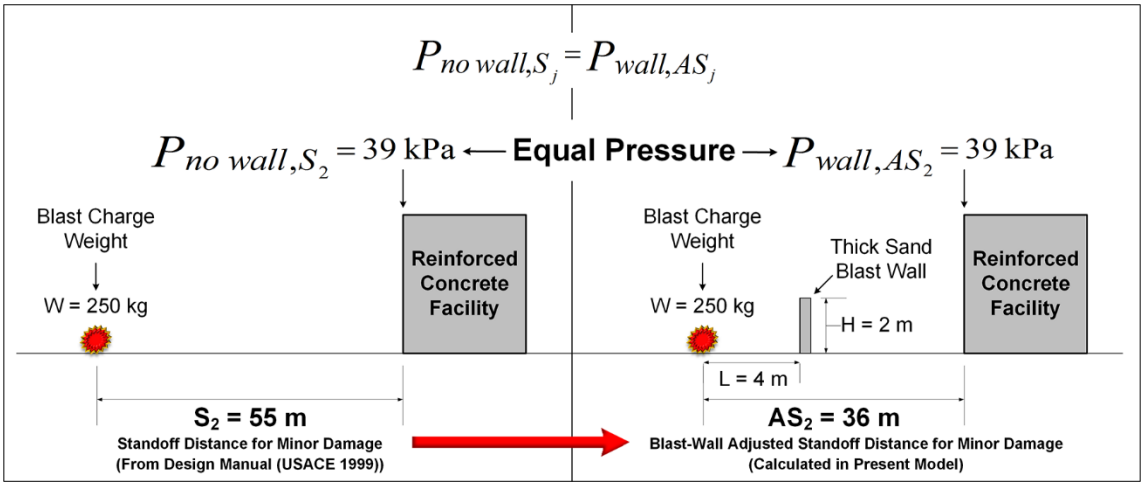

Figure 3.4 Blast Wall-Adjusted Standoff Distance

This step calculates blast wall-adjusted standoff distances (AS_j) that provide equivalent levels of protection for facilities behind blast walls compared to existing standoff distance required for facilities with no blast wall, as shown in Eqs. (3.7)-(3.8) and Figure 3.4. AS_j values are calculated in the present model for each combination of damage level (j), blast charge weight (W), feasible blast wall type, and building material. The calculation of AS_j is performed in three main steps: (1) determine the standoff distances (S_j) for facilities with no blast wall for each combination of damage level (j), blast charge weight (W) and building material from existing design manuals; (2) calculate the reflected pressure or impulse on a facility at these determined standoff distances using Eqs. (3.9)-(3.10) for pressure and Eq. (3.18) for impulse; and (3) compute the blast wall-adjusted standoff distances (AS_j) that maintain equal pressure or impulse to those determined in step two using a modification of the Powell hybrid method for nonlinear equations (Moré et al. 1980) to solve Eq. (3.7) or (3.8), as applicable. These three steps are discussed below.

$$P_{no\ wall,S_j} = P_{wall,AS_j} \tag{3.7}$$

$$I_{no\ wall,S_j} = I_{wall,AS_j} \tag{3.8}$$

where,

$P_{no\ wall}$ = reflected pressure load on a facility with no blast wall (kPa);

S_j = standoff distance for a facility with no blast wall at damage level j (m);

P_{wall} = reflected pressure load on a facility behind a blast wall (kPa);

AS_j = blast wall-adjusted standoff distance for a facility at damage level j (m);

j = damage level (minimal, minor, moderate, heavy, severe)

$I_{no\ wall}$ = reflected impulse load on a facility with no blast wall (kPa-ms/kg$^{1/3}$); and

I_{wall} = reflected impulse load on a facility behind a blast wall (kPa-ms/kg$^{1/3}$).

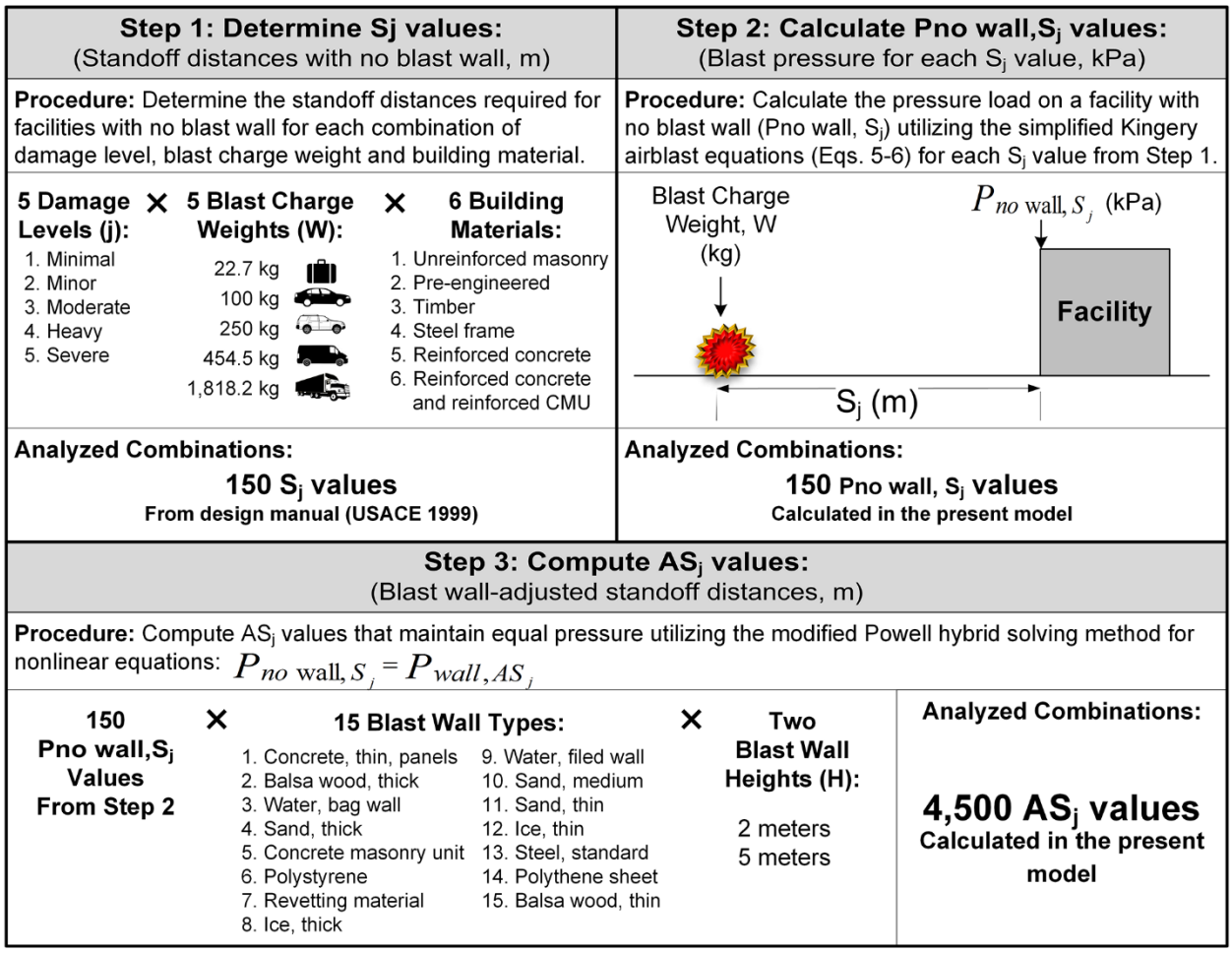

Figure 3.5 Calculation Steps of Blast Wall-Adjusted Standoff Distances

First, the standoff distances required for facilities with no blast wall are determined for each combination of damage level, blast charge weight, and building material, as shown in Figure 3.5. The present model utilizes data provided in ETL 1110-3-495 (USACE 1999) to determine these standoff distances for 150 feasible design

combinations (see Figure 3.5). These 150 feasible design combinations cover (1) the five aforementioned damage levels: minimal, minor, moderate, heavy and severe; (2) five blast charge weights based upon the most common method of delivery: luggage (22.7 kg), sedan (100 kg), sport utility vehicle (250 kg), full-size van (454.4 kg) and large truck (1,818.2 kg) (FEMA 2011); and (3) six prevalent building materials: unreinforced masonry, pre-engineered metal, timber, steel frame with lightly reinforced CMU infill walls, reinforced concrete, and reinforced concrete frame with lightly reinforced CMU infill walls, as shown in Figure 3.5.

Second, reflected pressure or impulse loads are calculated at these determined standoff distances utilizing the simplified Kingery airblast equations, where reflected pressure and impulse are a function of the scaled distance factor (standoff distance/blast charge weight$^{1/3}$) (Swisdak Jr 1994), as shown in Eqs. (3.9)-(3.11). These calculated reflected blast pressures are the $\mathrm{P}_{\mathrm{no\ wall,S_j}}$ and $I_{no\ wall,S_j}$ values utilized in Eqs. (3.7)-(3.8) above.

For:

$0.06 \leq \frac{S}{W^{1/3}} \leq 2.00$:

$$P_{no\ wall} = e^{\left(9.006-2.6893\,ln\left(\frac{S}{W^{1/3}}\right)-0.6295\left(ln\left(\frac{S}{W^{1/3}}\right)\right)^2+0.1011\left(ln\left(\frac{S}{W^{1/3}}\right)\right)^3+0.29255\left(ln\left(\frac{S}{W^{1/3}}\right)\right)^4+0.13505\left(ln\left(\frac{S}{W^{1/3}}\right)\right)^5+0.019736\left(ln\left(\frac{S}{W^{1/3}}\right)\right)^6\right)} \quad (3.9)$$

$2.00 < \frac{S}{W^{1/3}} \leq 40.00$:

$$P_{no\ wall} = e^{\left(8.8396-1.733\,ln\left(\frac{S}{W^{1/3}}\right)-2.64\left(ln\left(\frac{S}{W^{1/3}}\right)\right)^2+2.293\left(ln\left(\frac{S}{W^{1/3}}\right)\right)^3-0.8232\left(ln\left(\frac{S}{W^{1/3}}\right)\right)^4+0.14247\left(ln\left(\frac{S}{W^{1/3}}\right)\right)^5-0.0099\left(ln\left(\frac{S}{W^{1/3}}\right)\right)^6\right)} \quad (3.10)$$

For:

$0.06 \leq \frac{S}{W^{1/3}} \leq 40$:

$$I_{no\ wall} = e^{\left(6.7853-1.3466\,ln\left(\frac{S}{W^{1/3}}\right)+0.101\left(ln\left(\frac{S}{W^{1/3}}\right)\right)^2-0.01123\left(ln\left(\frac{S}{W^{1/3}}\right)\right)^3\right)} \quad (3.11)$$

Third, blast wall-adjusted standoff distances (AS_j) are computed to quantify the impact of integrating various blast wall designs on the aforementioned standoff distances. As shown in Figure 3.5, this step calculates the blast wall-adjusted standoff distances (AS_j) that maintain equal pressure or impulse to those determined in step two using the modified Powell hybrid method for nonlinear equations to solve Eqs. (3.7)-(3.8). This step computes 4,500 unique AS_j values by quantifying the performance of 30 feasible blast walls in reducing reflected pressure or impulse loading on facilities for each of the 150 design combinations of damage level, blast charge weight and building material identified above. These 30 blast walls cover all possible combinations of: (1) 15 blast wall types, including the 12 frangible walls with the newly developed effectiveness factors listed in Table 3.2, a standard rigid steel wall (Zhou and Hao 2008), and precast concrete panel and concrete masonry unit (CMU) walls (Bogosian and Piepenburg 2002); and (2) two blast wall heights of two meters and five meters. In order to perform these computations, it is necessary to quantify the performance of feasible frangible and rigid blast walls in reducing reflected pressure and impulse loading on facilities. This reduction in peak reflected pressure loading on facilities is quantified by multiplying the blast pressure on a facility when no wall is present ($P_{\text{no wall}}$) from Eqs. (3.9)-(3.10), by the appropriate blast wall pressure adjustment factor ($AF_{P_{max}}$), as shown in Eq. (3.12). The reduction in reflected impulse loading on facilities is quantified by multiplying the reflected impulse on a facility when no wall is present ($I_{\text{no wall}}$) from Eq. (3.11) by the appropriate blast wall impulse adjustment factor ($AF_{I_{max}}$), as shown in Eq. (3.13). Utilizing this process, the modified Powell hybrid method for nonlinear equations is then

used to solve Eqs. (3.7)-(3.8), as applicable, by computing the AS_j value where P_{wall,AS_j} equals the $P_{no\ wall,S_j}$ or I_{wall,AS_j} equals the $I_{no\ wall,S_j}$ calculated in step two.

$$P_{wall} = AF_{P_{max}} \times P_{no\ wall} \tag{3.12}$$

$$I_{wall} = AF_{I_{max}} \times I_{no\ wall} \tag{3.13}$$

The computations performed in the aforementioned three steps can be illustrated using a simple example, as shown in Figure 3.4. In this example, it is assumed that a reinforced concrete facility is required to be located outside the range of minor damage (j = 2) in the event of a 250 kg TNT explosive attack. The designers wish to compare the standoff distance required for the facility with no blast wall to the blast wall-adjusted standoff distance required when a two-meter tall, thick sand wall is constructed to protect the facility. In the first step, ETL 1110-3-495 (USACE 1999) is used to determine that a 55-meter standoff distance (S_j) is required to provide the desired level of protection for the facility with no blast wall. In the second step, the simplified Kingery airblast equations (Swisdak Jr 1994) are used to calculate the $P_{no\ wall,S_j}$ value for the standoff distance determined in the first step. At a standoff distance of 55 meters, solving Eq. (3.10) shows that the facility will experience a reflected pressure load of 39 kPa. In the third step, the blast wall-adjusted standoff distance for the facility protected by a two-meter tall, thick sand wall that results in an equal pressure load of 39 kPa is computed by solving Eq. (3.7) utilizing the modified Powell hybrid method for nonlinear equations. This computation yields a blast wall-adjusted standoff distance (AS_2) of 36 meters. This calculation can be verified and further explained by using Eq. (3.12). When AS_2 is 36 meters, $P_{wall,36m}$ is calculated by multiplying $P_{no\ wall}$ [calculated with Eq. (3.10)] at 36 meters by the $AF_{P_{max}}$ [calculated with Eq. (3.3)] for a two-meter tall, thick sand wall

that is assumed to be located four meters from the blast. Performing these calculations results in a $P_{no\ wall}$ of 76 kPa and a $AF_{P_{max}}$ of 0.51, which multiplied together verify $P_{wall,36m}$ as 39 kPa. This example demonstrates that frangible blast walls can substantially reduce the standoff distance required to provide an equivalent level of protection for a facility compared to the standoff distance required for a facility with no blast wall. Further, this reduction in required standoff distance greatly increases site layout planning flexibility, enabling designers to construct additional facilities in the freed-up site space or reduce the site footprint in order to realize real-estate savings.

3.3.3 Quantify the Percent Facility Area within Specified Damage Levels

This step quantifies the percent area of each facility within the five damage levels (PFAij) by calculating the area of intersection between blast damage areas, which are determined by utilizing the blast wall-adjusted standoff distances (AS_j) computed in the previous step, and the facility area (FA_i), as shown in Figure 3.3. Each damage level (DL_j) is represented as a ring, centered at the anticipated blast location, with a radius equal to the calculated standoff distance. The areas are then converted to percentages by dividing the area of intersection by the total facility area and multiplying by 100%, as shown in Eq. (3.14). This model utilizes the intersection function within Shapely, an existing Python package used for manipulation and analysis of planar geometric objects based on the GEOS (Geometry Engine, Open Source) and JTS (Java Topology Suite) libraries to automate these calculations (Gillies 2013). These percent areas of each facility within the five damage levels (PFA_{ij}) are utilized in the next section to compute the total facility damage level.

$$PFA_{ij} = \frac{FA_i \cap DL_j}{FA_i} \times 100\% \tag{3.14}$$

where,

PFA_{ij} = percent area of a facility i within damage level j;

i = facility number;

FA_i = area of facility i (m^2); and

DL_j = area of damage level j (m^2).

3.3.4 Compute Total Facility Damages

The final step in quantifying the blast effects on constructed facilities behind blast walls is computing the total percentage of damage to each facility (PFD_i). PFD_i is the sum of the percent facility area (PFA_j) multiplied by the percent destruction (PD_j) for all the five damage levels (j) considered in this model, as shown in Eq. (3.15). The PD_j value for these five damage levels (minimal, minor, moderate, heavy, and severe) is considered in this model to be 10%, 20%, 40%, 60%, and 100% respectively. These PD_j values are identified based on the upper limit of the reported ranges of destruction for each of these five damage levels in existing design manuals (USACE 1999; FEMA 2011; DoD 2012).

$$PFD_i = \sum_{j=1}^{5} PFA_{ij} \times PD_j \tag{3.15}$$

where,

PFD_i = total percentage of damage to facility i;

PFA_{ij} = percent area of facility i in damage category j; and

PD_j = percent destruction caused by damage category j.

The model is capable of quantifying the expected damages on multiple constructed facilities behind blast walls from a single explosive attack. The next section

discusses the output of 2-D visualizations of the impact of an explosive attack on multiple facilities to support designers in their critical task of identifying the most effective design for blast walls and facility hardening.

3.4 Blast Damage Visualization

This stage presents the development of blast damage visualizations that display the results calculated from the aforementioned blast effects assessment model. These calculations are performed using Python programming language (Rossum 1995) and the blast damage visualizations are generated using the 2-D plotting library matplotlib (Hunter 2007). The blast damage visualizations represent an effective tool to analyze the impact of various design combinations on the level of blast damages in all analyzed facilities. These generated visualizations provide designers with practical and reliable graphical illustrations that show the impact of a single blast on the level of damages in all facilities on site for each feasible design combination of blast charge weight, blast wall type, and building material.

The generated visualizations represent the five damage levels (DL_j) as rings, where each of these rings is centered at the anticipated blast location and has a radius equal to its corresponding calculated standoff distance (AS_j), as shown in Figure 3.6(a). The developed model enables designers to specify the color and line styles of these rings to support their blast damage analysis. For example, designers can specify varying colors for each of the rings representing the five damage levels when all facilities have the same building material, as shown in Figure 3.6(a), where dark red, red, orange, yellow, and green represent the severe, heavy, moderate, minor, and minimal damage levels, respectively. If the site consists of facilities constructed of

multiple building materials, designers can use various line styles to represent the damage level rings for different materials, as shown in Figure 3.6(b), where solid lines are used to represent the damage level rings for the timber facilities and dashed lines are used to represent the damage level rings for reinforced concrete facilities. In addition, the model enables designers to utilize hatch patterns to represent different building materials. For example, in Figure 3.6, the diagonal (/) pattern is used to represent timber facilities while the dotted pattern (.) is used to represent reinforced concrete facilities. Furthermore, facility colors can be used to represent the overall facility damage level, enabling designers to easily visualize the level of damage suffered by each facility.

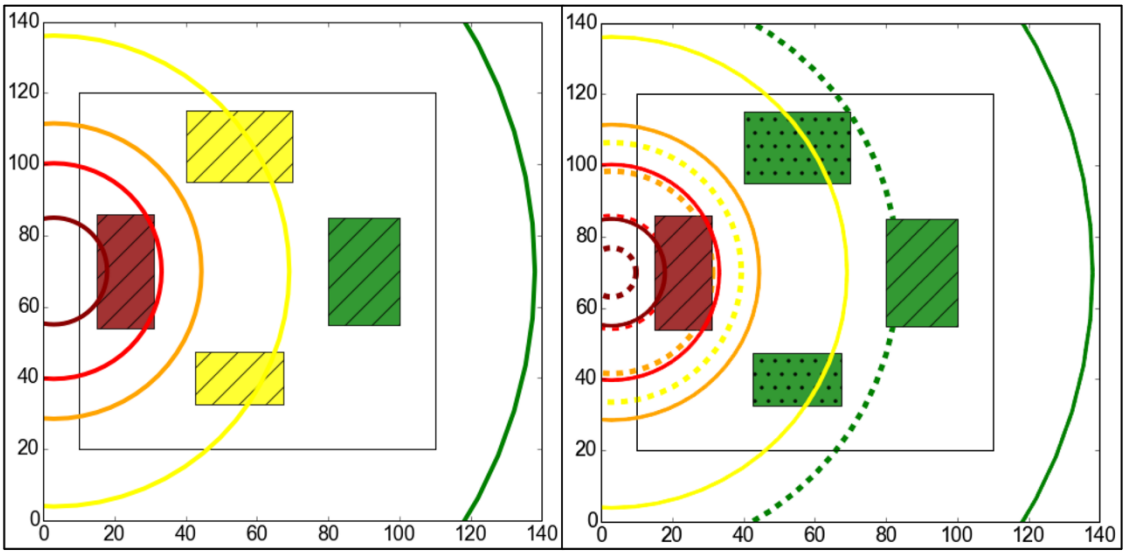

Building Material		Damage Level Rings			Facility Damage Level	
Material	Fill Pattern	Damage Level	Timber Facility	Reinforced Concrete Facility	Damage Level	Fill Pattern
Timber		Severe			Severe	
		Heavy			Heavy	
Reinforced Concrete		Moderate			Moderate	
		Minor			Minor	
		Minimal			Minimal	

Figure 3.6 Colored Rings Representing Five Damage Levels: (a) One Building Material; (b) Two Building Materials

These generated visualizations provide designers with a practical and reliable analysis tool to assess the results of the design scenario and determine the level of protection provided for each constructed facility. They enable designers to: (1) perform a visual risk management assessment of the design scenario; and (2) determine if any design changes are needed to provide the required level of protection for constructed facilities. For example, the generated visualization in Figure 3.7(a) presents a design scenario where the calculated damage level exceeds the designers' maximum acceptable facility damage level.

In this example, a five-meter-tall, steel blast wall is constructed to protect a timber facility from a 250 kg explosive attack at a standoff distance of 20 meters. The designers have specified an acceptable facility damage level of minimal for their design scenario; however, the blast damage visualizations and model output data show that this design results in a facility damage level of 40%, which corresponds to a heavy damage level. As the anticipated damage level exceeds the minimum acceptable level of protection for the facility, design changes are needed to reduce the security risks to site personnel and facilities from this explosive threat.

Figures Figure 3.7(b) and (c) provide examples of alternative design scenarios that utilize the two primary design strategies used to reduce blast effects on facilities in order to increase the anticipated level of protection. First, designers attempt to maximize the standoff distance between the facility and the anticipated location of the explosive, as shown in Figure 3.7(b). By increasing the standoff distance from 20 meters to 80 meters, the anticipated facility damage level is reduced from 40% to 10%, which is within the designer's maximum acceptable facility damage level. Second, if a

sufficient standoff distance to provide the desired level of protection cannot be achieved, designers must select blast walls and/or building materials that provide greater levels of blast protection. Figure 3.7(c) displays the results of one possible design alternative where a five-meter-tall, thick sand blast wall is constructed to protect a steel frame facility. This design alternative results in a facility damage level of 10%, corresponding to a minimal damage level, which meets the designer's acceptable facility damage level.

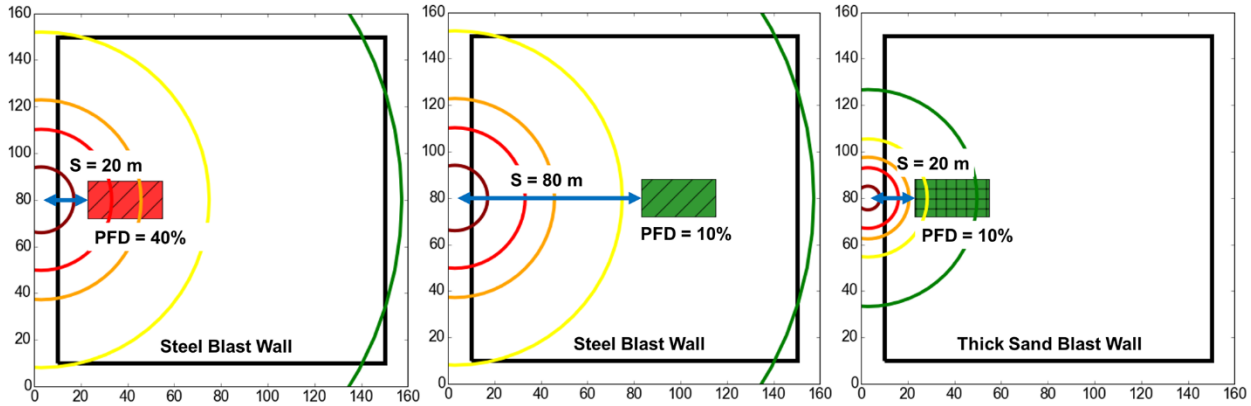

Building Material	Fill Pattern	Damage Level Rings	Ring Color	Facility Damage Level	Fill Pattern
Timber		Severe		Severe	
		Heavy		Heavy	
Steel Frame		Moderate		Moderate	
		Minor		Minor	
		Minimal		Minimal	

Figure 3.7 Alternative Design Scenarios to Minimize Damage Level in Constructed Facility (a) 20 m Standoff, Timber Facility, Steel Blast Wall; (b) 80 m Standoff, Timber Facility, Steel Blast Wall; (c) 20 m Standoff Distance, Steel Frame Facility, Thick Sand Blast Wall

3.5 Performance Analysis

The purpose of this stage is to analyze the performance of the present model by comparing its results to those generated by the Defense Threat Reduction Agency's Vulnerability Assessment and Protection Option (VAPO) software, version 6.2 (USACE PDC 2016). VAPO was selected in this analysis because of its: (1) capability of

simultaneously predicting blast loads on facilities and accounting for the structural response of individual building components; and (2) computational efficiency in generating and analyzing multiple designs scenarios in a relatively short time (Nichols and Doyle 2014). This performance analysis was performed by evaluating 114 design configurations that consisted of 54 configurations with no blast walls and 60 configurations with steel blast walls. The design configurations were analyzed using a 2.0 GHz quad-core Intel Core i7 processor with 6 MB of cache memory and 16 GB of SDRAM.

The performance of BEAM was analyzed using two metrics: accuracy and efficiency. The accuracy of the present model was evaluated by calculating the: (1) average difference between the generated reflected pressure and impulse by the present model and VAPO (ΔP and ΔI, respectively), as shown in Eqs. (3.16)-(3.17); and (2) the percent difference between the reflected pressure and impulse results generated by the two models ($\%P$ and $\%I$, respectively), as shown in Eqs. (3.18)-(3.19). These average and percent differences were calculated for a wide range of possible design scenarios that represent the most probable security threats faced by designers. In total, 114 combinations of building materials, blast charge weights, standoff distances and utilization of blast walls were analyzed, including 54 design configurations with no blast wall and 60 with blast walls. In the first set of analyzed design configurations with no blast walls, reflected pressure and impulse loads on facilities were calculated for 54 feasible combinations of: (1) six building materials (unreinforced masonry, pre-engineered metal, timber, steel frame with lightly reinforced CMU infill walls, reinforced concrete, and reinforced concrete frame with lightly reinforced CMU infill walls); and (2)

nine combinations of blast charge weights and standoff distances. As shown in Figure 3.8, these nine combinations of blast charge weights and standoff distances include: (a) blast charge weights of 100 and 250 kg at a standoff distance of 25 meters; (b) blast charge weights of 100, 250, 454.5, and 1,818.2 kg at a standoff distance of 50 meters; and (c) blast charge weights of 250, 454.5, and 1,1818.2 kg at a standoff distance of 100 meters. For each of these nine combinations of standoff distance and blast charge weight, the average reflected pressure that was calculated by the present model and VAPO for the analyzed six building materials is displayed in Figure 3.8.

In the second set of design configurations with blast walls, reflected pressure and impulse loads on facilities behind a five-meter-tall, steel blast wall were calculated for 60 feasible combinations of: (1) six building materials (unreinforced masonry, pre-engineered metal, timber, steel frame with lightly reinforced CMU infill walls, reinforced concrete, and reinforced concrete frame with lightly reinforced CMU infill walls); and (2) ten combinations of blast charge weights and standoff distances. As shown in Figure 3.9, these ten combinations of blast charge weights and standoff distances include: (a) blast charge weights of 100, 250 and 454.5 kg at a standoff distance of 25 meters; (b) blast charge weights of 100, 250, 454.5, and 1818.2 kg at a standoff distance of 50 meters; and (c) blast charge weights of 250, 454.5, and 1,1818.2 kg at a standoff distance of 100 meters. For each of these ten combinations of standoff distance and blast charge weight, the average reflected pressure that was calculated by the present model and VAPO for the analyzed six building materials is displayed in Figure 3.9.

The results of the conducted analysis verify that the methodology of calculating blast loads in this component of the model by utilizing the simplified Kingery airblast

equations (Swisdak Jr 1994) and the rigid wall adjustment factors (Zhou and Hao 2008) generates results that are very close to those generated by VAPO, as shown in Figure 3.8 and Figure 3.9. The average and percent reflected pressure differences between the two models were 1.9 kPa and 4.0% for the no wall configurations and 1.2 kPa and 3.9% for the steel wall configurations. The average and percent reflected impulse differences between the two models were 83 kPa-ms/kg$^{1/3}$ and 12.0% for the no wall configurations and 39 kPa-ms/kg$^{1/3}$ and 10% for the steel wall configurations. These differences in calculated blast loads between BEAM and VAPO are minor, and may only lead to slightly more conservative design outcomes.

$$\Delta P = \frac{\sum_{c=1}^{C}\left(P_{BEAM_c} - P_{VAPO_c}\right)}{C} \tag{3.16}$$

$$\Delta I = \frac{\sum_{c=1}^{C}\left(I_{BEAM_c} - I_{VAPO_c}\right)}{C} \tag{3.17}$$

$$\%P = \frac{\left(\sum_{c=1}^{C}\left(\frac{P_{BEAM_c} - P_{VAPO_c}}{P_{VAPO_c}}\right)\times 100\%\right)}{C} \tag{3.18}$$

$$\%I = \frac{\left(\sum_{c=1}^{C}\left(\frac{I_{BEAM_c} - I_{VAPO_c}}{I_{VAPO_c}}\right)\times 100\%\right)}{C} \tag{3.19}$$

where,

ΔP = average reflected pressure difference between BEAM and VAPO (kPa);

c = design configuration number;

C = total number of design configurations;

P_{BEAM} = reflected pressure load on a facility as calculated by the present blast effects assessment model for configuration c (kPa);

P_{VAPO} = reflected pressure load on a facility as calculated by VAPO for configuration c (kPa);

ΔI = average reflected impulse difference between BEAM and VAPO (kPa-ms/kg$^{1/3}$);

$\%P$ = average percent reflected pressure difference between BEAM and VAPO at a given standoff distance; and

$\%I$ = average percent reflected impulse difference between BEAM and VAPO at a given standoff distance.

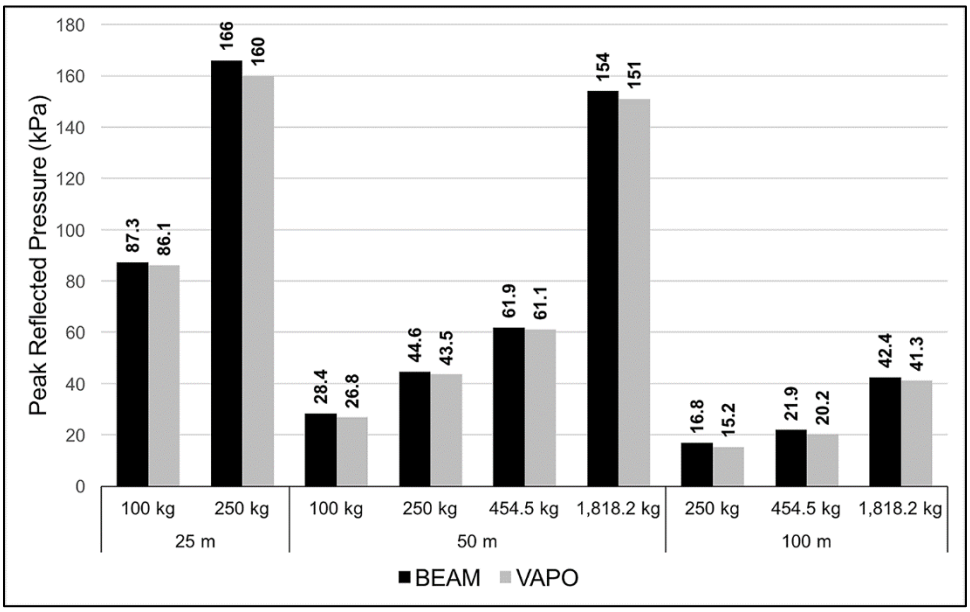

Figure 3.8 Average Peak Reflected Pressure for Six Building Materials and No Blast Wall

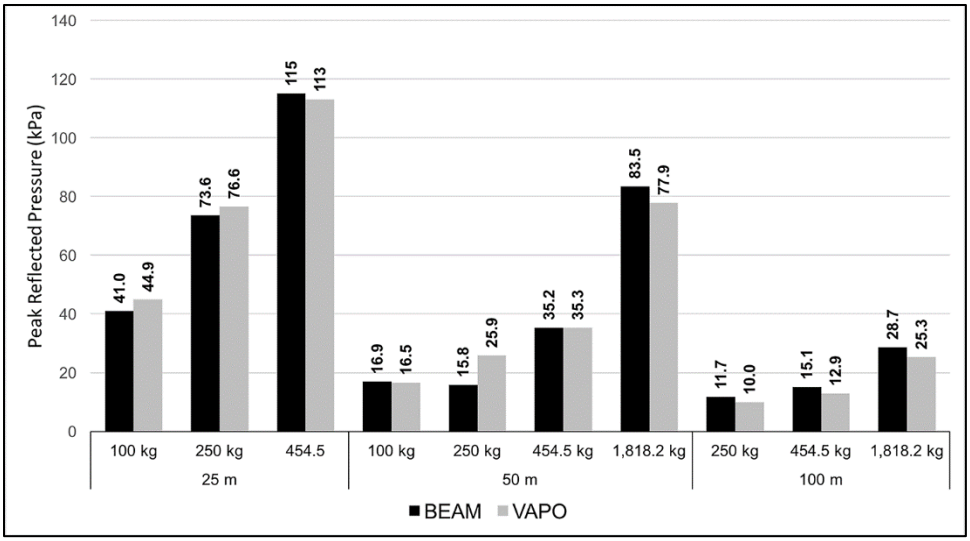

Figure 3.9 Average Peak Reflected Pressure for Six Building Materials and with Blast Wall

The efficiency of the present model was analyzed by recording the amount of time required by BEAM and VAPO to perform blast damage computations and generate blast damage visualizations for each design scenario. BEAM required an average completion time of 0.18 seconds per design scenario while VAPO required 11 seconds per design scenario. This illustrates that the present model requires only 1.7% of the computational time required by VAPO to perform facility blast damage assessments. The results of this performance analysis highlight the accuracy and efficiency of the developed model.

3.6 Case Study

The purpose of this stage is to analyze a case study to illustrate the use of the model and demonstrate its distinctive capabilities. To illustrate the use of the model, the case study seeks to identify the best design configuration for a 512 m^2 one-story constructed facility. The anticipated security threat in this case study is a 454.5 kg TNT explosive attack, assumed to be detonated on a road adjacent to the blast wall at a

distance of four meters from the blast wall. Designers are considering a wide range of feasible design alternatives that include 15 blast wall materials, two wall heights, six building materials and three possible facility locations. As shown in Figure 3.10, these feasible design parameters produce 540 design alternatives for this case study that need to be analyzed by designers to determine the design configuration that provides the greatest level of facility protection.

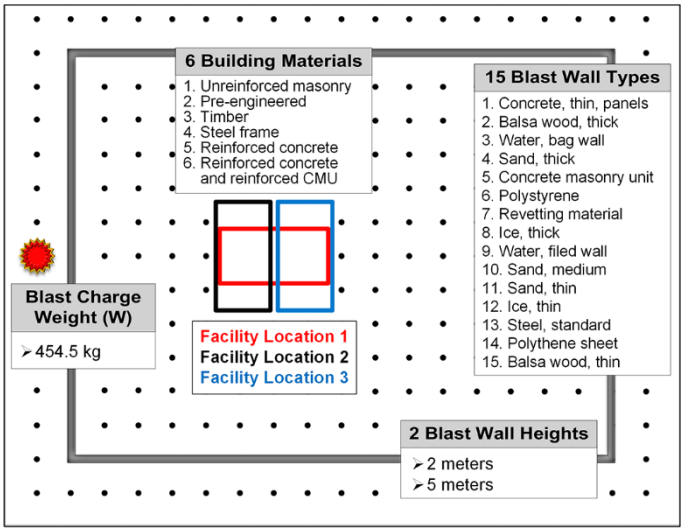

Figure 3.10 Case Study Feasible Design Alternatives

To analyze this case study, designers need to input: (1) the blast charge weight and its Cartesian coordinates, (2) facility dimensions, Cartesian coordinates of its centroid and its orientation (degrees), (3) selection of blast wall type from 30 feasible alternatives, and (4) selection of building material from six feasible alternatives. The output of the model contains the blast wall-adjusted standoff distances (AS_j) for each of the five damage levels (DL_j), the percent area of the facility within each of the five damage levels (PFA_j), the calculated total percentage of damage to the facility (PFD_i), and the generated 2-D visualizations of the anticipated facility damage areas for the

specified combination of blast charge weight (W), blast wall type, building material, and facility location, as shown in Figure 3.11.

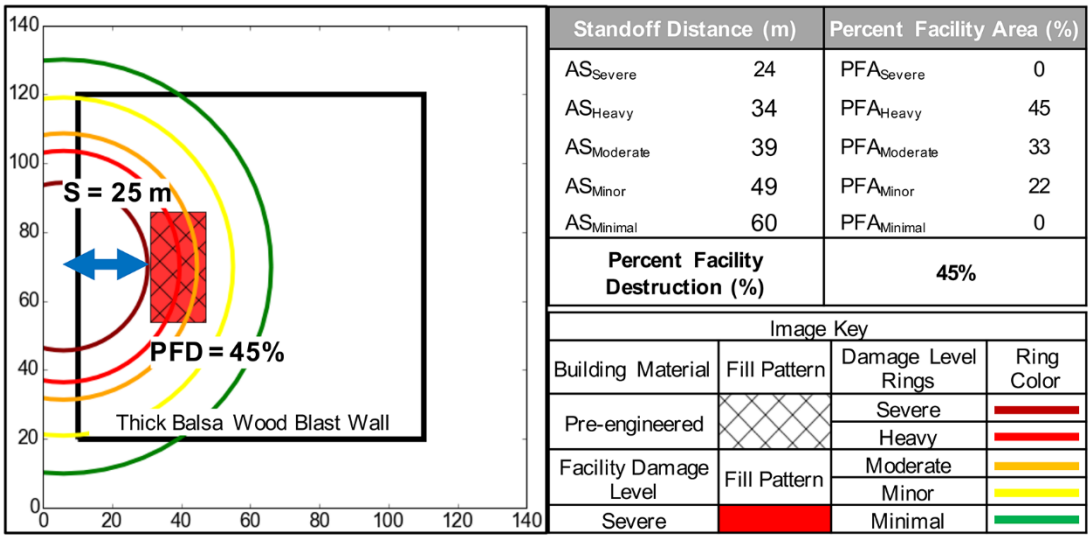

Standoff Distance (m)		Percent Facility Area (%)	
AS_{Severe}	24	PFA_{Severe}	0
AS_{Heavy}	34	PFA_{Heavy}	45
$AS_{Moderate}$	39	$PFA_{Moderate}$	33
AS_{Minor}	49	PFA_{Minor}	22
$AS_{Minimal}$	60	$PFA_{Minimal}$	0
Percent Facility Destruction (%)		**45%**	

Image Key			
Building Material	Fill Pattern	Damage Level Rings	Ring Color
Pre-engineered		Severe	
		Heavy	
Facility Damage Level	Fill Pattern	Moderate	
		Minor	
Severe		Minimal	

Figure 3.11 Model Output Data and Generated 2-D Visualization

The present model was used to analyze the aforementioned 540 design alternatives for this case study. The results of this analysis enabled designers to select the configuration that is most suitable for their specified needs. Absent project cost and material availability limitations, designers will select the configuration that provides the greatest level of facility protection. This configuration, shown in Figure 3.12(a), requires the construction of a reinforced concrete frame facility, behind a five-meter-tall, precast concrete panel blast wall at a standoff distance of 40 meters and a rotation of 90 degrees. This design configuration results in a total percent facility destruction level of 1%.

In addition, designers may need to explore other solutions that provide the lowest level of damage when using specified blast wall types and/or building materials that are available or cost effective in their location. For example, if designers require the construction of a CMU blast wall to protect their facility, the design configuration that

provides the greatest level of protection is shown in Figure 3.12(b). This configuration requires the construction of a reinforced concrete frame facility at a standoff distance of 40 meters and a rotation of 90 degrees, and the building of a five-meter-tall CMU blast wall. This design configuration results in a total percent facility destruction level of 10%.

Furthermore, designers may specify their preference for blast wall type, building material and/or facility location and seek to determine the configuration that provides the greatest level of protection while incorporating their stated design preferences. For example, designers may specify their preference to construct a timber facility. Figure 3.12(c) displays the configuration that provides the greatest level of protection for a timber facility. This configuration requires constructing a five-meter-tall, precast concrete panel blast wall and siting the facility at a standoff distance of 40 meters and a rotation of 90 degrees. This best-case scenario for a timber facility results in a total percent facility destruction level of 20%. The ability of the present model to analyze a wide range of feasible design alternatives enables designers to identify an optimal solution that best addresses the specified needs and limitations of their project.

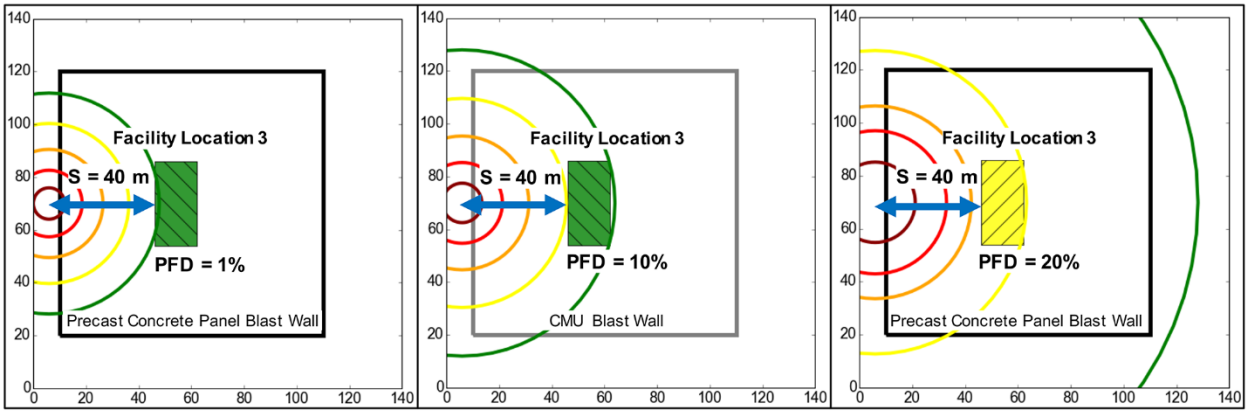

(a) (b) (c)

Building Material	Fill Pattern	Damage Level Rings	Ring Color	Facility Damage Level	Fill Pattern
Reinforced concrete and reinforced CMU		Severe		Severe	
		Heavy		Heavy	
Timber		Moderate		Moderate	
		Minor		Minor	
		Minimal		Minimal	

Figure 3.12 Sample Case Study Results

The analysis of the case study illustrates the unique capabilities of the present model in: (1) efficiently predicting the blast damage level on facilities for a wide range of feasible design alternatives of blast charge weight, blast wall type, building material and facility location; (2) quantifying the effectiveness of feasible frangible blast wall types in reducing blast loading on facilities; and (3) generating visualizations of the anticipated facility damage areas based upon the blast charge weight, blast wall type and building material combinations.

The first distinctive capability of the present model is its ability to efficiently predict the blast damage level on the constructed facility for all feasible design alternatives identified. The model gains its computational efficiency by incorporating a database that contains the aforementioned 30 blast wall types and six building materials, enabling designers to analyze all possible combinations in a single run without the need to input the values for each possible combination. This capability enabled the present model to analyze the 540 possible design combinations for this

case study, as shown in Figure 3.13, in a total computational time of 97 seconds or an average of 0.18 seconds per design scenario. BEAM's ability to efficiently analyze the performance of all feasible design scenarios for constructed facilities in resisting the effects of an explosive attack allows for improvement and optimization in facility design that was previously infeasible using existing blast models.

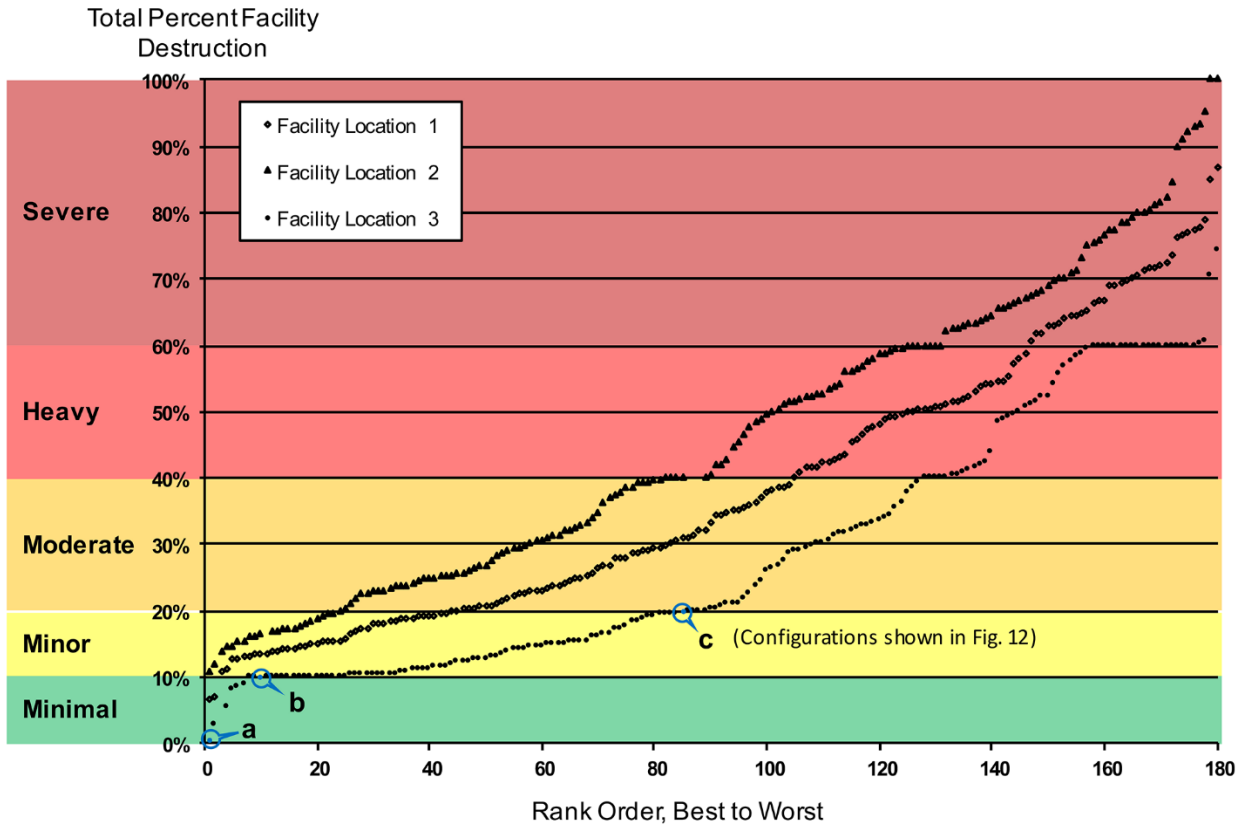

Figure 3.13 Generated Case Study Results

The second distinctive capability of the present model is its ability to quantify the effectiveness of feasible frangible blast wall types in reducing blast loading on facilities compared to a standard, rigid wall. This reduction in blast loading on facilities is capable of producing significant reduction in expected damages to the facility. Using facility location 1 from this case study as an example, the design configuration that returns the lowest percent facility destruction for a facility behind a rigid blast wall is to construct a

steel frame facility behind a five-meter-tall, steel blast wall. This design configuration results in a total percent facility destruction level of 18%. Constructing the same steel frame facility behind a frangible, five-meter-tall, precast concrete panel wall reduces the percent facility destruction level to 7%. Similar blast assessment models are incapable of considering frangible walls and their effectiveness in reducing blast loading on facilities. This inability to consider more effective frangible blast wall types limits the ability of designers to maximize the safety of their facilities and exposes their occupants to increased risk of loss of life, property damages, and economic losses in the event of an explosive attack.

The third distinctive capability of the present model is its ability to generate visualizations of the anticipated facility damage areas based upon the blast charge weight, blast wall type, and building material combinations. Existing models are incapable of generating visualizations that account for the pressure-mitigating effects of feasible rigid and frangible blast wall types. BEAM's ability to rapidly generate visualizations provides designers with a practical and reliable analysis tool to assess the impact of utilizing various frangible and rigid blast wall types to protect their constructed facilities. These generated visualizations enable designers to perform a visual risk management assessment of the design scenario and easily determine if any design changes are required to provide the desired level of protection for their constructed facilities.

3.7 Summary and Conclusions

This chapter presented a blast effects assessment model for quantifying and visualizing blast effects on constructed facilities behind rigid or frangible blast walls. The

model was developed in five main stages: (1) blast wall analysis stage that developed a methodology to quantify the performance of feasible frangible blast wall types including sand-filled, water-filled, and wood walls in reducing reflected pressure and impulse loading on facilities; (2) facility damage assessment stage that computed the percent area of each facility within five specified damage levels in order to calculate an overall facility damage level; (3) blast damage visualization stage that displayed anticipated facility damage areas based upon blast charge weight, blast wall type, and building material combinations; (4) performance analysis stage that evaluated the accuracy and efficiency of the developed model; and (5) case study stage that analyzed the performance of the developed model using an application example. The analysis of this case study illustrated the use of the model and demonstrated its unique capabilities. The model was able to efficiently predict the blast damage level for a constructed facility and generate blast damage visualizations for 540 feasible design alternatives comprised of 15 blast wall materials, two blast wall heights, six building materials, and three possible facility locations. The total computational time required for the model to analyze and generate results for these 540 feasible design alternatives was 97 seconds or an average of 0.18 seconds per design scenario.

The primary contribution of this research is the development of a novel model that enables designers to efficiently and accurately analyze and compare all feasible design alternatives in order to select an optimal design solution that minimizes the security risks to site personnel and facilities from the threat of an explosive attack. This developed model should prove useful for designers and construction managers of high-threat sites, allowing them to evaluate design options that may not have been previously

considered because of the significant computational time and effort required by numerical blast assessment models. The end result is a greater likelihood of designing a site that meets the functional and security requirements established by the site owners.

CHAPTER 4

FACILITY PROTECTION OPTIMIZATION MODEL

4.1 Introduction

The chapter presents the development of a multi-objective model for optimizing the site layout and selection of perimeter blast walls and building materials in order to minimize facility destruction levels from explosive attacks while minimizing site construction costs. The model is intended to equip planners of remote construction sites with the capability to efficiently analyze and compare all feasible design alternatives in order to construct remote sites that minimize the security risks to site personnel and facilities from the threat of explosive attacks in the most cost-effective manner. The model is developed in three main stages: (1) formulation stage that defines the relevant decision variables, formulates the objective functions, and identifies practical model constraints; (2) implementation stage that performs the optimization computations using multi-objective genetic algorithm; and (3) performance evaluation stage that analyzes an application example to evaluate and improve model performance. The following sections describe the three developmental stages of the present model.

4.2 Model Formulation

This stage presents the formulation of a novel multi-objective optimization model for optimizing the site layout and selection of perimeter blast walls and building materials for remote construction sites. This stage is accomplished in three steps: (1) defining the model decision variables; (2) formulating the facility destruction and construction cost objective functions; and (3) identifying all practical model constraints.

4.2.1 Decision Variables

The decision variables of the developed optimization model are selected to represent all feasible design alternatives of site layout and selection of perimeter blast walls and building materials. As shown in Figure 4.1, the model incorporates these decision variables in two main groups: (1) perimeter decision variables; and (2) facility decision variables. The first group represents all the decision variables that affect the location and performance of perimeter blast walls including perimeter location (PL), perimeter type (T) and perimeter height (H). The model enables planners to specify a feasible set of design alternatives for each of these three perimeter decision variables. The second group incorporates all the decision variables that affect the location and performance of site facilities including facility location (FLi), facility orientation (θ_i), and building material (Mi). Facility locations are defined within the model by the placement of their centroids on a user-specified grid system that allows planners to establish their preferred grid interval. Facility orientation is the degree that the facility is rotated about its centroid and is specified in this model to be 0 or 90°, which represents the most widely used orientations for rectangular shaped facility layouts. Facility location 1 (FL1) in Figure 4.1 shows the two possible facility rotation angles for a single facility location. Finally, building material will be selected from a set of feasible design alternatives that are specified by planners.

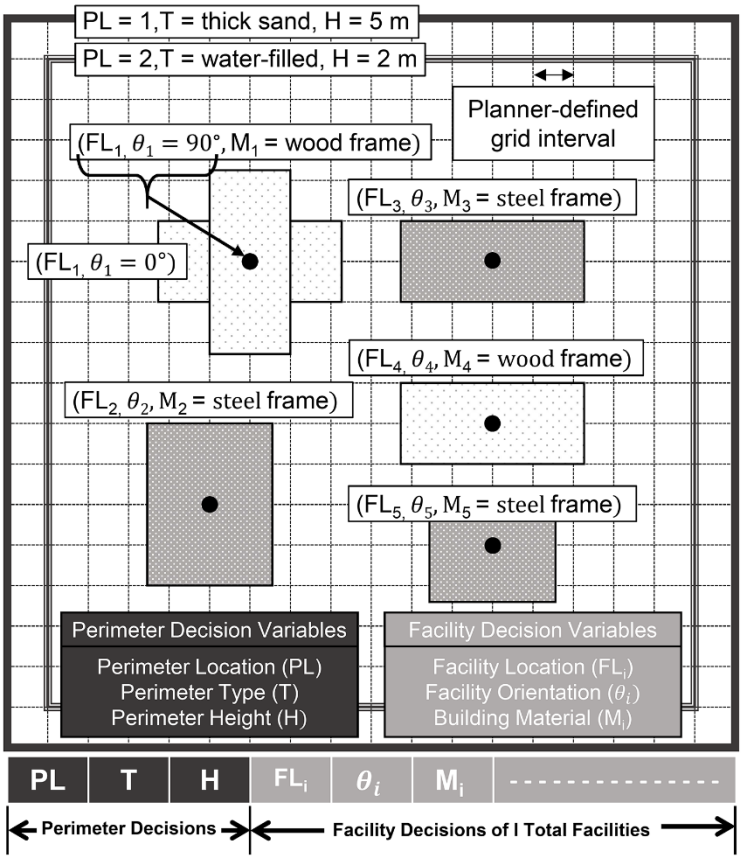

Figure 4.1 Model Decision Variables

4.2.2 Objective Functions

The present model is designed to accomplish two primary objectives: (1) minimize site facility destruction levels from explosive attacks; and (2) minimize site construction costs.

4.2.2.1 Minimizing Site Facility Destruction Levels

The first objective function in the present model is designed to minimize the destruction of site facilities inflicted by a specified explosive threat based on the performance of the selected site layout, perimeter blast walls and building materials. As shown in Eq. (4.1), the destruction of site facilities is quantified as the site destruction index (SDI), which ranges from 0% to 100%, where 0% represents no destruction and

100% represents complete destruction. SDI is quantified as the sum of the percent destruction of each facility $(\mathrm{PFD_i})$ multiplied by the importance weight of each facility on the site (w_i), as assigned by project planners. The use of importance weights provides planners with the flexibility to assign priority to facilities based on their criticality to the mission and purpose of the remote construction site.

The percent destruction of each facility $(\mathrm{PFD_i})$ is calculated using a recently developed model for quantifying blast effects on facilities behind blast walls (Schuldt and El-Rayes 2017) in five main phases that focus on: (1) establishing specified facility damage levels (j); (2) defining the percent destruction of each facility damage level (PD_j); (3) quantifying the standoff distances from an explosive at which each facility damage level is suffered; (4) determining the portion of every facility within each of the five damage level zones; and (5) computing the total percent destruction of each facility, as shown in Figure 4.2. The first phase of calculation establishes five facility damage levels (j), characterized by an increasing level of destruction: minimal, minor, moderate, heavy, and severe. This use of facility damage levels is consistent with established blast design practices and manuals (USACE 1999; DoD 2008b; FEMA 2011). The second phase defines the percent destruction for each facility damage level (PD_j) from a range of destruction as reported in existing design manuals (USACE 1999; FEMA 2011; DoD 2012). The PD_j values utilized in the present model for the five specified damage levels are 10%, 20%, 40%, 60%, and 100%, respectively, which represent the upper limit of these reported ranges in the aforementioned design manuals. The third phase quantifies the standoff distances at which the facility damage levels occur for each design scenario. These standoff distances form rings, centered at the blast location, that

define the zone in which each facility damage level (DL_j) is suffered. The fourth phase utilizes Shapely (Gillies 2013), a spatial analysis software package, to determine the portion of every facility within each of the five damage level zones. This phase employs automated computational geometry based on the defined grid-interval system to calculate the intersection areas of each facility and damage level zone. These intersection areas are expressed as the percent area of each facility within each of the five damage level zones (PFA_{ij}). The fifth phase computes the percent destruction of each facility (PFD_i) as the sum of the percent area of a facility within each of the five damage level zones (PFA_{ij}) multiplied by the corresponding percent destruction of each damage level (PD_j).

The aforementioned third phase requires detailed calculations to quantify the required standoff distances, which are the minimum acceptable separation distances between facilities and explosive attacks that will provide the specified levels of protection (U.S. Dept. of the Air Force 1997), for each feasible design combination that considers varying damage levels (j), blast charge weights (W), building materials (M), and perimeter blast wall types (T), and heights (H), if any. The present model is designed to provide the flexibility to quantify the required standoff distances for: (a) perimeter types that provide no blast attenuation, such as chain-link fence; and (b) rigid and frangible wall types that provide varying levels of blast attenuation. As shown in Figure 4.2, these detailed calculations of phase three are performed in three steps that are designed to: (1) identify the required standoff distances for perimeter types that provide no blast attenuation (S_j); (2) calculate blast loads on facilities at the identified

standoff distances; and (3) quantify the blast wall-adjusted standoff distances (AS_j) where blast loads on facilities are equal to those calculated in step two.

The first step identifies the required standoff distances for each combination of facility damage level (j), blast charge weight (W), and building material (M) for perimeter types that provide no blast attenuation, as shown in Figure 4.2. To determine these standoff distances, planners typically perform the time-consuming and often error-prone process of manually extracting the data for each design scenario from existing design manuals and charts (USACE 1999; DoD 2002, 2008a). The present model overcomes this limitation by automatically and accurately extracting the standoff distances for each design combination utilizing WebPlotDigitizer (Rohatgi 2016). The model integrates a constructed database containing the standoff distances for each combination of facility damage level, blast charge weights ranging from 22.7 kg to 18,182 kg, and the most commonly used building materials. This automated extraction process (a) eliminates the tedious requirement for planners to manually extract data for each design scenario; (b) ensures accuracy and high data fidelity levels within the model; and (c) greatly increases model computational efficiency. When blast walls are utilized, further calculations are necessary to quantify the blast wall-adjusted standoff distances (AS_j) required to provide an equivalent level of protection for facilities behind blast walls compared to the standoff distances (S_j) for facilities behind perimeter types that provide no blast attenuation.

The second step calculates the blast loads on facilities at the standoff distances identified in step one. This step computes the total applied force acting upon an identified facility that causes the specified level of damage. The present model is

designed to perform these calculations on the basis of peak reflected pressure (kPa) and reflected impulse (kPa-ms/kg$^{1/3}$). The listed equations in this paper present the performed calculations based on reflected impulse and it should be noted that the model computations based on reflected pressure are performed using a similar methodology. The reflected impulse loads are calculated for the standoff distances extracted from the aforementioned design manuals and charts in step one utilizing the Kingery-Bulmash equations (Kingery and Bulmash 1984), where reflected impulse is a function of scaled distance (standoff distance/blast charge weight$^{1/3}$).

The third step quantifies the blast wall-adjusted standoff distances (AS_j) where the reflected impulse loads on facilities behind rigid or frangible walls are equal to the reflected impulse loads at the standoff distances $\left(I_{\text{no wall},S_j}\right)$ calculated in step two, utilizing a hybrid solving method for nonlinear equations (Moré et al. 1980). Therefore, AS_j are the distances that provide an equivalent level of protection for facilities behind blast walls compared to the standoff distances for facilities behind perimeter types that provide no blast attenuation (S_j) identified in step one. The reflected impulse load behind a blast wall is calculated as the product of the impulse load when no wall is present $\left(I_{\text{no wall},AS_j}\right)$, the maximum reflected impulse adjustment factor for a rigid wall $\left(AF_{I_{max,R}}\right)$ (Zhou and Hao 2008), and the blast wall impulse effectiveness factor (EF_I), as shown in Eq. (4.2) and Figure 4.2. EF_I is a ratio that measures the performance of frangible blast wall types compared to a rigid blast wall in reducing impulse loading on facilities (Bogosian and Piepenburg 2002). As shown in Figure 4.3, the present model utilizes a newly developed set of effectiveness factors that expands the capability of $AF_{I_{max,R}}$ to consider the effectiveness of feasible frangible blast wall types, which have

been reported to provide comparable or greater levels of blast mitigation than a standard, rigid wall (Bogosian and Piepenburg 2002; Rose et al. 1998).

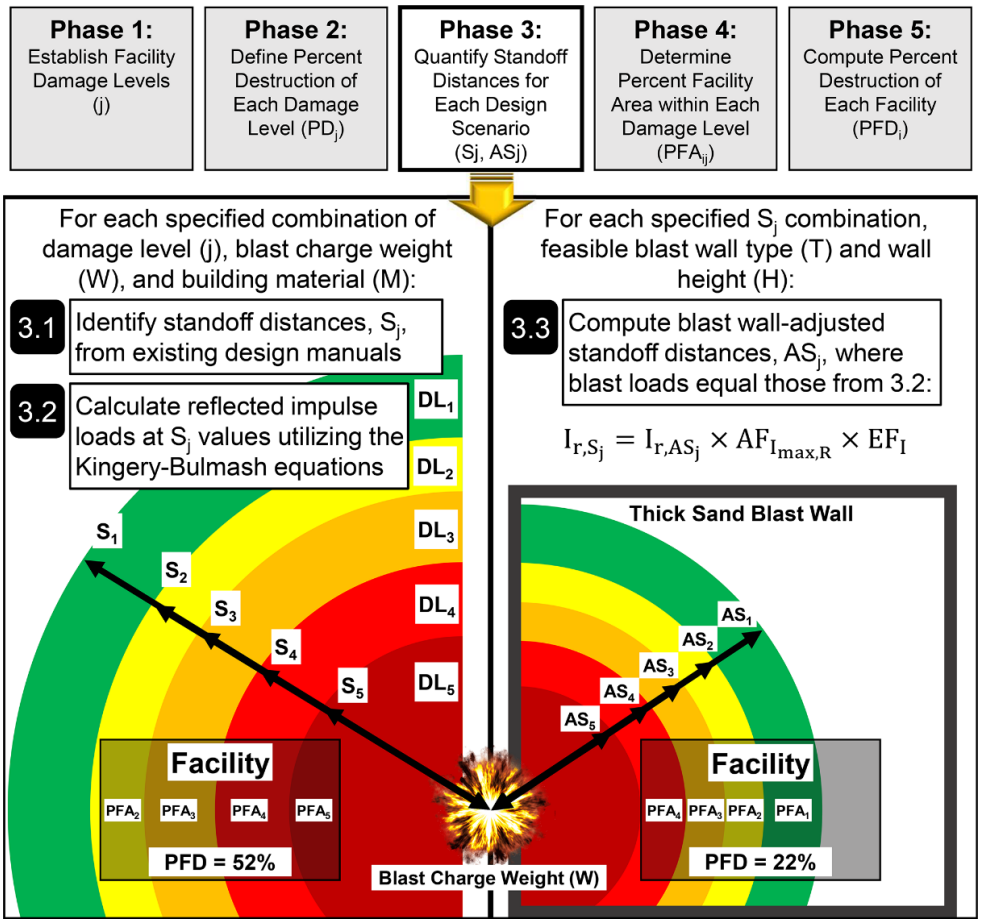

Figure 4.2 Phase Calculations of Percent Facility Destruction

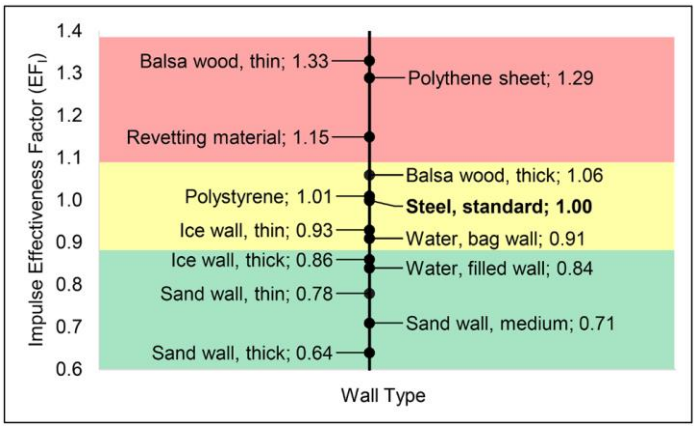

Figure 4.3 Newly Developed Set of Impulse Effectiveness Factors for 12 Frangible Wall Types

$$Minimize\ SDI = \sum_{i=1}^{I} w_i \times PFD_i \tag{4.1}$$

$$I_{r,S_j} = I_{r,AS_j} \times AF_{I_{max,R}} \times EF_I \tag{4.2}$$

where,

SDI = site destruction index;

i = facility number;

I = total number of facilities;

w_i = importance weight for each facility i, where $w_i > 0$ and $\sum_{i=1}^{I} w_i = 1$;

PFD_i = total percentage of destruction to facility i;

I_r = reflected impulse load on a facility (kPa-ms/kg1/3);

S_j = standoff distance for a facility with no blast wall at damage level j (m);

AS_j = blast wall-adjusted standoff distance for a facility at damage level j (m);

$AF_{I_{max,R}}$ = maximum reflected impulse adjustment factor for rigid walls; and

EF_I = blast wall impulse effectiveness factor.

4.2.2.2 Minimizing Construction Cost

The second objective function in the present model is designed to minimize the construction costs of integrating site security measures that include constructing perimeter blast walls and hardening site facilities. As shown in Eq. (4.3), the site construction cost (SCC) incorporates initial construction costs (ICC) and the present value of future wall replacement costs (WRC). First, ICC is comprised of the perimeter

wall construction costs and facility hardening costs [see Eq. (4.4)]. Perimeter wall costs are calculated as the product of the perimeter wall length (PL) and the wall construction unit cost ($WC_{T,H}$), as shown in Eq. (4.4). The total perimeter wall length is calculated based upon the selection of the blast wall location decision variable from the set of feasible alternatives defined by planners. The wall construction unit cost is the cost to construct a linear meter of the selected blast wall based upon the wall type (T) and wall height (H). Facility hardening costs are calculated using the facility area (FA_i) and the facility construction unit cost (FC_M). The facility construction unit cost is the cost to construct a square meter of the selected building material (M). The total facility hardening cost is equal to the sum of the facility area multiplied by the facility construction unit cost for all site facilities, as shown in Eq. (4.4).

Second, the present value of future perimeter wall replacement costs (WRC) is computed as the product of the perimeter wall length of the selected blast wall location (PL_{WL}), the number of times a wall must be replaced over the anticipated site lifespan, the wall replacement unit cost ($WR_{T,H}$), and discount rate (D) to calculate the present value of future costs as shown in Eq. (4.5). The number of times the selected wall will need to be replaced is calculated by rounding up the integer value of the anticipated site lifespan (LS) divided by the design life of the selected blast wall (DL) minus the initial wall construction, as shown in Eq. (4.5). For example, if a blast wall has a design life of six years and the anticipated site lifespan is twenty years, the blast wall will need to be replaced three times after the lifespan of the first constructed wall (20 divided by 6 – 1 = 2.33, rounded up to 3). The wall replacement unit cost is the cost to remove and

reconstruct a linear meter of the selected blast wall based upon the wall type (T) and wall height (H).

$$Minimize\ SCC = ICC + WRC \tag{4.3}$$

$$ICC = PL_{WL} \times WC_{T,H} + \sum_{i=1}^{I} FA_i \times FC_M \tag{4.4}$$

$$WRC = D\left(PL_{WL} \times \left\lceil \frac{LS}{DL_{T,H}} - 1 \right\rceil \times WR_{T,H}\right) \tag{4.5}$$

where,

SCC = site construction cost ($);

ICC = initial construction cost ($);

WRC = present value of future replacement costs of the perimeter wall ($);

PL_{WL} = perimeter wall length (m) based upon the selected option for wall location (WL);

$WC_{T,H}$ = wall construction unit cost based upon the selected wall type (T) and wall height (H) ($/m);

FA_i = area of facility i (m^2);

FC_M = facility construction unit cost based upon the selected building material (M) ($/$m^2$);

D = discount rate to calculate the present value of future costs (%);

LS = expected site lifespan (years);

$DL_{T,H}$ = design life of selected blast wall based upon the wall type (T) and wall height (H) (years); and

$WR_{T,H}$ = wall replacement unit cost based upon the selected wall type (T) and wall height (H) ($/m).

4.2.3 Model Constraints

The present model was designed to comply with all practical constraints that can be encountered in the planning of remote construction sites, including: (1) site boundary; (2) facility overlap; (3) minimum distance; and (4) maximum distance. These constraints, as shown in Figure 4.4, ensure model efficacy and enhance model performance by incorporating planner preferences. Each of the constraint types is briefly discussed below.

Site boundary and facility overlap constraints are mandatory to ensure the feasibility of generated solutions by avoiding spatial conflicts (El-Rayes and Said 2009; Zouein and Tommelein 1999). The first constraint type, site boundary, is employed to guarantee that all facilities are positioned within the selected site perimeter, as shown in Figure 4.4a. Boundary constraints are analyzed using automated computational geometry to calculate the area of each facility outside the site perimeter. The boundary constraint is violated when the calculated area of a facility outside the site perimeter is greater than zero. The second constraint type, facility overlap, is utilized to ensure that proposed facility locations do not overlap one another. Facility overlap constraints are tested by calculating the intersection area between each pair of proposed facility locations on the site. The facility overlap constraint is violated when the calculated intersection area between a pair of facilities is greater than zero. In Figure 4.4a, facility 1 violates the site boundary constraint but complies with the facility overlap constraint, while facilities 2 and 3 comply with the site boundary constraint but violate the facility

overlap constraint, and facility 4 complies with both the site boundary and facility overlap constraints.

Minimum and maximum distance constraints are incorporated into the present model to enforce compliance with security and safety requirements and to enable planners to integrate design preferences, as shown in Figure 4.4b. The third constraint of minimum distance establishes a buffer area around facilities in which other facilities cannot be constructed. For example, minimum separation distances between facilities may be required to allow for emergency vehicle access. Another example of this constraint is a specified minimum separation distance between hazardous materials (HAZMAT) storage areas and housing buildings. The fourth constraint of maximum distance establishes a buffer area around facilities in which other facilities must be located. For example, maximum distance constraints may be established to limit the walking distance of senior decision makers to the headquarters (HQ) office building in case of a rapid response scenario. Both minimum and maximum distance constraints are evaluated similarly to the aforementioned facility overlap constraints, where the intersection area between each pair of facilities is calculated; however, a buffer equal to the required minimum/maximum distance is added to the facility dimensions. The minimum distance constraint is violated when the calculated intersection area between a pair of facilities and their minimum separation distance is greater than zero. The maximum distance constraint is violated when the calculated intersection area is equal to zero. For example, there is a minimum separation distance from facility 1 in the layout in Figure 4.4b and therefore, facility 2 violates this constraint while facilities 3 and 4 comply with this constraint. Similarly, there is a maximum distance constraint imposed

around facility 1 in Figure 4.4b and accordingly both facilities 2 and 3 violate this constraint.

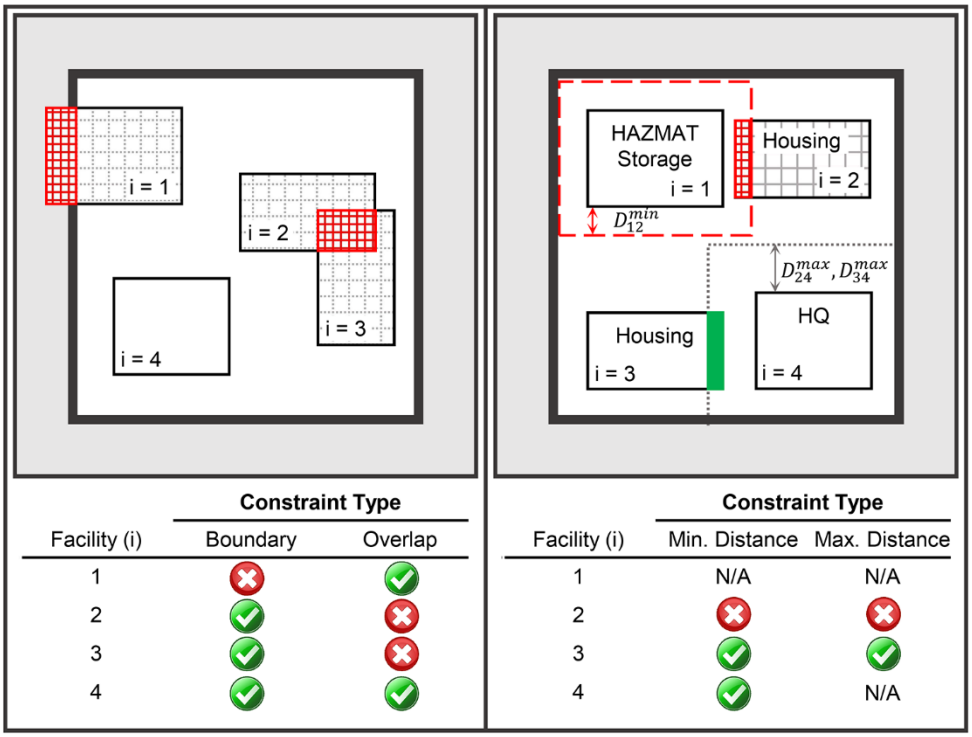

Facility (i)	Constraint Type: Boundary	Constraint Type: Overlap
1	✗	✓
2	✓	✗
3	✓	✗
4	✓	✓

(a)

Facility (i)	Constraint Type: Min. Distance	Constraint Type: Max. Distance
1	N/A	N/A
2	✗	✗
3	✓	✓
4	✓	N/A

(b)

Figure 4.4 Model Constraints: (a) Boundary and Overlap; (b) Minimum/Maximum Distance

4.3 Model Implementation

In order to support planners in their critical task of analyzing optimal tradeoffs between minimizing facility destruction levels from explosive attacks and minimizing site construction costs, the present model is implemented as a multi-objective genetic algorithm (MOGA). MOGA was selected to perform the model computations because of its proven capabilities in: (1) modeling non-linear objective functions and constraints; (2) identifying near optimal solutions within a practical computational time; and (3) successfully modeling previous facility layout and construction optimization problems (Said and El-Rayes 2010; Mawdesley et al. 2002; Elbeltagi et al. 2004; Khalafallah and

El-Rayes 2011). The present model was implemented utilizing the nondominated sorting genetic algorithm II (NSGA-II) (Deb et al. 2002) and executed with the Distributed Evolutionary Algorithms toolbox (Fortin et al. 2012) for Python (Rossum 1995). The model was implemented in four main steps: (1) data input; (2) initialization (3) fitness evaluation; and (4) data output, as shown in Figure 4.5 and described below.

In the first implementation step, planners need to provide two sets of input data that specify: (1) all required site layout and security measure data; and (2) MOGA search parameters. The first set of input data includes: (a) feasible blast walls characteristics including perimeter location, type, height, and design life; (b) available building materials; (c) blast wall and building material cost data; (d) facility geometries; (e) facility importance weights; (f) site lifespan; and (g) blast charge weight. The second set of input data specifies the required MOGA search parameters, including: (a) population size (P); (b) number of generations (G); (c) mutation rate (p_m); and (d) crossover rate (p_c).

The second implementation step initiates the search process by: (1) reading in the specified MOGA parameters; and (2) randomly generating an initial set of solutions (s = 1 to S) that forms the initial population (P_1) of the first generation (g = 1). This set of solutions represents feasible alternatives of facility layout, blast wall, and building material decisions.

The third implementation step evaluates the fitness of the generated solutions by: (1) calculating the site destruction index (SDI) based upon the facility layout and selected security measures for each solution (s) in generation (g); (2) calculating the site construction cost (SCC) of each solution (s) in generation (g) based upon the

selected blast wall and building materials; (3) computing a site penalty score for each solution (s) based upon the percent area of site facilities that violate specified geometric constraints; (4) selecting the fittest individuals within the population; and (5) utilizing selection, crossover, and mutation operators in order to generate a new offspring population (g = g+1). This five-step process is repeated until the specified number of generations (g = G) has been reached.

In the fourth implementation step, the model can be used to generate and visualize the optimization output data. This enables planners to: (1) produce a database of the generated optimal tradeoff solutions between the objectives of minimizing SDI and minimizing SCC; (2) graphically represent the tradeoff curves of the nondominated Pareto frontier solutions, as shown in Figure 4.5; and (3) generate visualizations of the optimal site layout plans using matplotlib (Hunter 2007) (Figure 4.5). The output data and visualizations enable planners to analyze and select the optimal facility layout and selection of security measures based upon their required level of facility protection or available construction budget.

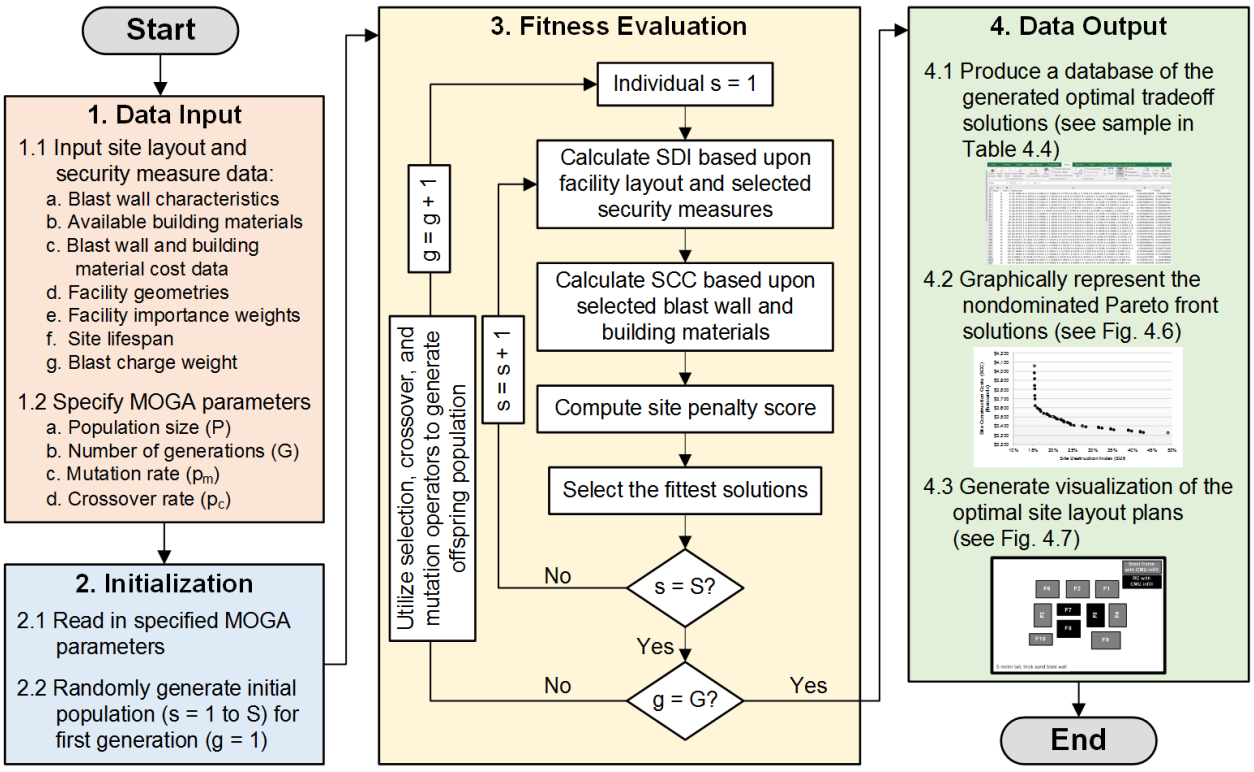

Figure 4.5 Model Implementation

4.4 Performance Evaluation

This stage analyzes an application example to evaluate the performance of the developed model and demonstrate its distinctive capabilities in optimizing remote construction site layouts and generating optimal tradeoffs between minimizing facility destruction levels from explosive attacks and minimizing site construction costs. The application example represents a hypothetical military forward operating base designed to house and support the operations of 75 personnel. In this example, the base is assumed to be: (1) located in a remote area in an overseas country with a construction area cost factor of 1.67 (USACE 2016); (2) positioned in an available site area of 90 meters by 60 meters; and (3) comprised of one-story facilities with a three-meter minimum separation distance between all facilities.

The application example requires the construction of ten facilities to house and support the operations of the military base, including a headquarters office facility, dormitories, a senior officer dormitory, a dining facility, a gymnasium, a maintenance facility, and a storage facility. In order to perform the optimization of this application example, planners need to specify the input data discussed in the model implementation phase, including the: (1) characteristics of feasible perimeter blast wall types, as shown in Table 4.1; (2) available facility building materials, as shown in Table 4.2; (3) estimated construction costs of blast walls and building materials, as well as replacement costs of blast walls, as shown in Table 4.1 and Table 4.2; (4) dimensions of each site facility (Lx, Ly), as shown in Table 4.3; (5) importance weight assigned to each site facility, as shown in Table 4.3; (6) expected operational lifespan of twenty years; and (7) anticipated maximum explosive threat of 454.5 kg (1,000 lb) based upon local intelligence, which is the design blast charge weight carried in a full-size van (FEMA 2011). This application example subjects the base to uniformly distributed threats from all four sides of the perimeter wall. It should be noted that the facility importance weights in Table 4.3 are assigned for the purpose of analyzing this application example and that the model provides the flexibility to assign priority to facilities based on their criticality to the mission and the purpose of the remote construction site.

Table 4.1 Characteristics of Available Blast Walls

ID	Wall type (WT)	Wall height H (m)	Construction Cost[a] $WC_{T,H}$ ($/m)	Replacement Cost[a] $WR_{T,H}$($/m)	Design Life $\mathrm{DL_{T,H}}$ (years)
1	Balsa wood, thick	2	544	816	20
2	Balsa wood, thick	5	1,361	2,042	20
3	Balsa wood, thin	2	436	654	20
4	Balsa wood, thin	5	1,089	1,634	20
5	CMU	2	438	657	10
6	CMU	5	1,094	1,641	10
7	Concrete, thin panel	2	431	647	15
8	Concrete, thin panel	5	1,077	1,616	15
9	Polystyrene	2	640	960	10
10	Polystyrene	5	1,598	2,397	10
11	Polythene sheet	2	561	842	10
12	Polythene sheet	5	1,402	2,103	10
13	Revetting material	2	601	902	10
14	Revetting material	5	1,501	2,252	10
15	Sand, thick	2	524	786	4
16	Sand, thick	5	624	936	4
17	Sand, medium	2	339	509	4
18	Sand, medium	5	458	687	4
19	Sand, thin	2	267	401	4
20	Sand, thin	5	386	579	4
21	Steel	2	1,015	1,523	20
22	Steel	5	2,537	3,806	20
23	Water, bag	2	752	1,128	7
24	Water, bag	5	1,002	1,503	7
25	Water, filled	2	534	801	7
26	Water, filled	5	668	1,002	7

[a]Costs were determined from the 2017 RS Means, when available, or Army Corps of Engineers subject matter experts

Table 4.2 Building Material Options and Construction Costs

ID	Building Material	Construction Cost FC_M ($/m2)
1	Wood frame	3,090
2	Pre-engineered metal	3,150
3	Unreinforced masonry	3,300
4	Steel frame with lightly reinforced CMU infill walls	3,380
5	Reinforced concrete	3,560
6	Reinforced concrete with lightly reinforced CMU infill walls	4,400

[a]Costs were determined from the 2017 RS Means, when available, or Army Corps of Engineers subject matter experts

Table 4.3 Site Facilities, Dimensions, and Importance Weights

		Dimensions		
ID	Description	Lx (m)	Ly (m)	w_i
F1	Dormitory	12	9	0.05
F2	Dormitory	12	9	0.05
F3	Dormitory	12	9	0.05
F4	Dormitory	12	9	0.05
F5	Dining Facility	12	9	0.2
F6	Gymnasium	12	9	0.05
F7	Headquarters	12	6	0.3
F8	Senior Officer Dormitory	12	9	0.2
F9	Storage	15	9	0.02
F10	Maintenance	12	6	0.03

The developed optimization model was used to search for and identify optimal site layout and security decisions for this remotely located base. The optimization model utilizes the aforementioned multi-objective genetic algorithm (MOGA) computations. The optimal MOGA search parameters were identified for this application example based on a large number of experiments that evaluated a wide range of population sizes, number of generations, mutation rates, crossover rates, and crossover types as shown in Table 4.4. Accordingly, these MOGA parameters were specified for this application example to be a population size of 150, 600 generations, a mutation rate of 0.01, and two-point crossover with a crossover rate of 0.50.

Table 4.4 MOGA Search Parameter Experiments

ID	Population	Generations	Mutation rate	Crossover rate	Crossover Type
1	50	150	0.001	0.10	one-point
2	50	150	0.001	0.10	two-point
3	50	150	0.001	0.25	one-point
4	50	150	0.001	0.25	two-point
5	50	150	0.001	0.50	one-point
6	50	150	0.001	0.50	two-point
7	50	150	0.001	0.75	one-point
8	50	150	0.001	0.75	two-point
9	50	150	0.001	0.90	one-point
10	50	150	0.001	0.90	two-point
11	50	150	0.002	0.10	two-point
12	50	150	0.002	0.25	two-point
13	50	150	0.002	0.50	two-point

Table 4.4 (cont.)

14	50	150	0.002	0.75	two-point
15	50	150	0.002	0.90	two-point
16	50	150	0.005	0.10	two-point
17	50	150	0.005	0.25	two-point
18	50	150	0.005	0.50	two-point
19	50	150	0.005	0.75	two-point
20	50	150	0.005	0.90	two-point
21	50	150	0.010	0.10	two-point
22	50	150	0.010	0.25	two-point
23	50	150	0.010	0.50	two-point
24	50	150	0.010	0.75	two-point
25	50	150	0.010	0.90	two-point
26	150	150	0.010	0.50	two-point
27	300	150	0.010	0.50	two-point
28	600	150	0.010	0.50	two-point
29	150	300	0.010	0.50	two-point
30	300	300	0.010	0.50	two-point
31[a]	150	600	0.010	0.50	two-point
32	150	1,500	0.010	0.50	two-point

[a]Provided the best combination of performance and computational time

The search space for this application example includes more than 17.5 million unique combinations of facility layout and security decisions, which represents the product of multiplying the total number of all feasible alternatives for the aforementioned six decision variable types. Each of these 17.5 million possible combinations represents varying performance in the aforementioned objectives of minimizing SDI and minimizing SCC. The developed optimization model, performed using MOGA, was used to perform an efficient and effective search of this large search space of feasible design alternatives in order to identify near-optimal solutions. The model generated a broad spectrum of 72 Pareto-optimal (i.e. nondominated) solutions that represent a unique and optimal tradeoff between the two optimization objectives. The generated Pareto-optimal solutions result in expected damage levels ranging from 14% to 68% and site construction costs between $5.25 million and $3.41 million, respectively, as shown in Figure 4.6.

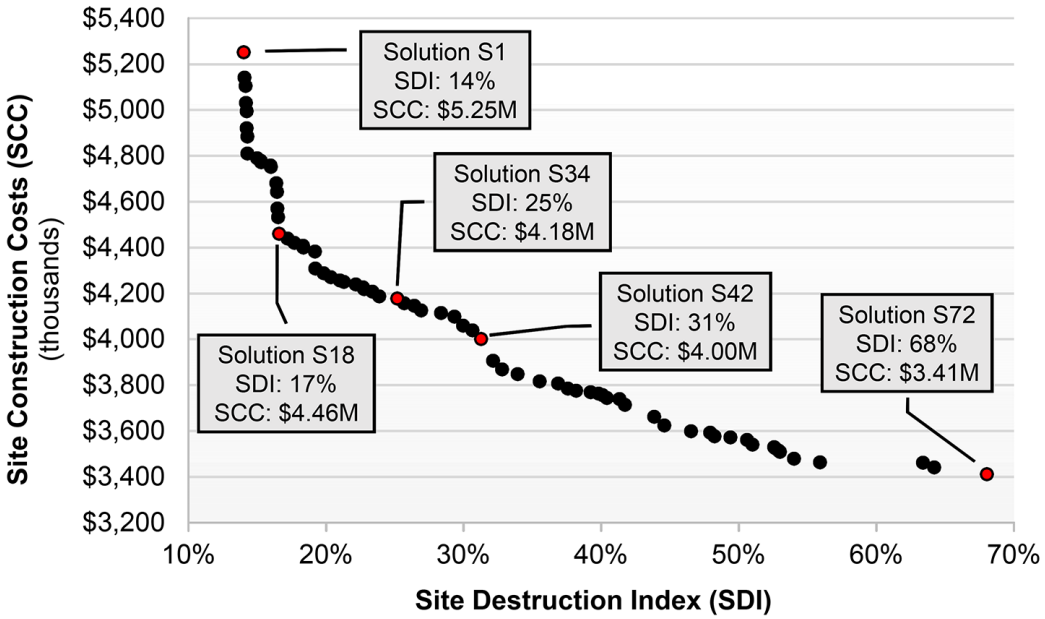

Figure 4.6 Generated Pareto-optimal Solutions

On one end of the spectrum, solution S1 represents the generated Pareto-optimal solution that results in the lowest overall level of site destruction (14%). This minimum SDI was achieved by: (1) utilizing the layout shown in Figure 4.7a, where the standoff distances between the facilities and site perimeter are as large as possible and the facilities with the highest importance weights (w_i) are placed near the center of the site; (2) constructing the most blast-resistant perimeter wall, a five-meter tall, thick sand blast wall; and (3) constructing all facilities from steel frame or reinforced concrete with lightly reinforced CMU infill walls, which provide the highest levels of blast-resistance. This solution, however, is the most expensive, with a site construction cost of $5.25 million.

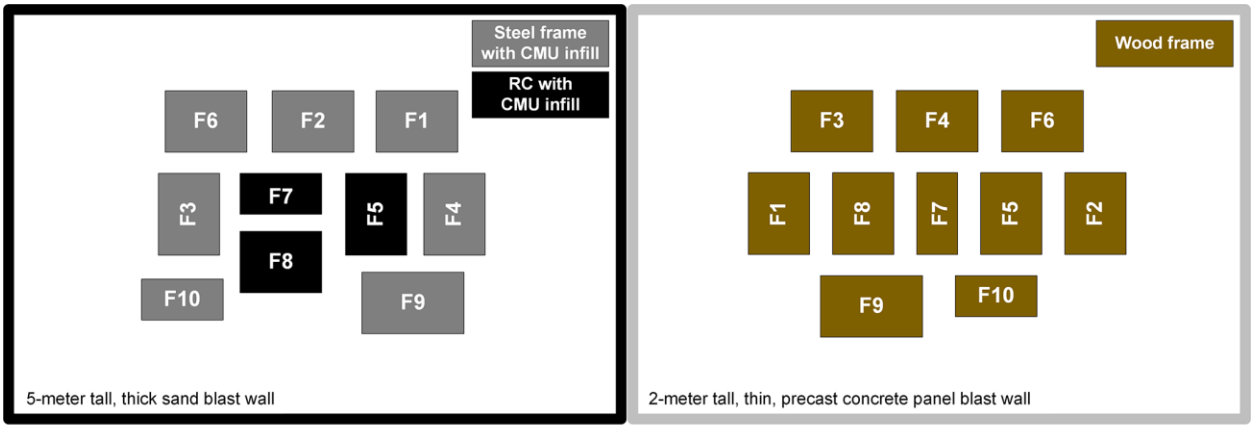

(a) (b)

Figure 4.7 Site Layout Plan for Solutions (a) S1 and (b) S72

At the other end of the spectrum, solution S72 represents the generated Pareto-optimal solution that results in the lowest site construction cost ($3.41 million). This minimum SCC was achieved by: (1) employing the site layout shown in Figure 4.7b; (2) building a two-meter tall, thin, balsa wood blast wall; and (3) selecting wood-frame construction for all ten buildings. While this solution does result in the lowest site construction cost, planners face an extremely high expected site damage level of 68% in the event of a 454.5 kg explosive attack. The similarity between the site layouts of solutions S1 and S72 clearly illustrate that increasing standoff distance by locating all facilities towards the center of the site layout has a significant impact on minimizing the potential effects of an explosive attack with little or no additional cost. To achieve further reduction in site destruction levels, solution S1 selects more costly alternatives for the perimeter blast wall and building materials, which provides additional protection at an increased cost.

Between the two ends of the spectrum, the model generated 70 other Pareto-optimal solutions that enable planners to analyze and select the design that best meets their unique project requirements based upon: (1) maximum acceptable level of site

destruction; (2) maximum available construction budget; and/or (3) minimizing site destruction levels with the least additional cost. For example, solution S34 represents the solution that costs the least amount of money to construct a site ($4.18 million) where the expected level of destruction does not exceed 25%. Likewise, solution S42 represents the solution that results in the lowest level of site destruction (31%) while complying with a maximum available construction budget of $4.00 million (see Figure 4.7). Similarly, solution S18 represents the solution that results in a site destruction level of 17%, which is near the lowest overall level of site destruction identified in solution S1 (14%), but is achieved at a substantially reduced cost of $4.46 million compared to $5.25 million for solution S1. Table 4.5 provides a sample of the optimal decision variable solutions for the solutions discussed in this section.

Table 4.5 Sample Optimization Results

Solution	Blast Wall	Building Material										SDI (%)	SCC ($M)
		F1	F2	F3	F4	F5	F6	F7	F8	F9	F10		
S1	8	4	4	4	4	6	4	6	6	4	4	14	5.25
S18	20	4	4	4	4	4	4	4	4	4	4	17	4.46
S34	22	4	1	4	1	4	1	4	4	1	4	25	4.18
S42	21	4	4	4	4	4	4	4	4	1	1	31	4.00
S72	29	1	1	1	1	1	1	1	1	1	1	68	3.41

4.5 Summary and Conclusions

A novel multi-objective optimization model was developed to identify optimal site layout and security decisions for remote construction sites. The model provides the capability of generating optimal tradeoffs between the two main objectives of minimizing facility destruction levels from explosive attacks and minimizing site construction costs. The model was developed in three main stages: (1) formulation stage that defined the relevant decision variables, formulated the objective functions and identified practical

model constraints; (2) implementation stage that performed the optimization computations using multi-objective genetic algorithm; and (3) performance evaluation stage that analyzed an application example to evaluate model performance. The application example optimized the design and construction decisions to protect a hypothetical remote military base against the identified threat of a 454.5 kg (1,000 lb) explosive attack. The results of this analysis demonstrated the model's distinctive capabilities in optimizing construction site layout and security decisions by generating 72 Pareto-optimal solutions that represent unique optimal tradeoffs between minimizing facility destruction levels from explosive attacks and minimizing site construction costs.

The primary contribution this research makes to the body of knowledge is the development of a novel model that is uniquely capable of: (a) optimizing both the site layout planning and selection of perimeter blast walls and building materials; and (b) generating optimal tradeoffs between minimizing facility destruction levels from explosive attacks and minimizing site construction costs. The developed model should prove useful for planners of high-threat, remote sites, enabling them to efficiently and effectively evaluate all feasible design alternatives. This capability results in the construction of cost-effective, high-performance sites that will lower the risks to site personnel and facilities from the devastating effects of an explosive attack.

CHAPTER 5

BLAST CONSEQUENCE MITIGATION MODEL

5.1 Introduction

This chapter presents the development of a novel multi-objective optimization model for the layout and security planning of remote construction sites that provides the capability of minimizing the consequences of an explosive attack and minimizing the construction cost of remote sites. Designers and site layout planners of remote sites often have limited construction budgets and confined site layout spaces with which to meet the mission requirements of the site and provide maximum security to site personnel and facilities. The model is intended to support designers in their critical task of searching for and identifying optimal remote construction site layouts in order to construct remote sites that minimize the personnel loss, psychological impact, economic loss, and operational impact in the event of an explosive attack while minimizing site construction costs. The model is developed in three main stages: (1) consequence identification stage that quantifies the consequences of explosive attacks targeting facilities; (2) formulation stage that identifies the relevant decision variables, formulates the objective functions, and defines all practical constraints; and (3) implementation stage that performs the optimization computations using genetic algorithm and specifies the model input and output data, as shown in Figure 5.1. The performance of the developed model is analyzed using a case study that is designed to illustrate the use of the model and demonstrate its unique capabilities. The following sections describe these three development stages.

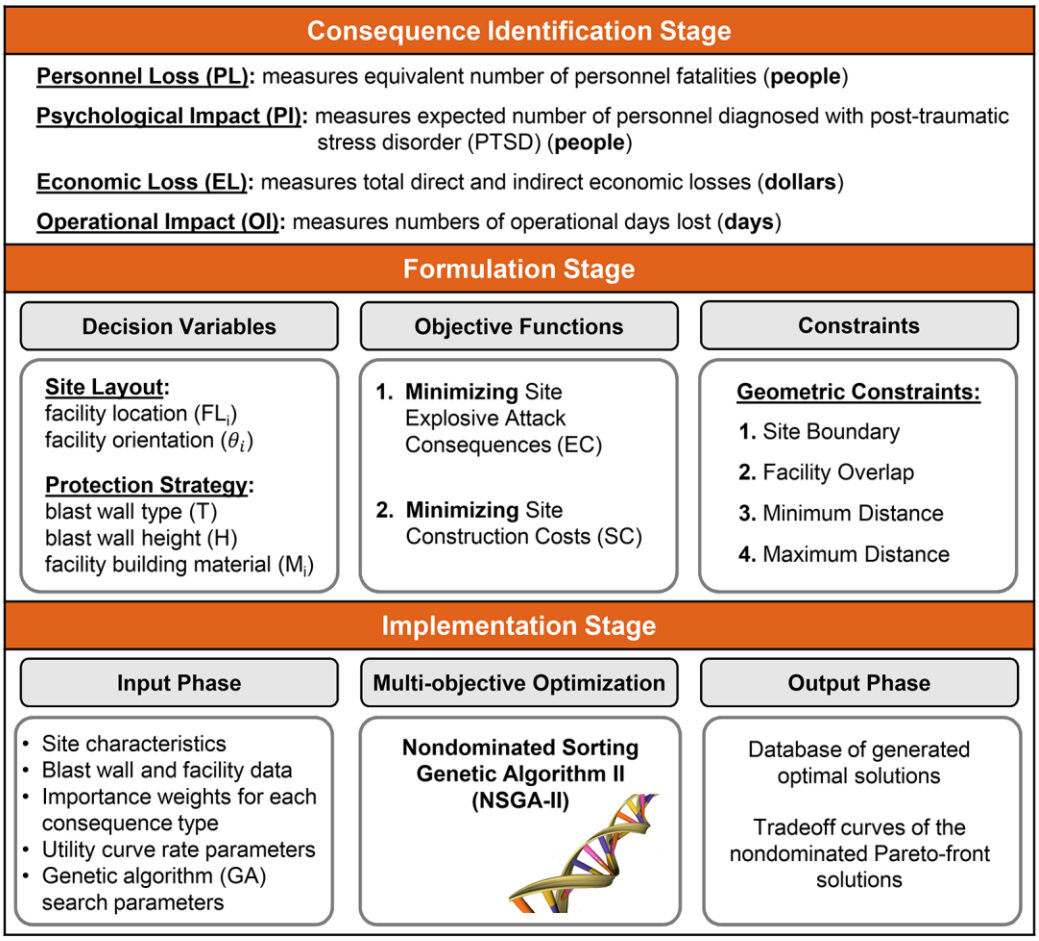

Figure 5.1. Optimization Model Development Stages

5.2 Consequence Identification

This stage of model development is designed to quantify the consequences of explosive attacks on remote construction sites. These consequences are identified and organized in the present model using a similar approach to the one adopted by the Federal Emergency Management Agency (FEMA). Accordingly, the present model quantifies four main consequences of explosive attacks: (1) personnel loss (PL); (2) psychological impact (PI); (3) economic loss (EL); and (4) operational impact (OI).

5.2.1 Personnel Loss (PL)

Personnel loss (PL) is designed to measure and minimize the extent of fatalities and injuries inflicted on occupants of a remote site from an explosive attack. The overall PL is presented as the site personnel loss equivalence (PLE_{site}), which is a measure of the total equivalent number of fatalities and is defined as the weighted sum of three personnel loss types: fatalities (P^F), serious injuries (P^{SI}), and minor injuries (P^{MI}), as shown in Eq. (5.1). The use of weights (w^{PL}) provides designers with the capability and flexibility to consider varying user-specified weights to represent the relative impact of these three personnel losses types (w^F, w^{SI}, w^{MI}), which differs from one decision maker to another. For example, the model utilizes default weights of 1.0, 0.7 and 0.085 for fatalities, serious injuries and minor injuries, respectively, based on the reported compensations provided for these three personnel loss types after the 9/11 terrorist attacks (Dixon and Stern 2004).

$$PLE_{site} = \lceil P^F \times w^F + P^{SI} \times w^{SI} + P^{MI} \times w^{MI} \rceil \quad (5.1)$$

where,

PLE_{site} = equivalent number of personnel fatalities on site;

P^F, P^{SI}, P^{MI} = number of personnel expected to suffer fatalities, serious injuries and minor injuries, respectively; and

w^F, w^{SI}, w^{MI} = importance weight for fatalities, serious injuries and minor injuries, respectively, where $0 \leq w^{PL} \leq 1$.

Each of the aforementioned personnel loss types: fatalities (P^F), serious injuries (P^{SI}), and minor injuries (P^{MI}) is calculated in two main steps that are designed to

compute: (1) the percent area of each facility within specified damage levels; and (2) the number of personnel expected to suffer fatalities, serious injuries and minor injuries.

The first step is designed to compute the percent area of each facility that is subjected to either minimal, minor, moderate, heavy, or severe damage levels ($PFA_{i,j}$) resulting from an explosive attack, as shown in Figure 5.2. The computations in this step are performed using a recently developed model for quantifying blast effects on facilities behind blast walls (Schuldt and El-Rayes 2017). The area of the aforementioned five damage levels are represented as concentric rings, centered at the blast location, with radii equal to the standoff distance at which each facility damage level occurs.

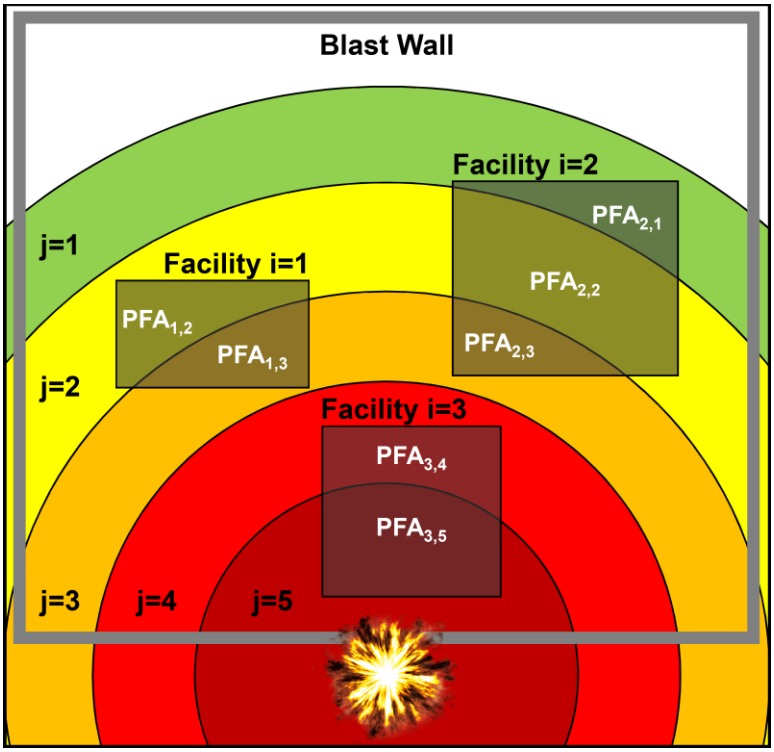

Figure 5.2 Percent facility area within each damage level ($PFA_{i,j}$)

The second step computes the total number of personnel expected to suffer fatalities, serious injuries and minor injuries in all facilities on site. Each of these

personnel loss types is calculated as the product of multiplying the percent facility area within each damage level ($PFA_{i,j}$), the assigned facility population (Pop_i), and the ratio of the facility population expected to suffer each personnel loss type within each facility damage level $\left(R_j^{PL}\right)$. For example, Eq. (5.2) illustrates the computations of the total number of fatalities in all facilities on site. Similarly, the total number of serious injuries and minor injuries in the entire site are calculated using similar equations to Eq. (5.2). These computations are based on two assumptions: (1) the assigned Pop_i is assumed to be uniformly distributed within each facility and is calculated based on the prorated amount of time individuals occupy a facility each day; and (2) R_j^{PL} represents the upper limit of reported ranges of injury levels as identified in existing design manuals (DoD 2012; USACE 1999), as shown in Figure 5.3.

$$P^F = \sum_{i=1}^{I} \sum_{j=1}^{5} PFA_{i,j} \times Pop_i \times R_j^F \tag{5.2}$$

where,

i = facility number;

I = total number of facilities on site;

j = facility damage level, where j = 1,2,3,4,5 represents minimal, minor, moderate, heavy, and severe damage, respectively;

$PFA_{i,j}$ = percent facility area (i) that suffers damage level (j);

Pop_i = number of personnel assigned to facility i; and

R_j^F = ratio of personnel expected to suffer fatalities per damage level (j).

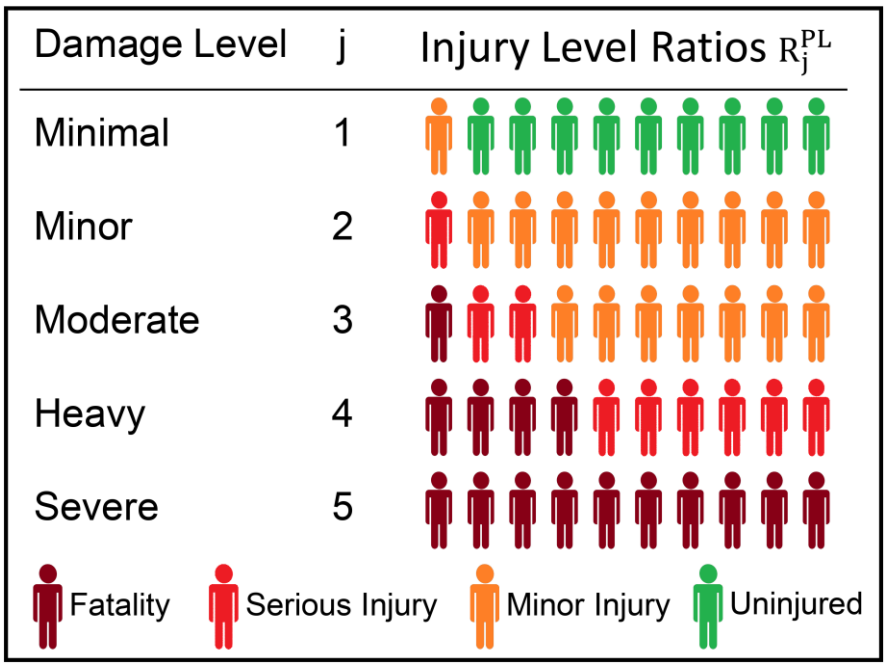

Figure 5.3 Ratio of personnel expected to suffer injury levels within each facility damage level $\left(R_j^{PL}\right)$

5.2.2 Psychological Impact Index

Psychological impact (PI) is designed to evaluate and minimize the degree of emotional and psychological disorders suffered by the survivors of explosive attacks on remote sites. Accordingly, the present study quantifies PI by the prevalence of post-traumatic stress disorder (PTSD) among survivors because PTSD is the most studied, best-defined, and one of the most frequent and debilitating psychological disorders experienced in the aftermath of explosive attacks (Butler et al. 2003; Gabriel et al. 2007; Neria et al. 2008).

Psychological impact is calculated as the total number of personnel expected to suffer PTSD on the site (PI_{site}). The rate that survivors of explosive attacks experience PTSD is reported to vary by personnel degree of exposure. Specifically, the prevalence of PTSD among personnel injured in an explosive attack is reported to range from 30-40%, while the reported PTSD rate of uninjured personnel is between 5% and 10%

(Neria et al. 2008). To consider the most critical design cases, the present model utilizes the upper limit of these reported ranges (40% and 10%) to define the expected PTSD rates for injured (P^I) and uninjured (P^U) survivors, as shown in Eq. (5.3). The number of injured personnel is calculated using Eq. (5.4) and the number of uninjured personnel is equal to the site population (Pop_{site}) minus the number of personnel fatalities and injured personnel, as shown in Eq. (5.5).

$$PI_{site} = \lceil 0.4 \times P^I + 0.1 \times P^U \rceil \tag{5.3}$$

$$P^I = P^{SI} + P^{MI} \tag{5.4}$$

$$P^U = Pop_{site} - (P^F + P^I) \tag{5.5}$$

where,

PI_{site} = number of site personnel expected to be diagnosed with PTSD;

P^I = number of injured personnel on site;

P^U = number of uninjured personnel on site; and

Pop_{site} = total site population.

5.2.3 Economic Loss Index

Economic loss (EL) is designed to assess and minimize the total economic loss inflicted on a site by an explosive attack. The overall EL represents the site total economic loss (TEL_{site}) that consists of: (a) the sum of all facility direct losses (DL_i), including damages to facilities and assets, and (b) facility indirect losses (IL_i) resulting from facility interruptions that degrade the capability of the site to provide goods and services (Pelling et al. 2002), as shown in Eq. (5.10). TEL_{site} is computed in four main steps that are designed to calculate: (1) the total percent destruction of each facility; (2)

the direct losses for each facility; (3) the indirect losses for each facility; (4) site total economic loss.

The first step is designed to calculate the percent destruction inflicted on each facility from an explosive attack (PFD_i). The quantification of these percent facility destruction values are performed using the aforementioned model for quantifying blast effects on facilities behind blast walls (Schuldt and El-Rayes 2017). The second step is to calculate the direct losses for each facility. Direct losses consist of both facility reconstruction costs (FRC_i) and asset replacement costs (ARC_i), as shown in Eq. (5.6). First, FRC_i is calculated using the PFD_i, facility reconstruction unit cost (FR_M), which is the cost to reconstruct a square meter of the selected building material (M), and the facility area (FA_i). When the PFD_i is low, building owners usually prefer to repair the damaged facility, as shown in Eq. (5.7). When the cost of repairing the damaged facility exceeds a certain percentage of the replacement cost, building owners typically decide to replace the damaged facility instead of repairing it. The present model utilizes FEMA P-58's recommendation to reconstruct a facility when it suffers more than 40% damage (FEMA 2012), as shown in Eq. (5.7). Second, ARC_i is the cost to replace the assets within a facility that are destroyed or damaged by an explosive attack. ARC_i is calculated as the product of multiplying the total value of assets within a facility (FAV_i) and its percent facility destruction (PFD_i), where the assets are assumed to be uniformly distributed within the facility, as shown in Eq. (5.8).

$$DL_i = FRC_i + ARC_i \tag{5.6}$$

$$\begin{aligned} FRC_i &= PFD_i \times FR_M \times FA_i \quad \text{for } PFD_i < 0.40 \\ FRC_i &= FR_M \times FA_i \quad \text{for } PFD_i \geq 0.40 \end{aligned} \tag{5.7}$$

$$ARC_i = FAV_i \times PFD_i \quad (5.8)$$

where,

DL_i = direct losses for facility i ($);

FRC_i = facility reconstruction cost for facility i ($);

ARC_i = cost to replace destroyed assets in facility i ($);

PFD_i = total percentage of destruction to facility i;

FR_M = facility reconstruction unit cost based upon the selected building material (M) ($/m^2);

FA_i = area of facility i (m^2); and

FAV_i = total value of assets within facility i ($).

The third step is to calculate the indirect losses for each facility (IL_i). IL_i is calculated as the product of facility downtime (FD_i) and facility productivity rate (FPR_i), as shown in Eq. (5.9). The downtime of a facility following an explosive attack includes the time necessary to plan, design, finance, and complete the required repairs on the damaged facility. As show in Table 5.1, this facility downtime (FD_i) is identified in the present model based on the percent facility destruction (PFD_i) and the required repair time for different categories of repair that were reported by Comerio (2006). The fourth step computes the total economic loss for the entire site by summating the direct losses and indirect losses for all facilities on site, as shown in Eq. (5.10).

$$IL_i = FD_i \times FPR_i \quad (5.9)$$

$$TEL_{site} = \sum_{i=1}^{I} (DL_i + IL_i) \quad (5.10)$$

where,

IL_i = indirect losses for facility i ($);

FD_i = downtime of facility i (months); and

FPR_i = productivity rate for facility i ($/month).

Table 5.1 Facility Downtime Based on Facility Damage Level

Percent Facility Destruction (PFD_i)	Repair Category	Repair Time[a] (FD_i) (months)
< 5%	Minimal Effort	N/A
5-10%	Cleanup	0.25
10-20%	Minor Repair	2
20-30%	Moderate Repair	4
30-40%	Major Repair	20
> 40%	Replacement	36

[a] Reported repair time for facilities with an area less than 7,500 m^2 (Comerio 2006)

5.2.4 Operational Impact Index

Operational impact (OI) is designed to measure and minimize the reduction in site operational capacity due to the downtime of critical facilities damaged by an explosive attack. This impact is represented in the model using the site total operational impact (TOI_{site}), which is a measure of the total number of days the site will be unable to perform its primary mission. TOI_{site} is calculated in four steps that are designed to compute the: (1) mission dependency index of each facility; (2) effective mission dependency index based on facility destruction level; (3) site daily mission disruption; and (4) site total operational impact.

The first step is designed to compute the mission dependency index of each facility (MDI_i) using the standard measure of infrastructure criticality adopted by the United States Department of Defense (Antelman et al. 2008; Grussing et al. 2010). MDI_i is measured on a normalized scale of 0% to 100% that represents the percentage degradation in the overall site operations if the facility is unable to perform its primary

function. MDI_i is calculated using Eq. (5.11) (Grussing et al. 2010), where mission intra- and interdependency scores (MD_W and MD_B, respectively) are assigned from a scoring matrix based upon designers' answers to questions designed to assess the: (a) length of time a facility can be inoperable before having an adverse impact on the site mission; (b) ability of another facility to perform the mission of the damaged facility; and (c) difficulty to replace the services provided by the damaged facility (Grussing et al. 2010).

The second step calculates the effective mission disruption index of each facility ($EMDI_i$) based on the total percentage of destruction to facility i (PFDi), as shown in Eq. (5.12). MDI_i is incapable of quantifying the level of operational degradation when the facility suffers partial damage because it assumes the facility is completely destroyed or out of service. Accordingly, $EMDI_i$ accounts for the actual degradation of operational capacity based on the destruction level of each facility by multiplying the MDI_i by the PFD_i. For example, if a facility has an MDI value of 75% and is 100% damaged, the overall site operational capacity will be degraded 75%. If the same facility is only 10% damaged, the overall site operational capacity will only be degraded 7.5%.

The third step calculates the overall daily mission disruption (DMD_t) for each day (t) that site facilities are unable to perform their primary functions, as shown in Eq. (5.13). DMD_t is calculated by summing up the $EMDI_i$ for all damaged facilities on day t while considering: (a) the time needed to restore each facility to its full operational capacity (TRO_i); and (b) that DMD_t at any given day t should not exceed 100%, which represents complete disruption of site operations on that day. TRO_i is a user input that varies based upon the local conditions of the remote site and the availability of contract support to construct temporary facilities to restore functionality while long-term repairs

are conducted to repair damaged facilities. The fourth step calculates the site total operational impact (TOI_{site}) by summing the site DMD_t values for each day until all facilities are returned to full operational capacity (TRO_{site}+1), as shown in Eq. (5.14). Therefore, the TOI_{site} represents the total number of days the site will be unable to perform its primary mission.

$$MDI_i = MD_W \times \left(1 + \left(MD_{B,avg} + ln(n)\right)/100\right) \tag{5.11}$$

$$EMDI_i = MDI_i \times PFD_i \tag{5.12}$$

$$\begin{aligned} DMD_t &= \textstyle\sum_{i=1}^{I} EMDI_{i,t} && \text{for } \textstyle\sum_{i=1}^{I} EMDI_{i,t} < 100\% \\ DMD_t &= 100\% && \text{for } \textstyle\sum_{i=1}^{I} EMDI_{i,t} \geq 100\% \end{aligned} \tag{5.13}$$

$$TOI_{site} = \sum_{t=1}^{TRO_{site}+1} DMD_t \tag{5.14}$$

where,

MDI_i = mission dependency index value for facility i (0% to 100%);

MD_w = measure of mission intra-dependency;

$MD_{B,avg}$ = average measure of mission interdependency;

n = number of interdependencies with other function areas on site;

$EMDI_i$ = effective mission dependency index value for facility i (0% to 100%);

DMD_t = the overall site daily mission disruption on day (t);

t = day number;

TRO_{site} = time to restore all site facilities to full operational capacity; and

TOI_{site} = total site operational impact (number of operational days lost).

The calculation of TOI_{site} can be illustrated using a simplified example of a site consisting of five facilities with MDI_i, PFD_i, EMD_i, and TRO_i values as shown in Table 5.2. On day one, all five facilities are damaged and $DMD_{t=1}$ is calculated as 150% using Eq. (5.13). As shown in Figure 5.4, DMD_t is capped at 100% to reflect the complete degradation of operational capacity on a given day. On day two, facility F3 has been restored to full operational capacity and $DMD_{t=2}$ is equal to 112% and capped at 100%. On day three, facilities F3 and F1 have been restored to full operational capacity and the site $DMD_{t=3}$ is now 81%, meaning that the site is operating at 19% its full operational capacity. $DMD_{t=4}$ and $DMD_{t=5}$ are calculated in the same manner and are equal to 56% and 24%, respectively. The site is restored to full operational capacity on day six. TOI_{site} is then calculated by summing the DMD_t values from day one to day six (TRO_{site}+1) and is equal to 3.57 days, which represents the total number of days the site will be unable to perform its primary mission.

Table 5.2 Daily Mission Disruption Example

ID	Mission dependency index (MDI_i) (%)	Percent facility destruction (PFD_i) (%)	Effective mission disruption index ($EMDI_i$) (%)	Time to restore full operational capacity (TRO_i) (days)
F1	80	25	20	2
F2	60	60	36	3
F3	50	75	38	1
F4	40	80	32	4
F5	30	80	24	5

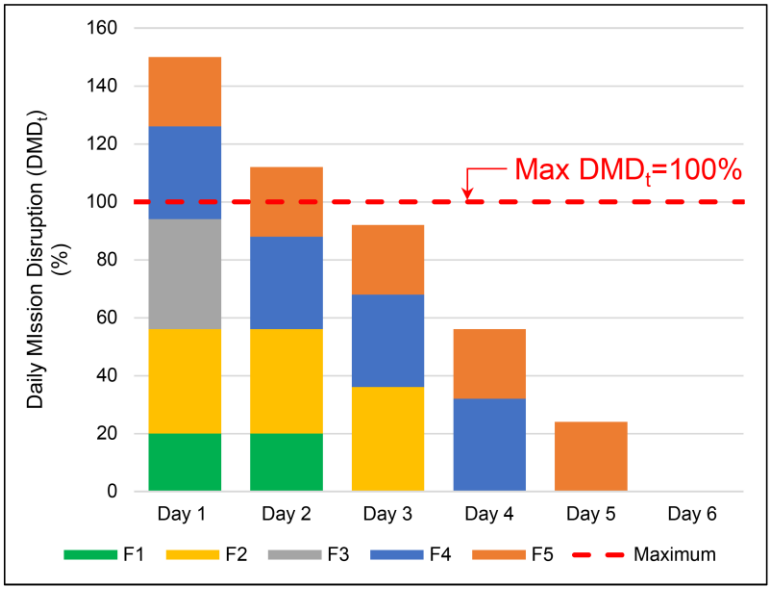

Figure 5.4 Daily Mission Disruption Example Calculations

5.3 Model Formulation

This stage focuses on formulating a multi-objective optimization model that is capable of optimizing the site layout and protection strategies in order to minimize the explosive attack consequences (EC) and minimize the site construction costs (CC) of remote sites. The model is formulated in three steps that focus on: (1) identifying the relevant decision variables, (2) defining the objective functions, and (3) specifying all practical constraints.

5.3.1 Decision Variables

The decision variables in the present model are selected to represent all relevant site layout and protection strategy decisions that have an impact on the aforementioned optimization objectives. Accordingly, the model incorporates these decision variables into two main categories: (1) site layout decision variables, and (2) protection strategy decisions variables, as shown in Figure 5.5. Site layout decision variables include the facility location (FL_i) and facility orientation (θ_i). The model defines facility locations by

the placement of their centroids on a user-specified grid system that allows site layout planner to select their preferred grid interval. Facility orientation represents the degree that a facility is rotated about its centroid and is specified in the present model to be 0 or 90°, which represents the conventional orientations for rectangular shaped facility layouts. Protection strategy decision variables consist of the facility building material (M_i), blast wall type (T), and blast wall height (H).

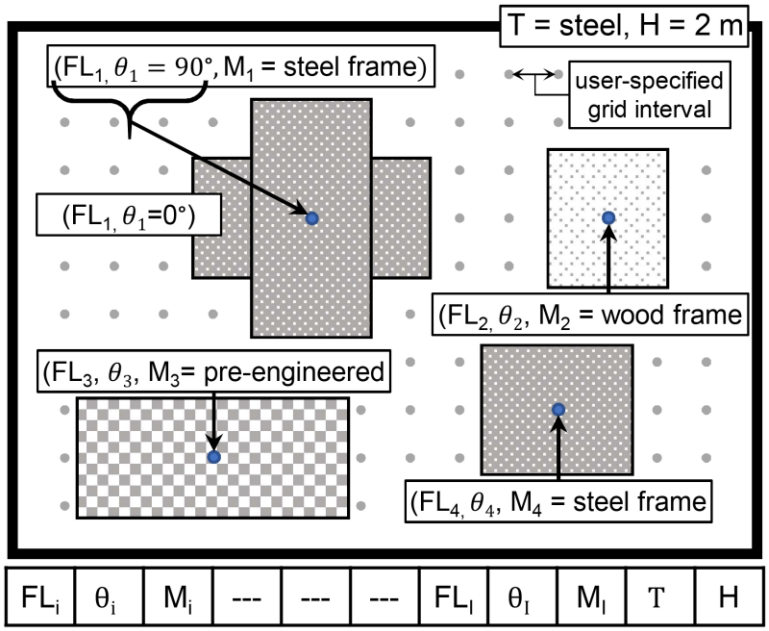

Figure 5.5 Model Decision Variables

5.3.2 Objective Function(s)

The model is designed to generate optimal tradeoffs between the two primary objectives of: (1) minimizing the explosive attack consequences (EC) for remote construction sites; and (2) minimizing the site construction costs (CC).

5.3.2.1 Minimizing Site Explosive Attack Consequences

The first objective function in the present model is designed to calculate and minimize the explosive attack consequences (EC) on remote sites, where 0%

represents no suffered consequences and 100% represents the highest level of consequences (see Eq. (5.15)). In this objective function, an overall EC index is calculated to represent the collective performance of the remote site in each of the earlier described four consequence types. Due to the various units that are used to measure these consequences, they cannot be directly aggregated to evaluate the overall level of site consequences. Accordingly, the present model transforms each of the aforementioned consequence measurements to an index that ranges from 0% to 100% by utilizing utility functions with designer-specified utility curve rate parameters. The use of utility functions enables designers to: (1) aggregate and standardize the four consequence types that have inherently different units of measurements; and (2) integrate their individual risk tolerance levels for each of the various consequence types.

The objective function is then calculated as the weighted sum of the four consequence indices. The use of weights provides designers and site layout planners with the flexibility to assign higher priority to the consequence types that are most critical to the mission and purpose of their remote construction site. Additionally, the utility curve rate parameters (r_c) provide designers with the flexibility to incorporate their own acceptable level of risk tolerance for each consequence type, where: (i) $r_c < 1$ defines a concave curve shape, which represents risk averse designers; (ii) $r_c = 1$ defines a linear function; which represents risk neutral designers, and (iii) $r_c > 1$ defines a convex function, which represents a risk tolerant design approach (El-Anwar et al. 2009), as shown in Figure 5.6. The utility functions for the personnel loss index (PLI), psychological impact index (PII), economic loss index (ELI), and operational impact index (OII) are shown in Eqs. (5.16), (5.17), (5.18) and (5.19), respectively.

$$\min EC = w_1 \times PLI + w_2 \times PII + w_3 \times ELI + w_4 \times OII \quad (5.15)$$

$$PLI = \left(\frac{PLE_{site}}{Pop_{site}}\right)^{r_{PL}} \times 100\% \quad (5.16)$$

$$PII = \left(\frac{PI_{site}}{Pop_{site}}\right)^{r_{PI}} \times 100\% \quad (5.17)$$

$$ELI = \left(\frac{TEL_{site}}{TEL_{max}}\right)^{r_{EL}} \times 100\% \quad (5.18)$$

$$OII = \left(\frac{TOI_{site}}{TOI_{max}}\right)^{r_{OI}} \times 100\% \quad (5.19)$$

where,

EC = explosive attack consequences;

w_c = importance weight for each consequence type, where $w_c > 0$ and $\sum_{c=1}^{4} w_c = 1$;

PLI = personnel loss index score for the site;

r_{PL} = personnel loss utility curve rate parameter;

PII = psychological impact index score for the site;

r_{PI} = psychological impact utility curve rate parameter;

ELI = economic loss index score for the site;

TEL_{max} = maximum total economic loss for the site ($);

r_{EL} = economic loss utility curve rate parameter;

OII = operational impact index score for the site;

TOI_{max} = maximum total operational impact for the site (days); and

r_{OI} = operational impact utility curve rate parameter.

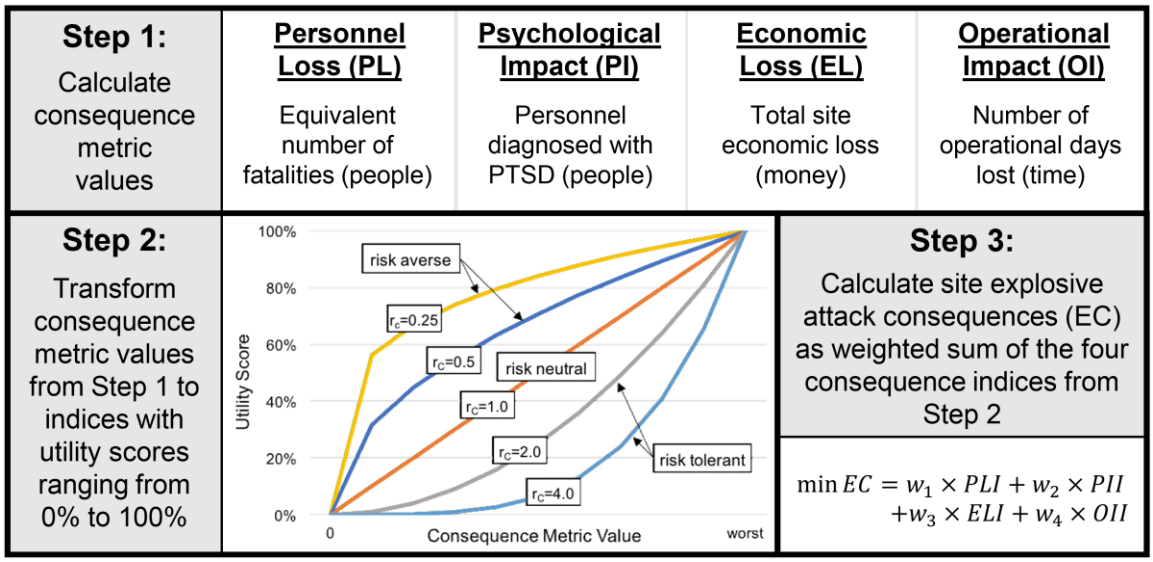

Figure 5.6 Calculation Steps of Site Explosive Attack Consequences

5.3.2.2 Minimizing Site Construction Cost

The model's second objective function is designed to calculate and minimize total site construction cost (CC), as shown in Eq. (5.20). CC includes the construction cost of all site facilities and the perimeter wall, as well as wall replacement costs based on the number of times the wall may need to be replaced over the site lifespan. Wall replacement costs are necessary for wall types such as sand-filled containers, which have a design life of 3-5 years.

$$Min\ CC = \sum_{i=1}^{I} (\mathrm{FA_i} \times \mathrm{FC_M}) + \mathrm{PL}\left(\mathrm{WC_{T,H}} + D \times R_T \times \mathrm{WR_{T,H}}\right) \tag{5.20}$$

where,

CC = total site construction cost ($);

PL = perimeter wall length (m);

$WC_{T,H}$ = wall construction unit cost based on the selected wall type (T) and wall height (H) ($/m);

D = discount rate to calculate the present value of future costs (%);

R_T = number of wall replacements over the site lifespan based on the selected wall type (T);

$WR_{T,H}$ = wall replacement unit cost based on the selected wall type (T) and wall height (H) ($/m);

FA_i = area of facility i (m^2); and

FC_M = facility construction unit cost based on the selected building material (M) ($/$m^2$).

5.3.3 Model Constraints

The present facility layout optimization model is designed to comply with all practical geometric constraints, including: (1) site boundary, which ensures that all facilities are constructed within the available site area; (2) facility overlap, which ensures that proposed facility locations do not overlap one another; (3) minimum distance, which allows designers to establish minimum separation distances between facilities or minimum standoff distances from the site perimeter to enforce security and safety requirements; and (4) maximum distance, which allow designers to specify the maximum distances between facilities, such as locating emergency personnel near the fire station or hospital in the event of a rapid-response scenario. Automated computational geometry is utilized to analyze each of these geometric constraints and to ensure feasible site layout solutions are generated.

5.4 Model Implementation

The present model is implemented using multi-objective genetic algorithm (GA) to enable the generation of optimal site layout plans that present optimal tradeoffs

between minimizing site explosive attack consequences and minimizing site construction costs. GA was selected as the optimization algorithm based on its proven performance in handling non-linear objective functions and constraints, and successfully modeling facility layout and construction optimization problems (Abotaleb et al. 2016; Khalafallah and El-Rayes 2011; Said and El-Rayes 2010, 2013; Tong 2016). The model utilizes the nondominated sorting genetic algorithm II (NGSA-II) (Deb et al. 2002) and is written in Python (Rossum 1995). Model computations are accomplished in three main phases: (1) input phase to collect, integrate, and store data for the project site, blast wall, facility, and cost, as well as designer-specified importance weights and risk tolerance factors and GA search parameters; (2) multi-objective optimization phase that initializes the model, evaluates the fitness of generated solutions, selects the fittest individuals, generates a new offspring population utilizing the GA search parameters, and repeats until the specified number of generations is completed; and (3) output phase that facilities the retrieval and visualization of the generated optimal site layout plans by producing a database of the generated optimal tradeoff solutions, and graphically representing the tradeoff curves of the nondominated Pareto frontier solutions.

5.5 Model Assumptions

The development of the present model was based on a number of assumptions, including: (1) certainty in the specified input data; (2) utilization of single-story constructed facilities; (3) explosive attacks detonate near ground level; (4) use of conservative design values for facility destruction levels and rates of fatalities, injuries,

and post-traumatic stress disorder; and (5) remote construction site populations up to 250 people.

5.6 Case Study

The performance of the developed model is analyzed using a case study that is designed to demonstrate the use of the model and display its unique capabilities in optimizing remote construction site layouts and generating optimal tradeoffs between minimizing site explosive attack consequences and minimizing site construction costs. The case study focuses on optimizing the site layout and protection strategies for a hypothetical military base that is located in a remote area of an overseas country with a construction area cost factor of 1.80 (USACE 2016). The base has an available site area of 90 x 60 meters in which to construct the 13 facilities that are required to house and support the operations of 110 personnel (see Table 5.3).

The present model requires site layout planners and designers to specify a number of input parameters in order to carry out the optimization computations. Project site input data includes an expected site operational lifespan of 20 years and an anticipated maximum explosive threat of 454.5 kg, which is the design blast charge weight carried in a full-size van (FEMA 2011). Blast wall characteristics include the available blast wall types, blast wall heights, and their design lives, as shown in Table 5.4. Facility characteristics consist of available building materials (see Table 5.5), facility dimensions (Lx and Ly) and the assigned facility population (Pop_i), asset value (FAV_i), productivity rate (FPR_i), and mission dependency index value (MDI_i), as shown in Table 5.3. Cost data is provided for blast walls (Table 5.4) and building materials (Table 5.5). A three-meter minimum separation distance between all facilities is also specified. The

importance weight (w_c) and utility curve rate parameter value (r_c) for each consequence type are selected based upon the mission and purpose of the remote construction site and the risk tolerance levels of site designers. Accordingly, the model enables designers to specify these input parameters, which can vary from one decision maker to another. For the analysis of this case study, importance weights are set to 0.5, 0.1, 0.1, and 0.3, and utility curve rate parameters are set to 0.5, 1.0, 1.0, and 0.75 for personnel loss, psychological impact, economic impact and operational impact, respectively. These importance weights and utility curve rate parameters reflect that the designers place greater emphasis on and are more sensitive to the consequences of personnel loss and operational impact.

Table 5.3 Facility Input Data

ID	Description	Dimensions		Assigned Population (Pop_i)	Asset Value (FAV_i) ($)	Productivity Rate (FPR_i) ($/month)	Mission Dependency Index (MDI_i)
		Lx (m)	Ly (m)				
F1-F4	Dormitory (x4)	15	10	12	25,000	1,000	17
F5	Dining Facility	12	9	20	150,000	50,000	69
F6	Headquarters	12	9	10	250,000	250,000	81
F7	Senior Leader Dormitory	15	10	3	50,000	2,500	27
F8	Storage	8	8	0	10,000	500	5
F9	Gymnasium	15	10	12	100,000	5,000	51
F10	Communications Building	8	8	2	375,000	100,000	81
F11	Maintenance	8	8	3	50,000	25,000	69
F12	Emergency Response	12	9	5	150,000	50,000	81
F13	Medical Clinic	16	12	7	200,000	50,000	81

Table 5.4 Blast Wall Input Data

ID	Wall type (WT)	Wall height H (m)	Construction Cost[a] $WC_{T,H}$ ($/m)	Replacement Cost[a] $WR_{T,H}$($/m)	Design Life $\mathrm{DL_{T,H}}$ (years)
1	Balsa wood, thick	2	588	881	20
2	Balsa wood, thick	5	1,467	2,201	20
3	Balsa wood, thin	2	469	704	20
4	Balsa wood, thin	5	1,174	1,760	20
5	CMU	2	472	708	10

Table 5.4 (cont.)

6	CMU	5	1,179	1,769	10
7	Concrete, thin panel	2	465	698	15
8	Concrete, thin panel	5	1,161	1,741	15
9	Polystyrene	2	690	1,035	10
10	Polystyrene	5	1,722	2,583	10
11	Polythene sheet	2	605	907	10
12	Polythene sheet	5	1,512	2,268	10
13	Revetting material	2	648	972	10
14	Revetting material	5	1,619	2,428	10
15	Sand, thick	2	566	849	4
16	Sand, thick	5	674	1,011	4
17	Sand, medium	2	366	549	4
18	Sand, medium	5	494	741	4
19	Sand, thin	2	288	432	4
20	Sand, thin	5	416	624	4
21	Steel	2	1,094	1,642	20
22	Steel	5	2,736	4,104	20
23	Water, bag	2	811	1,216	7
24	Water, bag	5	1,080	1,620	7
25	Water, filled	2	576	864	7
26	Water, filled	5	720	1,080	7

[a]Costs were determined from the 2017 RS Means, when available, or Army Corps of Engineers subject matter experts

Table 5.5 Building Material Costs

ID	Building Material	Construction Cost[a] FC_M ($/m^2)
1	Wood frame	3,341
2	Pre-engineered metal	3,398
3	Unreinforced masonry	3,557
4	Steel frame with lightly reinforced CMU infill walls	3,643
5	Reinforced concrete	3,830
6	Reinforced concrete with lightly reinforced CMU infill walls	4,738

[a]Costs were determined from the 2017 RS Means, when available, or Army Corps of Engineers subject matter experts

The aforementioned input data were utilized by the present model to perform the optimization computations for this case study in order to generate optimal site layout solutions that provide an optimal tradeoff between minimizing site explosive attack consequences and minimizing site construction costs. The multi-objective genetic

algorithm (GA) computations are performed in four steps. First, the model randomly generates an initial set of solutions that forms the initial population of the first generation. This set of solutions represents feasible site layout and protection measure decisions. Second, the model evaluates the fitness of each solution and ranks them based on nondomination criteria (Deb et al. 2002). Third, the model selects the fittest individuals within the population. Fourth, utilizing selection, crossover, and mutation operators, the model generates a new offspring population. Steps two through four are repeated until the model termination conditions are reached. The optimization GA search parameters were established for this case study based on a large number of experiments that evaluated a wide range of population sizes, number of generations, mutation rates, crossover types, and crossover rates. Accordingly, these GA parameters were specified in the present case study to be a population size of 200, 500 generations, a mutation rate of 0.01, two-point crossover with a crossover rate of 0.75.

The developed optimization model was used to optimize the selection of facility locations and protection strategies to minimize the explosive attack consequences (EC) and minimize the construction cost (CC) of the remote construction site. The model generated a total of 53 nondominated optimal solutions, where each solution represents a unique and optimal tradeoff between the two optimization objectives, as shown in Figure 5.7. An analysis of this broad spectrum of generated nondominated solutions illustrates that the model was able to identify two extreme nondominated solutions. At one of end of the spectrum, solution S1 represents the nondominated solution that results in the lowest overall EC (14.8%) at the highest CC ($6.80 million). This minimum EC solution was achieved by: (1) constructing a five-meter tall, thick sand blast wall; (2)

utilizing the layout shown in Figure 5.7(a); and (3) constructing all facilities using steel frame or reinforced concrete with lightly reinforced CMU infill walls, which provide the highest levels of blast resistance, as shown in Table 5.6. This solution anticipates 5 fatality equivalents, 27 personnel to be diagnosed with PTSD, $2.38 million in total economic losses, and 4.9 operational days lost. At the other end of the spectrum, solution S53 represents the nondominated solution that results in the lowest CC ($5.57 million) but is expected to suffer the highest EC (54.3%). This lowest cost solution was achieved by: (1) constructing a two-meter tall, thick balsa wood blast wall; (2) utilizing the layout shown in Figure 5.7(b); and (3) constructing all facilities using wood-frame construction, which is the least expensive building material. This design solution anticipates individual consequence values of 47 fatality equivalents, 34 personnel to be diagnosed with PTSD, $20.1 million in total economic losses, and 21 operational days lost, as shown in Table 5.6.

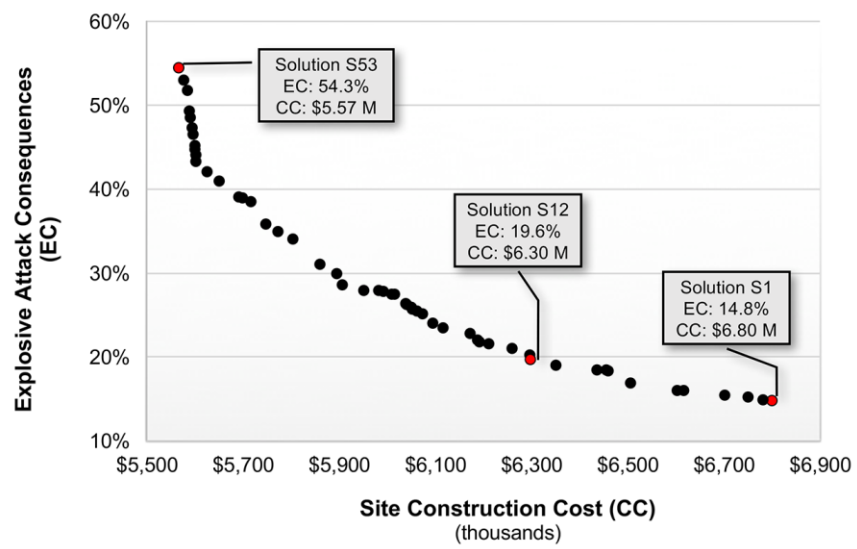

Figure 5.7 Generated Nondominated Solutions

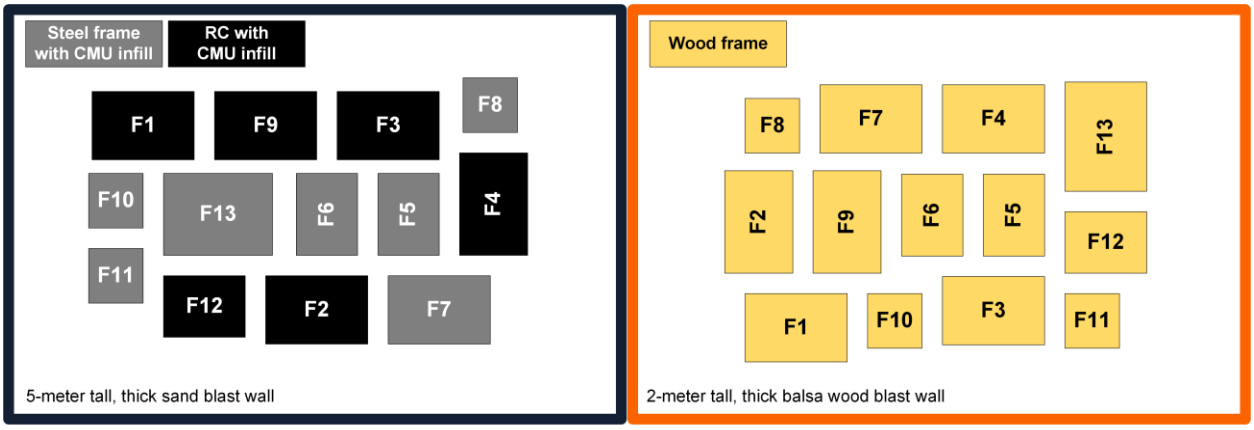

(a) (b)

Figure 5.8 Site Layout Plan for Solutions (a) S1 and (b) S53

Between these two extreme solutions, the model generated a wide range of 51 optimal tradeoff solutions. Designers can analyze the optimal tradeoff solutions and select the optimal site layout and protection strategy that best fits the specific requirements of their project based on their: (1) maximum acceptable level of explosive attack consequences; or (2) maximum available construction budget. For example, solution S12 represents the design that has the lowest construction cost ($6.30 million) where the anticipated EC does not exceed 20%, as shown in Figure 5.7. This design solution anticipates that the site will suffer the following consequences in the event of a 454.5 kg explosive attack: 11 fatality equivalents, 15 personnel to be diagnosed with PTSD, $2.35 million in total economic losses, and 11.5 operational days lost. Table 5.6 presents a sample of the optimal decision variable selections for the design solutions discussed in this section.

Table 5.6 Sample Nondominated Solutions

Solution	Blast Wall	Building Materials	EC (%)	SC ($ M)	PLE_{site} (people)	PI_{site} (people)	TEL_{site} ($ M)	TOI_{site} (days)
S1	16	(6,6,6,6,4,4,4,4,6,4,4,6,4)	14.8	6.80	5	27	2.38	4.9
S12	21	(4,4,4,4,6,4,2,3,4,5,2,3,4)	19.6	6.30	11	15	2.35	11.5
S53	1	(1,1,1,1,1,1,1,1,1,1,1,1,1)	54.3	5.57	47	34	20.1	21

The results of this case study analysis highlight the significance and practicality of the developed optimization model. The model was able to efficiently quantify the consequences of an explosive attack in order to generate a broad spectrum of optimal site layout solutions and protection strategies that provide optimal tradeoffs between minimizing the consequences of explosive attacks and minimizing site construction costs. In quantifying the explosive attack consequences, the model was able to: (1) compute the number of expected fatality equivalents that accounts for the total number of fatalities, serious injuries, and minor injuries resulting from the explosive attack; (2) quantify the extent of psychological impacts on survivors of the attack; (3) calculate the total economic loss from direct facility and asset damage as well as facility productivity losses; and (4) compute the number of operational days lost. These capabilities enable designers to select the optimal site layout and protection strategy that best meets the mission requirements of their remote construction site.

5.7 Summary and Conclusions

This chapter presented the development of a novel multi-objective optimization model for the layout and security planning of remote construction sites. The model was implemented using multi-objective genetic algorithms to search for and identify solutions that provide optimal tradeoffs between the competing objectives of minimizing site explosive attack consequences and minimizing site construction costs. The model was developed in three main stages that focused on: (1) quantifying the consequences of explosive attacks targeting facilities; (2) formulating the model by identifying the relevant decision variables, formulating the objective functions, and defining all practical constraints; and (3) implementing the model by specifying the input and output data and

performing the optimization computations using genetic algorithms. A case study was analyzed to demonstrate the use of the model and display its unique capabilities in selecting optimal design configurations for a hypothetical 110-person remote military base exposed to a 454.5 kg explosive attack. The results of analysis illustrate the new capabilities of the model in: (a) efficiently quantifying the consequences of explosive attacks on both unprotected and protected facilities; (b) evaluating the impact of serious and minor injuries on total personnel losses; (c) quantifying the extent of PTSD among survivors of explosive attacks; (d) measuring the total number of days the site is unable to perform its primary mission following an explosive attack; and (e) generating optimal tradeoffs between the conflicting objectives of minimizing site explosive attack consequences and minimizing site construction costs. The developed model should prove valuable to site layout planners and designers of remote construction sites in high-threat areas, enabling them to search for and select the optimal design configuration based on the mission of the remote construction site. This capability will result in the construction of cost-effective, secure sites that will reduce the risk of personnel loss, psychological impact, economic loss and operational impact in the event of an explosive terrorist attack.

CHAPTER 6

CONCLUSIONS

6.1 Summary

The present research study focused on the design and construction decisions of remote construction sites in order to minimize the security risks to site personnel and facilities from the threat of an explosive attack. The new research developments of this study include: (1) an innovative blast effects assessment model; (2) an original facility protection optimization model; and (3) a novel blast consequence mitigation model.

First, an innovative blast effects assessment model was developed enabling designers to accurately and efficiently quantify and visualize blast effects on constructed facilities behind rigid or frangible blast walls. The model was developed in five main stages: (1) blast wall analysis stage that developed a methodology to quantify the performance of feasible frangible blast wall types including sand-filled, water-filled, and wood walls in reducing reflected pressure and impulse loading on facilities; (2) facility damage assessment stage that computed the percent area of each facility within five specified damage levels in order to calculate an overall facility damage level; (3) blast damage visualization stage that displayed anticipated facility damage areas based upon blast charge weight, blast wall type, and building material combinations; (4) performance analysis stage that evaluated the accuracy and efficiency of the developed model; and (5) case study stage that analyzed the performance of the developed model using an application example. The case study analysis demonstrated the model's unique capability to efficiently predict the blast damage level for a constructed facility and generate blast damage visualizations for all feasible facility location, blast wall type,

and building material design alternatives. This new capability should prove useful for designers and construction managers of high-threat sites, allowing them to evaluate design options that may not have been previously considered because of the significant computational time and effort required by numerical blast assessment models. This should also contribute to enhancing the design of remote construction sites in order to meet the functional and security requirements established by the site owners.

Second, an original multi-objective facility protection optimization model was developed to optimize the site layout and selection of perimeter blast walls and building materials in order to minimize the facility destruction levels from explosive attacks while minimizing site construction costs. The model equips planners of remote construction sites with the capability to efficiently identify, from a set of feasible alternatives, optimal solutions for remote construction sites that minimize the site facility destruction levels resulting from explosive attacks in the most cost-effective manner. The model was developed in three main stages: (1) formulation stage that defined the relevant decision variables, formulated the objective functions, and identified practical model constraints; (2) implementation stage that performed the optimization computations using multi-objective genetic algorithm; and (3) performance evaluation stage that analyzed an application example to evaluate and improve model performance.

Third, a novel multi-objective blast consequence mitigation model was developed to optimize the site layout and security planning of remote construction sites in order to minimize the consequences of an explosive attack and minimize the construction costs of remote sites. The model was developed to support designers in their critical task of searching for and identifying optimal remote construction site layouts that minimize the

personnel loss, psychological impact, economic loss, and operational impact in the event of an explosive attack. The model was developed in three main stages: (1) consequence identification stage that quantified the consequences of explosive attacks targeting facilities; (2) formulation stage that identified the relevant decision variables, formulated the objective functions, and defined all practical constraints; and (3) implementation stage that performed the optimization computations using genetic algorithm and specified the model input and output data. The performance of the developed model was analyzed using a case study that was designed to illustrate the use of the model and demonstrate its unique capabilities.

6.2 Research Contributions

The main research contributions of this study include the development of:

1. Novel analytical formulas and effectiveness factors capable of quantifying the performance of feasible frangible blast wall types in reducing reflected pressure and impulse loading on site facilities from explosive attacks.
2. Innovative blast effects assessment model (BEAM) capable of efficiently quantifying and visualizing blast effects on constructed facilities behind blast walls.
3. Original multi-objective model for optimizing the site layout and selection of perimeter blast walls and building materials that provides the unique capability of generating optimal tradeoffs between minimizing the destruction of site facilities from an explosive attack and minimizing site construction costs.
4. New metric for evaluating the impact of serious and minor injuries on total personnel losses resulting from an explosive attack.

5. Novel methodology to quantify the extent of psychological impacts on survivors of explosive attacks.
6. Innovative metric for measuring the impact of explosive attacks on the operational capacity of remote construction sites.
7. Novel blast consequence mitigation model that is capable of identifying optimal site layout and protection strategies that minimize the consequences of explosive attacks on remote construction sites.

6.3 Research Impact

The aforementioned research developments and contributions are expected to have significant and broad impacts on the current practices for designing and constructing remote construction sites. They have a strong potential to: (1) enhance site protection through the use of frangible blast walls that provide comparable and often greater reductions in blast loading than rigid walls; (2) minimize facility destruction levels in remote construction sites resulting from explosive attacks; and (3) increase overall security of remote construction sites by minimizing the personnel losses, psychological impacts, economic losses, and operational impacts suffered from an explosive attack.

6.4 Future Research Work

While the present study fully achieved its research objectives, additional research areas have been identified to expand and build upon the completed research work. These future research opportunities include: (1) expanding blast modeling capabilities; (2) developing a bilevel optimization model that can consider the competing objectives of attackers; and (3) producing a multi-objective sustainability planning model for remote construction sites.

6.4.1 Expanding Blast Modeling Capabilities

The present study considers the most relevant and important design parameters and decision variables in quantifying blast effects on constructed facilities behind blast walls, including: blast charge weight, blast wall type, blast wall height, building size, building material, explosive-to-wall distance, and wall-to-facility distance. The methodology developed in the present study yields highly accurate blast analysis results, as shown by the performance analysis of the present model compared to the Defense Threat Reduction Agency's Vulnerability Assessment and Protection Option (VAPO) software (Schuldt and El-Rayes 2017). The integration of additional decision variables and design parameters can expand the use of the model to consider a wider range of remote construction sites. These additional modeling considerations may include: (1) accounting for uncertainty in model input data; (2) utilizing multi-story facilities and various window material and glazing options; and (3) modeling battalion- and division-sized camps.

6.4.2 Utilizing Bilevel Optimization to Consider Attacker Objectives

This research study focuses on accurately and efficiently evaluating all feasible design alternatives for remote construction sites in order to minimize the security risks to site personnel and facilities from the threat of explosive attacks. The optimization models developed in this study quantify the consequences of an explosive attack based upon the highest level of total facility damage inflicted from 20 possible attack locations. Developing a bilevel optimization model would enable decision makers to consider competing objectives of intelligent attackers. Bilevel optimization models utilize a leader-follow scenario or a Stackelberg game (Simaan and Cruz Jr 1973), where designers

make construction site layout decisions and the attacker responds by selecting the attack location that will maximize his objective. The attacker's strategies will in turn affect the designer's strategies. This bilevel scenario may result in more resilient remote construction site protection strategies.

6.4.3 Producing a Sustainability Planning Model for Remote Construction Sites

Remote construction sites are normally not connected to a local utility grid. This lack of established infrastructure creates unique sustainability and environmental challenges, including: (1) a heavy reliance on the delivery of resources such as fuel and water; and (2) difficulty in treating and disposing of generated wastes. These challenges result in several consequences, including: (1) increased energy consumption due to generating power on site and transporting fuel and water to the site; (2) higher construction and operating costs; (3) deleterious environmental impacts due to additional air emissions, natural resource consumption and disposal of generated wastes; and (4) adverse impacts on human health due to the level of noise produced by generators and harmful emissions from waste incineration. Accordingly, there is a need for an innovative multi-objective sustainability planning model for remote construction sites that is capable of generating optimal tradeoffs between maximizing site sustainability and minimizing construction and operating costs.

REFERENCES

Abbotts, R., Harrison, S., and Cooper, G. (2007). “Primary Blast Injuries to the Eye: A Review of the Evidence.” Journal of the Royal Army Medical Corps, 153(2), 119–123.

Abdallah, M. (2014). “Optimizing the selection of sustainability measures for existing buildings.” Ph.D. Thesis, University of Illinois at Urbana-Champaign.

Abenhaim, L., Dab, W., and Salmi, L. R. (1992). “Study of civilian victims of terrorist attacks (France 1982–1987).” Journal of Clinical Epidemiology, 45(2), 103–109.

Abotaleb, I., Nassar, K., and Hosny, O. (2016). “Layout optimization of construction site facilities with dynamic freeform geometric representations.” Automation in Construction, 66, 15–28.

Air3D. (2001). “A computational tool for airblast calculations.” An approach to the evaluation of blast loads on finite and semi-infinite structures, T.A. Rose, ed., Cranfield Univ., Shrivenham, U.K.

Ansys. (2013). AUTODYN, software for modeling the nonlinear dynamics of solids, fluids, gases and their interactions. Canonsburg, PA.

Antelman, A., Dempsey, J., and Brodt, B. (2008). “Mission Dependency Index–A Metric for Determining Infrastructure Criticality.” Infrastructure Reporting and Asset Management, American Society of Civil Engineers, 141–146.

ASCE. (2011). Blast Protection of Buildings. Standards, American Society of Civil Engineers.

Ataei, H., and Anderson, J. C. (2012). “Mitigating the Injuries from Flying Glass Due to Air Blast.” Forensic Engineering 2012, American Society of Civil Engineers, 133–142.

Avidan, V., Hersch, M., Armon, Y., Spira, R., Aharoni, D., Reissman, P., and Schecter, W. P. (2005). “Blast lung injury: clinical manifestations, treatment, and outcome.” The American Journal of Surgery, 190(6), 945–950.

Ayyub, B. M., McGill, W. L., and Kaminskiy, M. (2007). “Critical Asset and Portfolio Risk Analysis: An All-Hazards Framework.” Risk Analysis, 27(4), 789–801.

Bailey, J. R., and Levitan, M. L. (2008). “Lessons learned and mitigation options for hurricanes.” Process Safety Progress, 27(1), 41–47.

Baykasoglu, A., Dereli, T., and Sabuncu, I. (2006). “An ant colony algorithm for solving budget constrained and unconstrained dynamic facility layout problems.” Omega, 34(4), 385–396.

Bernal-Agustín, J. L., Dufo-López, R., and Rivas-Ascaso, D. M. (2006). “Design of isolated hybrid systems minimizing costs and pollutant emissions.” Renewable Energy, 31(14), 2227–2244.

Bewick, B., Flood, I., and Chen, Z. (2011). “A Neural-Network Model-Based Engineering Tool for Blast Wall Protection of Structures.” International Journal of Protective Structures, 2(2), 159–176.

Beyer, M. E. (1986). Blast loads behind vertical walls. DTIC Document.

Blomberg, S. B., Hess, G. D., and Orphanides, A. (2004). “The macroeconomic consequences of terrorism.” Journal of Monetary Economics, 51(5), 1007–1032.

Bogosian, D., Ferritto, J., and Shi, Y. (2002). Measuring uncertainty and conservatism in simplified blast models. DTIC Document.

Bogosian, D., and Piepenburg, D. (2002). “Effectiveness of frangible barriers for blast shielding.” Proceedings of the 17th International Symposium on the Military Aspects of Blast and Shock, Las Vegas, Nevada, USA.

Boussaïd, I., Lepagnot, J., and Siarry, P. (2013). “A survey on optimization metaheuristics.” Information Sciences, 237, 82–117.

Britt, J. R., Ranta, D. E., and Ohrt, A. P. (1999). A user’s manual for the BLASTX code, version 4.1. U.S. Army Engineer Waterways Experiment Station, Vicksburg, Miss.

Butler, A. S., Panzer, A. M., Goldfrank, L. R., and Institute of Medicine (U.S.) (Eds.). (2003). Preparing for the psychological consequences of terrorism: a public health strategy. National Academies Press, Washington, D.C.

Caramia, M., and Dell’Olmo, P. (2008). “Multi-objective optimization.” Multi-objective Management in Freight Logistics: Increasing Capacity, Service Level and Safety with Optimization Algorithms, 11–36.

Carper, K. (2011). “Design and Construction for Blast Resistance.” Journal of Performance of Constructed Facilities, 25(5), 357–357.

Cave, K. M., Cornish, E. M., and Chandler, D. W. (2007). “Blast Injury of the Ear: Clinical Update from the Global War on Terror.” Military Medicine, 172(7), 726–730.

Central Intelligence Agency (CIA). (2015). “The world factbook: crude oil - proved reserves.” <https://www.cia.gov/library/publications/the-world-factbook/rankorder/2244rank.html> (May 8, 2015).

Chapman, T. C., Rose, T. A., and Smith, P. D. (1995a). “Reflected blast wave resultants behind cantilever walls: A new prediction technique.” International Journal of Impact Engineering, 16(3), 397–403.

Chapman, T. C., Rose, T. A., and Smith, P. D. (1995b). “Blast wave simulation using AUTODYN2D: A parametric study.” International Journal of Impact Engineering, 16(5–6), 777–787.

Chen, L., Zhang, L., Fang, Q., and Mao, Y. (2015). “Performance based investigation on the construction of anti-blast water wall.” International Journal of Impact Engineering, 81, 17–33.

Chu, Y., Mi, H., Liao, H., Ji, Z., and Wu, Q. H. (2008). “A Fast Bacterial Swarming Algorithm for high-dimensional function optimization.” IEEE Congress on Evolutionary Computation, 2008. CEC 2008. (IEEE World Congress on Computational Intelligence), 3135–3140.

Coello, C. A. C. (1999). “A comprehensive survey of evolutionary-based multiobjective optimization techniques.” Knowledge and Information systems, 1(3), 269–308.

Comerio, M. C. (2000). “The Economic Benefits of a Disaster Resistant University: Earthquake Loss Estimation for UC Berkeley.” Institute of Urban & Regional Development.

Comerio, M. C. (2006). “Estimating Downtime in Loss Modeling.” Earthquake Spectra, 22(2), 349–365.

Comerio, M. C., and Blecher, H. E. (2010). “Estimating Downtime from Data on Residential Buildings after the Northridge and Loma Prieta Earthquakes.” Earthquake Spectra, 26(4), 951–965.

Crepeau, J. (1998). “SHAMRC second-order hydrodynamic automatic mesh refinement code, vol. 2: user’s manual.” Applied Research Associates, Inc., Albuquerque, NM.

Crowe, T. D. (2000). Crime Prevention Through Environmental Design, Second Edition. Butterworth-Heinemann, Boston, Mass.

Deb, K., Pratap, A., Agarwal, S., and Meyarivan, T. (2002). “A fast and elitist multiobjective genetic algorithm: NSGA-II.” Evolutionary Computation, IEEE Transactions on, 6(2), 182–197.

Department of Defense (DoD). (2002). “Design and analysis of hardened structures to conventional weapons effects.” UFC 3-340-01, Washington, DC.

Department of Defense (DoD). (2008a). “Structures to resist the effects of accidental explosions.” UFC 3-340-02, Washington, DC.

Department of Defense (DoD). (2008b). “DoD security engineering facilities planning manual.” UFC 4-020-01, Washington, DC.

Department of Defense (DoD). (2012). “DoD minimum antiterrorism standards for buildings.” UFC 4-010-01, Washington, DC.

Dillon, R. L., Liebe, R. M., and Bestafka, T. (2009). “Risk-Based Decision Making for Terrorism Applications.” Risk Analysis, 29(3), 321–335.

Dixon, L. S., and Stern, R. K. (2004). Compensation for losses from the 9/11 attacks. RAND, Santa Monica, CA.

Dorigo, M., Maniezzo, V., and Colorni, A. (1996). “Ant system: optimization by a colony of cooperating agents.” Systems, Man, and Cybernetics, Part B: Cybernetics, IEEE Transactions on, 26(1), 29–41.

Eberhart, R. C., and Kennedy, J. (1995). “A new optimizer using particle swarm theory.” Proceedings of the sixth international symposium on micro machine and human science, New York, NY, 39–43.

El-Anwar, O., El-Rayes, K., and Elnashai, A. S. (2009). “Maximizing the sustainability of integrated housing recovery efforts.” Journal of Construction Engineering and Management, 136(7), 794–802.

Elbeltagi, E., Hegazy, T., and Eldosouky, A. (2004). “Dynamic layout of construction temporary facilities considering safety.” Journal of construction engineering and management, 130(4), 534–541.

Elbeltagi, E., Hegazy, T., and Grierson, D. (2005). “Comparison among five evolutionary-based optimization algorithms.” Advanced Engineering Informatics, 19(1), 43–53.

El-Rayes, K., and Khalafallah, A. (2005). “Trade-off between Safety and Cost in Planning Construction Site Layouts.” Journal of Construction Engineering and Management, 131(11), 1186–1195.

El-Rayes, K., and Said, H. (2009). “Dynamic Site Layout Planning Using Approximate Dynamic Programming.” Journal of Computing in Civil Engineering, 23(2), 119–127.

Enders, W. (2007). “Chapter 26 Terrorism: An Empirical Analysis.” Handbook of Defense Economics, Elsevier, 815–866.

Enders, W., and Olson, E. (2012). “Measuring the economic costs of terrorism.” The Oxford Handbook of the Economics of Peace and Conflict, 874.

Federal Emergency Management Agency (FEMA). (2011). “Reference manual to mitigate potential terrorist attacks against buildings.” FEMA-426/BIPS-06 Edition 2, Washington, DC.

Federal Emergency Management Agency (FEMA). (2012). “Seismic Performance Assessment of Buildings, Volume 1 - Methodology.” FEMA P-58-1, Washington, DC.

Feng, X., Lau, F. C. M., and Gao, D. (2009). “A New Bio-inspired Approach to the Traveling Salesman Problem.” Complex Sciences, Lecture Notes of the Institute for Computer Sciences, Social Informatics and Telecommunications Engineering, J. Zhou, ed., Springer Berlin Heidelberg, 1310–1321.

Fister Jr., I., Yang, X.-S., Fister, I., Brest, J., and Fister, D. (2013). “A Brief Review of Nature-Inspired Algorithms for Optimization.” arXiv:1307.4186 [cs].

Fortin, F.-A., Rainville, D., Gardner, M.-A. G., Parizeau, M., Gagné, C., and others. (2012). “DEAP: Evolutionary algorithms made easy.” The Journal of Machine Learning Research, 13(1), 2171–2175.

Foulds, L. R., Hamacher, H. W., and Wilson, J. M. (1998). “Integer programming approaches to facilities layout models with forbidden areas.” Annals of Operations Research, 81(1–4), 405–417.

Gabriel, R., Ferrando, L., Cortón, E. S., Mingote, C., García-Camba, E., Liria, A. F., and Galea, S. (2007). “Psychopathological consequences after a terrorist attack: An epidemiological study among victims, the general population, and police officers.” European Psychiatry, 22(6), 339–346.

Galea, S., Ahern, J., Resnick, H., Kilpatrick, D., Bucuvalas, M., Gold, J., and Vlahov, D. (2002). “Psychological sequelae of the September 11 terrorist attacks in New York City.” New England Journal of Medicine, 346(13), 982–987.

Garth, R. J. N. (1995). “Blast injury of the ear: an overview and guide to management.” Injury, 26(6), 363–366.

Gillies, S. (2013). “The Shapely user manual.” Toblerity, <http://toblerity.org/shapely/manual.html> (Dec. 8, 2015).

Goel, M. D., and Matsagar, V. (2014). “Blast-Resistant Design of Structures.” Practice Periodical on Structural Design and Construction, 19(2), 04014007.

Goldberg, D. E. (1989). Genetic Algorithms in Search, Optimization and Machine Learning. Addison-Wesley Longman Publishing Co., Inc., Boston, MA, USA.

Grassie, R. P., Johnson, A. J., and Schneider, W. J. (1990). “Countermeasures selection and integration: a delicate balancing act for the security designer.”

Security Technology, 1990. Crime Countermeasures, Proceedings. IEEE 1990 International Carnahan Conference on, IEEE, 116–123.

Grussing, M. N., Gunderson, S., Canfield, M., Falconer, E., Antelman, A., and Hunter, S. L. (2010). “Development of the Army Facility Mission Dependency Index for Infrastructure Asset Management.” <http://www.dtic.mil/dtic/tr/fulltext/u2/a552791.pdf> (Nov. 17, 2016).

Havens, T. C., Spain, C. J., Salmon, N. G., and Keller, J. M. (2008). “Roach Infestation Optimization.” IEEE Swarm Intelligence Symposium, 2008. SIS 2008, 1–7.

Hibbitt, Karlsson & Sorensen, Inc. (2004). ABAQUS/CAE user’s manual, v. 6.5. Pawtucket, RI.

Hicks, M. J., Snell, M. S., Sandoval, J. S., and Potter, C. S. (1999). “Physical protection systems cost and performance analysis: a case study.” Aerospace and Electronic Systems Magazine, IEEE, 14(4), 9–13.

Holland, J. H. (1975). Adaptation in natural and artificial systems. The University of Michigan Press, Ann Arbor, MI.

Hulton, F. G., Smith, P. D., and Rose, T. A. (1995). “Blast resultants behind cantilever walls: comparison between full-scale and model-scale experiments.” Proceedings of the 14th International Symposium on Military Aspects of Blast and Shock, Las Cruces, New Mexico, USA.

Hunter, J. D. (2007). “Matplotlib: A 2D Graphics Environment.” Computing in Science Engineering, 9(3), 90–95.

Hunter, J., and Perkins, R. (2015). “Explosive States: AOAV’s Explosive Violence Monitor 2014.” AOAV, <https://aoav.org.uk/2014/aoav-explosive-violence-data-2014/> (Jan. 28, 2016).

Hyde, D. W. (1988). Microcomputer Programs CONWEP and FUNPRO, Applications of TM 5-855-1, “Fundamentals of Protective Design for Conventional Weapons” (User’s Guide).

Institute for Economics and Peace. (2015). “2015 Global terrorism impact: measuring and understanding the impact of terrorism.” IEP, <http://economicsandpeace.org/wp-content/uploads/2015/11/2015-Global-Terrorism-Index-Report.pdf> (Dec. 12, 2015).

Johnson, K., and Gilbert, D. (2013). “Poorly Secured Remote Energy Facilities Invite Terrorist Attacks.” Wall Street Journal.

Jones, P. S., Vitaya-Udom, K. P., and Watt, J. M. (1987). Design of structures to resist terrorist attack: Report 1. Vicksburg, Miss.

Karydas, D. M., and Gifun, J. F. (2006). “A method for the efficient prioritization of infrastructure renewal projects.” Reliability Engineering & System Safety, 91(1), 84–99.

Kazimi, A. A., and Mackenzie, C. A. (2016). “The economic costs of natural disasters, terrorist attacks, and other calamities: An analysis of economic models that quantify the losses caused by disruptions.” 2016 IEEE Systems and Information Engineering Design Symposium (SIEDS), 32–37.

Khalafallah, A., and El-Rayes, K. (2008). “Minimizing Construction-Related Security Risks during Airport Expansion Projects.” Journal of Construction Engineering and Management, 134(1), 40–48.

Khalafallah, A., and El-Rayes, K. (2011). “Automated multi-objective optimization system for airport site layouts.” Automation in Construction, 20(4), 313–320.

Kim, J.-G., and Kim, Y.-D. (2000). “Layout planning for facilities with fixed shapes and input and output points.” International Journal of Production Research, 38(18), 4635–4653.

Kingery, C. N., and Bulmash, G. (1984). Air blast parameters from TNT spherical air burst and hemispherical surface burst. Ballistic Research Laboratories, Aberdeen Proving Ground, MD.

Komarudin, and Wong, K. Y. (2010). “Applying Ant System for solving Unequal Area Facility Layout Problems.” European Journal of Operational Research, 202(3), 730–746.

Koutroulis, E., Kolokotsa, D., Potirakis, A., and Kalaitzakis, K. (2006). “Methodology for optimal sizing of stand-alone photovoltaic/wind-generator systems using genetic algorithms.” Solar Energy, 80(9), 1072–1088.

Li, Z., Shen, W., Xu, J., and Lev, B. (2015a). “Bilevel and multi-objective dynamic construction site layout and security planning.” Automation in Construction, 57, 1–16.

Li, Z., Xu, J., Shen, W., Lev, B., and Lei, X. (2015b). “Bilevel multi-objective construction site security planning with twofold random phenomenon.” Journal of Industrial and Management Optimization, 11(2), 595–617.

Little, R., Meacham, B., and Smilowitz, R. (2002). “A performance-based multiobjective decision framework for security and natural hazard mitigation.” Proc., National Symp. on Comprehensive Force Protection, Society of American Military Engineers Alexandria, Va.

Livermore Software Technology Corporation (LSTC). (2016). LS-DYNA, v. 971 keyword user’s manual. Livermore, CA.

Longinow, A., and Mniszewski, K. R. (1996). “Protecting buildings against vehicle bomb attacks.” Practice Periodical on Structural Design and Construction, 1(1), 51–54.

Malakooti, B. (1987). “Computer-aided facility layout selection (CAFLAS) with applications to multiple criteria manufacturing planning problems.” Large scale systems, 12(2), 109–123.

Mallonee, S., Shariat, S., Stennies, G., Waxweiler, R., Hogan, D., and Jordan, F. (1996). “Physical Injuries and Fatalities Resulting From the Oklahoma City Bombing.” JAMA, 276(5), 382–387.

Marzouk, M. M., Abdelhamid, M. S., and Elsheikh, M. T. (2012). “Selecting Building Materials Using System Dynamics and Ant Colony Optimization.” Reston, VA: ASCEProceedings of the 2011 International Conference on Sustainable Design and Construction| d 20120000, American Society of Civil Engineers.

Mawdesley, M., Al-jibouri, S., and Yang, H. (2002). “Genetic Algorithms for Construction Site Layout in Project Planning.” Journal of Construction Engineering and Management, 128(5), 418–426.

McGill, W. L., Ayyub, B. M., and Kaminskiy, M. (2007). “Risk Analysis for Critical Asset Protection: Risk Analysis for Critical Asset Protection.” Risk Analysis, 27(5), 1265–1281.

McGlaun, J. M., Thompson, S. L., and Elrick, M. G. (1990). “CTH: A three-dimensional shock wave physics code.” International Journal of Impact Engineering, 10(1), 351–360.

Mellor, S. G. (1992). “The relationship of blast loading to death and injury from explosion.” World Journal of Surgery, 16(5), 893–898.

Monismith, D. R., and Mayfield, B. E. (2008). “Slime Mold as a model for numerical optimization.” IEEE Swarm Intelligence Symposium, 2008. SIS 2008, 1–8.

Moore, J., and Chapman, R. (1999). “Application of particle swarm to multiobjective optimization.” Department of Computer Science and Software Engineering, Auburn University.

Moré, J. J., Garbow, B. S., and Hillstrom, Kenneth E. (1980). User Guide for MINIPACK-1. Argonne National Laboratory, Argonne, IL.

Morley, M. G., Nguyen, J. K., Heier, J. S., Shingleton, B. J., Pasternak, J. F., and Bower, K. S. (2010). “Blast eye injuries: a review for first responders.” Disaster Medicine and Public Health Preparedness, 4(2), 154–160.

Neria, Y., Nandi, A., and Galea, S. (2008). “Post-traumatic stress disorder following disasters: a systematic review.” Psychological Medicine, 38(04).

Ngo, T., Mendis, P., Gupta, A., and Ramsay, J. (2007). “Blast loading and blast effects on structures–an overview.” Electronic Journal of Structural Engineering, 7, 76–91.

Ngo, T., Nguyen, N., and Mendis, P. (2004). “An investigation on the effectiveness of blast wall and blast-structure interaction.” Developments in mechanics of structures and materials, Perth, Australia, 961–7.

Nichols, J. F., and Doyle, G. (2014). “Current Engineering Models and Capabilities in the Vulnerability Assessment and Protection Option (VAPO) Software.” Structures Congress 2014, American Society of Civil Engineers, 176–187.

North, C. S., Nixon, S. J., Shariat, S., Mallonee, S., McMillen, J. C., Spitznagel, E. L., and Smith, E. M. (1999). “Psychiatric disorders among survivors of the Oklahoma City bombing.” JAMA, 282(8), 755–762.

North, C. S., Tivis, L., McMillen, J. C., Pfefferbaum, B., Spitznagel, E. L., Cox, J., Nixon, S., Bunch, K. P., and Smith, E. M. (2002). “Psychiatric Disorders in Rescue Workers After the Oklahoma City Bombing.” American Journal of Psychiatry, 159(5), 857–859.

Norville, H. S., Harvill, N., Conrath, E. J., Shariat, S., and Mallonee, S. (1999). “Glass-Related Injuries in Oklahoma City Bombing.” Journal of Performance of Constructed Facilities, 13(2), 50–56.

Ohmori, S., Yoshimoto, K., and Ogawa, K. (2010). “Solving Facility Layout Problem via Particle Swarm Optimization.” 2010 Third International Joint Conference on Computational Science and Optimization (CSO), 409–413.

Pachakis, D., and Kiremidjian, A. S. (2004). “Estimation of downtime-related revenue losses in seaports following scenario earthquakes.” Earthquake Spectra, 20(2), 427–449.

Pelling, M., Özerdem, A., and Barakat, S. (2002). “The macro-economic impact of disasters.” Progress in Development Studies, 2(4), 283–305.

Perkins, R. (2015). “Four years of harm: Explosive Violence Monitor 2011-2014.” AOAV, <https://aoav.org.uk/2015/four-years-of-harm-impact-of-explosive-weapons-2011-2014/> (Nov. 16, 2016).

Piacenza, J., Tumer, I. Y., Hoyle, C., and Fields, J. (2012). “Power Grid System Design Optimization Considering Renewable Energy Strategies and Environmental Impact.” ASME 2012 International Mechanical Engineering Congress and Exposition, American Society of Mechanical Engineers, 1859–1869.

Porter, K., and Ramer, K. (2012). “Estimating earthquake-induced failure probability and downtime of critical facilities.” Journal of business continuity & emergency planning, 5(4), 352–364.

Pour, H. D., and Nosraty, M. (2006). “Solving the facility and layout and location problem by ant-colony optimization-meta heuristic.” International Journal of Production Research, 44(23), 5187–5196.

ProSAir. (2009). “Propagation of shocks in air.” A computational fluids dynamics code, Cranfield Univ., Oxfordshire, U.K.

Remennikov, A. M. (2003). “A review of methods for predicting bomb blast effects on buildings.” Journal of Battlefield Technology, 6(3), 5.

Remennikov, A. M., and Rose, T. A. (2007). “Predicting the effectiveness of blast wall barriers using neural networks.” International Journal of Impact Engineering, 34(12), 1907–1923.

Rezazadeh, H., Ghazanfari, M., Saidi-Mehrabad, M., and Sadjadi, S. J. (2009). “An extended discrete particle swarm optimization algorithm for the dynamic facility layout problem.” Journal of Zhejiang University SCIENCE A, 10(4), 520–529.

Rickman, D. D., Murrell, D. W., and Armstrong, B. J. (2006). “Improved predictive methods for airblast shielding by barrier walls.” St. Louis, MO, USA: ASCE Structures Congress.

Rohatgi, A. (2016). WebPlotDigitizer. Austin, TX, USA.

Rose, A. Z. (2009). “A framework for analyzing the total economic impacts of terrorist attacks and natural disasters.” Journal of Homeland Security and Emergency Management, 6(1).

Rose, A. Z., and Blomberg, S. B. (2010). “Total economic consequences of terrorist attacks: Insights from 9/11.” Peace Economics, Peace Science and Public Policy, 16(1).

Rose, T. A., Smith, P. D., and Mays, G. C. (1995). “The effectiveness of walls designed for the protection of structures against airblast from high explosives.” Proceedings of the Institution of Civil Engineers - Structures and Buildings, 110(1), 78–85.

Rose, T. A., Smith, P. D., and Mays, G. C. (1997). “Design charts relating to protection of structures against airblast from high explosives.” Proceedings of the ICE-Structures and Buildings, 122(2), 186–192.

Rose, T. A., Smith, P. D., and Mays, G. C. (1998). “Protection of structures against airburst using barriers of limited robustness.” Proceedings of the Institution of Civil Engineers - Structures and Buildings, 128(2), 167–176.

Rossum, G. (1995). Python Reference Manual. CWI (Centre for Mathematics and Computer Science), Amsterdam, The Netherlands, The Netherlands.

Said, H., and El-Rayes, K. (2010). “Optimizing the planning of construction site security for critical infrastructure projects.” Automation in Construction, 19(2), 221–234.

Said, H., and El-Rayes, K. (2013). “Performance of global optimization models for dynamic site layout planning of construction projects.” Automation in Construction, 36, 71–78.

Sasser, S. M., Sattin, R. W., Hunt, R. C., and Krohmer, J. (2006). “Blast Lung Injury.” Prehospital Emergency Care, 10(2), 165–172.

Scherbatiuk, K., and Rattanawangcharoen, N. (2008). “Experimental testing and numerical modeling of soil-filled concertainer walls.” Engineering Structures, 30(12), 3545–3554.

Schlenger, W. E., Caddell, J. M., Ebert, L., Jordan, B. K., Rourke, K. M., Wilson, D., Thalji, L., Dennis, J. M., Fairbank, J. A., and Kulka, R. A. (2002). “Psychological Reactions to Terrorist Attacks: Findings From the National Study of Americans’ Reactions to September 11.” JAMA, 288(5), 581–588.

Schuldt, S., and El-Rayes, K. (2017). “Quantifying Blast Effects on Constructed Facilities behind Blast Walls.” Journal of Performance of Constructed Facilities, 04017027.

Schuster, M. A., Stein, B. D., Jaycox, L. H., Collins, R. L., Marshall, G. N., Elliott, M. N., Zhou, A. J., Kanouse, D. E., Morrison, J. L., and Berry, S. H. (2001). “A National Survey of Stress Reactions after the September 11, 2001, Terrorist Attacks.” New England Journal of Medicine, 345(20), 1507–1512.

Simaan, M., and Cruz Jr, J. B. (1973). “On the Stackelberg strategy in nonzero-sum games.” Journal of Optimization Theory and Applications, 11(5), 533–555.

Smith, P. D. (2010). “Blast walls for structural protection against high explosive threats: A review.” International journal of protective structures, 1(1), 67–84.

Sorensen, A., and McGill, W. L. (2012). “Utilization of Existing Blast Analysis Software Packages for the Back-Calculation of Blast Loads.” Journal of Performance of Constructed Facilities, 26(4), 544–546.

Stewart, M. G. (2008). “Cost Effectiveness of Risk Mitigation Strategies for Protection of Buildings against Terrorist Attack.” Journal of Performance of Constructed Facilities, 22(2), 115–120.

Stewart, M. G., and Netherton, M. D. (2015). “Reliability-Based Design Load Factors for Explosive Blast Loading.” Journal of Performance of Constructed Facilities, 29(5), B4014010.

Strobel, K., and Liel, A. (2013). “Snow load damage to buildings: physical and economic impacts.” Proceedings of the Institution of Civil Engineers - Forensic Engineering, 166(3), 116–133.

Stuhmiller, J. H., Ho, K. H.-H., Vander Vorst, M. J., Dodd, K. T., Fitzpatrick, T., and Mayorga, M. (1996). “A model of blast overpressure injury to the lung.” Journal of Biomechanics, 29(2), 227–234.

Swisdak Jr, M. M. (1994). Simplified Kingery airblast calculations. DTIC Document.

Tam, C., Tong, T., Leung, A., and Chiu, G. (2002). “Site Layout Planning using Nonstructural Fuzzy Decision Support System.” Journal of Construction Engineering and Management, 128(3), 220–231.

Thompson, D., Brown, S., Mallonee, S., and Sunshine, D. (2004). “Fatal and non-fatal injuries among U.S. Air Force personnel resulting from the terrorist bombing of the Khobar Towers.” The Journal of Trauma, 57(2), 208–215.

Tong, Z. (2016). “A genetic algorithm approach to optimizing the distribution of buildings in urban green space.” Automation in Construction, Computational and generative design for digital fabrication: Computer-Aided Architectural Design Research in Asia (CAADRIA), 72, Part 1, 46–51.

United States Energy Information Administration (USEIA). (2015). “International Energy Statistics.” <http://www.eia.gov/cfapps/ipdbproject/IEDIndex3.cfm> (May 26, 2015).

U.S. Army Corps of Engineers (USACE). (1984). “Fundamentals of protective designs for conventional weapons.” TM 5-855-1, Vicksburg, MS.

U.S. Army Corps of Engineers (USACE). (1999). “Estimating damage to structures from terrorist bombs field operations guide.” ETL 1110-3-495, Washington, DC.

U.S. Army Corps of Engineers (USACE). (2016). “DoD Area Cost Factor, 31 March 2016.” <http://www.usace.army.mil/Cost-Engineering/Programming-Administration-and-Execution-System-Ne/> (Feb. 21, 2017).

U.S. Dept. of the Air Force. (1997). “Installation force protection guide.” Washington, DC.

U.S. Dept. of the Army. (1990). “Structures to resist the effects of accidental explosions.” TM 5-1300, Washington, DC.

USACE PDC. (2016). “VAPO — PDC.” Document, <https://pdc.usace.army.mil/software/vapo/> (Mar. 30, 2016).

Vázquez, C., Hervás, G., and Pérez-Sales, P. (2008). “Chronic thought suppression and posttraumatic symptoms: Data from the Madrid March 11, 2004 terrorist attack.” Journal of Anxiety Disorders, 22(8), 1326–1336.

Verger, P., Dab, W., Lamping, D. L., Loze, J.-Y., Deschaseaux-Voinet, C., Abenhaim, L., and Rouillon, F. (2004). “The Psychological Impact of Terrorism: An Epidemiologic Study of Posttraumatic Stress Disorder and Associated Factors in Victims of the 1995–1996 Bombings in France.” American Journal of Psychiatry, 161(8), 1384–1389.

Ward, S. P. (2004). “Retrofitting Existing Masonry Buildings to Resist Explosions.” Journal of Performance of Constructed Facilities, 18(2), 95–99.

Weise, T. (2008). Global Optimization Algorithms: Theory and Application.

Wightman, J. M., and Gladish, S. L. (2001). “Explosions and blast injuries.” Annals of Emergency Medicine, 37(6), 664–678.

Wolf, S. J., Bebarta, V. S., Bonnett, C. J., Pons, P. T., and Cantrill, S. V. (2009). “Blast injuries.” The Lancet, 374(9687), 405–415.

Wu, C., and Hao, H. (2007). “Safe Scaled Distance for Masonry Infilled RC Frame Structures Subjected to Airblast Loads.” Journal of Performance of Constructed Facilities, 21(6), 422–431.

Yang, H., Zhou, W., Lu, L., and Fang, Z. (2008). “Optimal sizing method for stand-alone hybrid solar–wind system with LPSP technology by using genetic algorithm.” Solar Energy, 82(4), 354–367.

Yang, X.-S. (2009). “Firefly Algorithms for Multimodal Optimization.” Stochastic Algorithms: Foundations and Applications, Lecture Notes in Computer Science, O. Watanabe and T. Zeugmann, eds., Springer Berlin Heidelberg, 169–178.

Yang, X.-S. (2010). “A New Metaheuristic Bat-Inspired Algorithm.” Nature Inspired Cooperative Strategies for Optimization (NICSO 2010), Studies in Computational Intelligence, J. R. González, D. A. Pelta, C. Cruz, G. Terrazas, and N. Krasnogor, eds., Springer Berlin Heidelberg, 65–74.

Yang, X.-S. (2014). Nature-Inspired Optimization Algorithms. Elsevier.

Yuan, Y., Yuan, J., Du, H., and Li, L. (2012). “An improved multi–objective ant colony algorithm for building life cycle energy consumption optimisation.” International Journal of Computer Applications in Technology, 43(1), 60–66.

Zhang, H., and Wang, J. Y. (2008). “Particle swarm optimization for construction site unequal-area layout.” Journal of Construction Engineering and Management, 134(9), 739–748.

Zhou, A., Qu, B.-Y., Li, H., Zhao, S.-Z., Suganthan, P. N., and Zhang, Q. (2011). “Multiobjective evolutionary algorithms: A survey of the state of the art.” Swarm and Evolutionary Computation, 1(1), 32–49.

Zhou, X. Q., and Hao, H. (2008). “Prediction of airblast loads on structures behind a protective barrier.” International Journal of Impact Engineering, 35(5), 363–375.

Zouein, P. P., and Tommelein, I. D. (1999). “Dynamic layout planning using a hybrid incremental solution method.” Journal of construction engineering and management, 125(6), 400–408.